

A MOLECULAR ORBITAL THEORY OF POLYMERS

A MOLECULAR ORBITAL THEORY
OF POLYMERS

By
JAMES FRANCIS O'SHEA, B.Sc.

A Thesis
Submitted to the Faculty of Graduate Studies
in Partial Fulfilment of the Requirements
for the Degree
Doctor of Philosophy

McMaster University
March 1973

© James Francis O'Shea 1973

DOCTOR OF PHILOSOPHY (1973)
(Chemistry)

McMASTER UNIVERSITY
Hamilton, Ontario

TITLE: A Molecular Orbital Theory of Polymers

AUTHOR: James Francis O'Shea, B.Sc. (National University of Ireland)

SUPERVISOR: Professor D. P. Santry

NUMBER OF PAGES: ix, 140

SCOPE AND CONTENTS:

The molecular orbital method and the underlying approximations are reviewed. A molecular orbital method appropriate to the study of polymers is then developed in the Complete Neglect of Differential Overlap approximation. The resulting equations, which are discussed in some detail, are used to study a number of real and model polymers which have regular structures. The model systems are chosen to represent a wide range of physical characteristics. A discussion of the results of these calculations which show that the method gives physically reasonable results is presented. Some problems specific to the theory of polymers are identified, discussed, and, in a number of cases, resolved.

The limitations on the method imposed by the assumption that the structure of the polymer is regular are discussed. A method, based on self-consistent perturbation theory, is proposed which permits the calculation of the effects of small irregularities on the electronic structure of polymers. The characteristics of the method are discussed using as examples calculations on small molecules. A formalism appropriate to the study of

polymers is then developed. Model calculations on a chain of hydrogen molecules are used to demonstrate the effectiveness and potential uses of the method. The linear chain of equally-spaced hydrogen molecules is shown to be stable with respect to distortions along the axis of the chain.

ACKNOWLEDGEMENT

I would like to thank Dr. David P. Santry for his help and encouragement throughout my stay at McMaster. He and Shirley have meant much to me.

I would further like to thank the people of Canada for their generous support through the National Research Council of Canada, and through McMaster University.

Any attempt to thank explicitly the many people in the Departments of Chemistry and Physics who have stimulated my interest in science would be inadequate; I thank them all anyway. To those who actively hindered my research by providing alternative interests I also say "thanks". Finally, I thank Judy.

This work is dedicated to my tolerant family.

7

TABLE OF CONTENTS

	Page
INTRODUCTION	1
CHAPTER 1	
Molecular Orbital Theory	7
Complete Neglect of Differential Overlap	13
The Infinite Polymer	17
CHAPTER 2	
The Hydrogen Chain	36
The Infinite Polyene	42
Polyethylene	56
The Carbon Chain	67
Beryllium	71
Lithium Fluoride Chains	76
Hydrogen Fluoride	84
CHAPTER 3	
A Perturbation Theory of Molecular Distortions	90
CHAPTER 4	
Perturbation Theory of Polymer Distortions	103
CHAPTER 5	
Final Discussion	121
APPENDIX 1	126
APPENDIX 2	132
REFERENCES	136

LIST OF FIGURES

FIGURE		PAGE
1	Schematic representation of the effect, on the band structure, of doubling the unit cell in the direct lattice.	37
2	The band structure of the optimum linear lattice of H ₂ molecules.	40
3	Diagram of the polyene unit cell.	44
4	The band structure of the optimum alternant polyene.	48
5	Diagram of the polyethylene molecule.	58
6	Diagram of the helix parameters.	8
7	The band structure of polyethylene.	59
8	Plot of E _{cell} against the helix parameter w for polyethylene.	62
9	Experimental results for the effect of increasing chain length on the first excitation energy of polyenes, cumulenes and polyynes.	68
10	Band structure of the optimum carbon chain.	72
11	The band gap of the beryllium chain as a function of the lattice constant.	74
12	The band structure of the beryllium chain.	75
13	The band structure of the lithium fluoride chain.	79
14	Diagram of the unit cell of the zig-zag hydrogen fluoride chain.	86
15	The band structure of the zig-zag hydrogen fluoride chain.	88
16	The P.T. and S.C.F. results for the variation in the energy of the methanol molecule with carbon-oxygen bond length.	99
17	P.T. and S.C.F. results for the variation of z component of the dipole moment of methanol with carbon-oxygen bond length.	100
18	A plot of the first-order energy versus the wave vector q for the lattice distortion in the hydrogen chain having $\underline{u}_1 = -\underline{u}_2 = (0,0,0.05 \text{ \AA})$.	117

LIST OF FIGURES (cont'd.)

FIGURE		PAGE
19	A plot of the first-order energy versus the wave vector q for the lattice distortion in the hydrogen chain having $\underline{u}_1 = \underline{u}_2 = (0,0,0.05 \text{ \AA})$.	119

LIST OF TABLES

TABLE		PAGE
1	A complete list of CNDO electron repulsion integrals for the polymer.	27
2	Relationships among the matrix elements in the basis of translational-symmetry functions.	31
3	Matrix elements of the Fock operator in the basis of translational-symmetry functions.	33
4	Density matrix elements within the origin unit cell of the optimum alternant polyene.	49
5	Comparison of density matrix elements for the symmetric and alternant polyenes.	50
6	The effect of truncation of lattice sums in the polyene calculation.	55
7	Density matrix elements for the optimum carbon chain.	70
8	Comparison of density matrices resulting from a calculation using truncated lattice sums with one using lattice sums evaluated by the Ewald transformation.	83
9	Comparison of P.T. and S.C.F. results for geometry variations in ethylene.	96
10	Comparison of P.T. and S.C.F. results for geometry variations in carbon dioxide.	98
11	Matrix elements of the Fock operator for the distorted polymer.	109
12	Comparison of S.C.F. and P.T. results for lattice distortions.	114
13	Comparison of displacement resulting from lattice waves of sine and cosine types.	115
14	Lattice sums for $k = 0.4$ and $k = 0.0125$ calculated by direct summation.	129
15	Recommended values of λ for various ranges of k and the value for the corresponding origin integral in k space.	129

LIST OF TABLES (cont'd.)

TABLE		PAGE
16	Phase modulated lattice sum calculated by Ewald's method using different values for the convergence parameter R.	131
17	Data demonstrating convergence with respect to N, the number of unit cells in the Born-Von Karman segment.	134
18	Data demonstrating convergence with respect to N, the number of unit cells included in the coulomb ^c lattice sum.	135

INTRODUCTION

In the last fifty years, chemistry and physics have unravelled many of the difficult problems relating to the structure of molecules^(1,2). The emphasis has naturally focused on small molecules where the principles which determine molecular structures are most easily seen. While small molecules are of considerable interest and importance it is clear that an increasing amount of effort will in the future be devoted to the study of macro-molecules. Giant molecules are the building blocks of which are made our bodies, our food, our clothes--even the ground on which we stand. The study of these molecules crosses the boundaries of many conventional disciplines and uses a wide variety of techniques. However, without exception, the understanding of polymers is based ultimately on the simple valence theory of molecules.

The most striking advance in the field of biophysics came when Pauling and Corey⁽³⁾, using experience gained in the study of small molecules, predicted and confirmed the α -helix structure of proteins. Watson and Crick⁽¹⁴⁾ using similar models succeeded in determining the double helix structure of D.N.A. Recently published is Max Perutz's⁽⁵⁾ beautiful study of the structure and function of the haemoglobin molecule, a milestone in the understanding of biological systems, which would have been impossible without the earlier experimental and theoretical work.

In the study of small molecules, the introduction of simple valence theories caused an advance in understanding and capability which would have seemed impossible even a few decades before. After this initial breakthrough, theory and experiment developed in parallel and the interplay between them has been very productive. While the study of large molecules has benefitted greatly from the advances in experimental methods, little progress has been made in

the development of a theory of macro-molecules. This is hardly surprising since these large molecules have two major drawbacks from a theoretical viewpoint, their size and their conformational freedom. The former means that computations will be long and difficult and the latter suggests that the simplifications which are possible, to a first approximation, in solid-state calculations cannot be used. Tackling the problems of polymer structure with conventional techniques is akin to cleaning the Stygian stables with a toy shovel.

The difficulties are not merely procedural; a considerable controversy is in progress over the applicability of time-independent quantum mechanics to large molecular systems⁽²⁵⁾. It is not clear whether or not quantum mechanics supplies an adequate description of such systems. Further problems exist relating to the interpretation of quantum mechanical results for such systems. The outcome of this debate is assumed in this work; this position is supported by the excellent correlation obtained between experimental results and quantum mechanical predictions in small molecule^(1,2,6,9,10) and solid-state studies^(2,7).

What is to be done? It is clear that the field of macro-molecules is so diverse that a range of methods can be employed. Simple polymers such as the synthetic stereo-regular ones and silica-type polymers can probably be handled by conventional methods. More complex polymers such as the peptide chains in biological systems will likely have to be dealt with in other ways. A study of simpler systems by conventional methods would be valuable in a number of ways. It would help to identify unusual characteristics of polymer systems or problems which are specific to such systems. A working theory for simple polymers would prove a valuable tool in calibrating non-conventional approaches to the problem; indeed, results such as the sensitivity of the

electronic energy bands to structural parameters might well provide an insight into the form of theory which should be used to handle the more general case.

Why use molecular orbital theory^(2,6)? M.O. theory was chosen because it represents the most commonly used method in the theory of small molecules, a method whose characteristics are well understood and whose usefulness has been proven. The study of a new area presents a range of problems in its own right without compounding the difficulties by using methods of uncertain value; interpretation is much easier when results which are due to approximations in the method can be distinguished from the results which are truly characteristic of the system. However, this method has a number of added limitations when applied to polymers; the first, the restriction to simple macro-molecules having a single building block or unit cell, is due to the need to reduce the calculation to a reasonable size; the second, which is the assumption of perfect translational symmetry, is necessary so that simplifying methods used in the theory of the solid state⁽⁷⁾ can be incorporated into the calculations. This regularity is found to a good approximation only in crystalline polymers. An approach to the problem of adapting the method to deal with structural irregularities forms the final part of this thesis.

The immediate object of this work then is to develop a molecular orbital theory of simple polymers, to test it, and to apply it to some simple systems. The characteristics of these systems will be studied and special problems relating to a theory of polymer structure identified and, in some cases, resolved.

For computational convenience and economy, an approximate form of the M.O. method, the Complete Neglect of Differential Overlap (CNDO)⁽⁸⁻¹⁰⁾ method, is used. The general features of this method are introduced and discussed in

Chapter One. A more complete treatment of this method and representative results obtained by the use of it are given in the books by Pople and Beveridge⁽⁹⁾ and by Daudel and Sandorfy⁽¹⁰⁾. This method which treats all valence electrons employs a number of parameters in the approximation of certain integrals while other integrals are neglected (see Chapter I). Selective approximation of the kind used in this method reduces the amount of calculation required while retaining many of the useful features of ab initio methods where all integrals are calculated directly. It represents a compromise between the Hückel^(6,9,10) method, where the Hamiltonian is almost completely parameterized, and ab initio^(2,6) methods; it couples the economy of the former to the explicit treatment of electron interaction in the latter.

Because of the conformational freedom of polymers, methods treating π electrons alone cannot be expected to give an adequate description even of their planar conjugated sections. This is best illustrated by reference to earlier calculations of the band structure of graphite; in spite of the strict planarity of the graphite sheets and the wide inter-sheet separation, it has been shown that significant σ - π overlap occurs⁽²⁶⁾. In polymers, where strict symmetry is rare, the separation of σ and π electrons is not generally a good approximation. Ab initio molecular orbitals, while having a certain mathematical elegance which semi-empirical methods do not, are exceedingly expensive and ultimately cannot be expected to provide more than a semi-quantitative description of electron distribution⁽²⁷⁾.

Semi-empirical wavefunctions are adequate for many purposes; because of the ease of calculation they may be best suited to the study of polymer systems, which involve large numbers of atoms and of conformational variables.

Attempts to formulate a theory of polymer structure are by no means a new phenomenon. As early as 1937, J. E. Lennard-Jones⁽¹¹⁾ discussed the behaviour of the π electrons in an infinite conjugated polyene. He employed the Huckel^(6,9,10) molecular orbital method to determine the ground state electronic configuration of the π -electron system. This particular polymer was the only one to be studied until quite recently because the only tractable method of dealing with large molecules available until ten years ago was not capable of dealing with the σ -electron framework of molecules. Lennard-Jones predicted that the alternation observed in open chain polyenes would decrease with increasing chain length until, in the case of the infinite polyene, it would disappear leaving a symmetrical structure (see Fig. 3). He further predicted a linear decrease with increasing chain length of the energy of the lowest electronic transition, until it too vanished. Coulson (1938)⁽¹²⁾, and Herzfeld and Sklar (1942)⁽¹³⁾ came to the same conclusion. Kuhn⁽¹⁴⁾, using the free electron method (F.E.M.) adapted from the study of metals, challenged this result. He suggested that the experimental data⁽¹⁵⁾, which show a finite limit for the first excitation energy, can only be explained by the persistence of bond alternation. The resulting controversy⁽¹⁵⁾, which is continued in Chapter 2, has outlived many of the protagonists. The first self-consistent field (S.C.F.) calculations, those of Ooshika (1957)⁽¹⁶⁾, were done on the same molecule. Extended Huckel theory, which can deal with σ electrons, was first applied to polyethylene only in 1968⁽¹⁷⁾. A complete formalism for the application of S.C.F. theory to polymers was derived in 1967⁽¹⁸⁾ and the first worked example of an ab initio calculation was published in 1969⁽¹⁹⁾. In the winter of 1970-71 three independent applications of CNDO/2 to the study of polymers⁽²⁰⁻²²⁾ were published, those by Morokuma⁽²⁰⁾, and by Fujita and

Imamura⁽²¹⁾ being essentially the formulation introduced by Ladik et al, and that by O'Shea and Santry⁽²²⁾ being an alternative but equivalent formulation. INDO and MINDO/2⁽⁹⁾ versions of the theory in the nearest neighbour approximation were published by Beveridge, Jano, and Ladik in 1972⁽²³⁾. This outline indicates the development of the theory. A considerable number of calculations have been reported at the various levels of approximation mentioned here (see for example references (11) to (24) and references cited therein).

The general molecular orbital method is briefly reviewed in the first chapter and the approximate method to be used is discussed in some detail. Following that, the formalism for the polymer calculations is developed in this approximation and the computational formulae are presented. Chapter 2 presents some representative samples of calculations on perfect polymers. In Chapter 3 the perturbation method required to deal with distortions is developed and its capabilities demonstrated by applying it to small-molecule calculations. Chapter 4 contains the theory for the distorted polymer, and preliminary results. A final summary and discussion is presented in Chapter 5.

CHAPTER 1

MOLECULAR ORBITAL THEORY

The molecular orbital form of the Hartree-Fock^(2,6) method to be used in the study of polymers is introduced here. This section outlines the general problem and the necessary approximations, as applied to small molecules.

A wavefunction, Ψ , for a system of interacting nuclei and electrons is found by solving the quantum mechanical form of the dynamical equation, the Schrodinger equation. Only stationary properties of such systems will be discussed here, and so the time-independent form of the equation may be used. It can be written

$$H\Psi = E\Psi \quad [1]$$

The operator⁽⁶⁾ H is the Hamiltonian or total energy operator, and E is the total energy of the system described by Ψ . Many of the terms in H are small relativistic corrections⁽²⁷⁾ which will be neglected here. The effective Hamiltonian then becomes ($r_{AB} = |r_A - r_B|$)

$$\begin{aligned}
 H &= -\sum_A \frac{\hbar^2}{2M_A} \nabla_A^2 - \sum_i \frac{\hbar^2}{2m} \nabla_i^2 - \sum_A \sum_i \frac{e^2 Z_A}{r_{iA}} + \sum_{A < B} \frac{e^2 Z_A Z_B}{R_{AB}} + \sum_{i < j} \frac{e^2}{r_{ij}} \\
 &= T_N + T_E + V_{EN} + V_{NN} + V_{EE}
 \end{aligned} \quad [2]$$

The terms in H are explained here:

$$T_N = -\sum_A \frac{\hbar^2}{2M_A} \nabla_A^2$$

is the quantum mechanical representation of the kinetic energy of the nuclei A of mass M_A ; the sum is over all nuclei, A .

$$T_E = -\sum_i \frac{\hbar^2}{2M} \nabla_i^2$$

is the kinetic energy of the electrons of mass M .

$$V_{EN} = -\sum_i \sum_A \frac{e^2 Z_A}{r_{iA}}$$

is the mutual electrostatic attraction of the electrons of charge $-e$ and the nuclei of charge eZ_A for one another; it is summed over all nuclei and all electrons.

$$V_{NN} = \sum_{A<B} \frac{e^2 Z_A Z_B}{R_{AB}}$$

is the electrostatic repulsion among the nuclei; it is summed over all pairs of nuclei.

$$V_{EE} = \sum_{i<j} \frac{e^2}{r_{ij}}$$

is the electron-electron repulsion; it is summed over all pairs of electrons.

In atomic units[†] H can be written as

$$\begin{aligned} H &= -\sum_A \frac{\nabla_A^2}{2M_A} - \sum_i \frac{\nabla_i^2}{2} - \sum_{A,i} \frac{Z_A}{r_{Ai}} + \sum_{AB} \frac{Z_A Z_B}{R_{AB}} + \sum_{i<j} \frac{1}{r_{ij}} \\ &= -\sum_A \frac{\nabla_A^2}{2M_A} - \sum_i H_i^C + \sum_{A,B} \frac{Z_A Z_B}{R_{AB}} + \sum_{i<j} \frac{1}{r_{ij}} \end{aligned} \quad [3]$$

H_i^C , defined by this equation, acts on coordinates of only one electron. The coordinates and momenta of all the particles are coupled by this equation which is generally insoluble.

The Born-Oppenheimer⁽²⁸⁾ approximation simplifies this equation by

[†]Atomic units are defined by

$$e^2/a_0 = 1; a_0 = 1; M = 1$$

where e , M are respectively the charge and mass of the electron. a_0 is the Bohr radius ($= 0.529167 \text{ \AA}$).

writing the wavefunction as a product of wavefunctions, one for the nuclei and one for the electrons

$$\Psi(\underline{r}, \underline{R}) = \psi_n(\underline{r}, R) \phi(\underline{R}) \quad [4]$$

By rewriting the Hamiltonian and neglecting some small cross terms, the equation for Ψ can be factored into two related equations

$$H_{EL} \psi_n(\underline{r}, R) = E_n(R) \psi_n(\underline{r}, R) = (T_E + V_{EN} + V_{EE} + V_{NN}) \psi_n(\underline{r}, R) \quad [5a]$$

$$[T_N + E_n(R)] \phi(R) = \epsilon \phi(R) \quad [5b]$$

The scalar R in the ψ_n implies a parametric dependence of ψ_n on the nuclear positions, while n stands for a complete set of electron quantum numbers. If the wavefunction is to describe a physical system it must be continuous, single-valued, and quadratically integrable; as a result of these boundary conditions the equation has a set of discrete solutions, ψ_n , with characteristic energies, E_n , corresponding to allowed electron distributions $\rho_n(\underline{r})$. $E_n(R)$ acts as a potential field in the equation [5b] determining the nuclear wavefunction $\phi(\underline{R})$. For molecules in which the ground state is well separated from the lowest excited state this is a good approximation, even in the restrictive "clamped nuclei" form which is most frequently used⁽²⁹⁾.

Equation [5a] determining $\psi_n(\underline{r}, R)$ is still insoluble and must be further simplified. This is done by writing the many-electron wavefunction as a product of one-electron wavefunctions. Electrons obey Fermi-Dirac statistics⁽³⁰⁾, and so the product used must be antisymmetric under the exchange of the coordinates of any two electrons. This is achieved as follows. Each electron is assigned to a spin orbital^(2,6) which describes the motion of the electron in space, and its spin characteristics. A spin orbital is given by

$$S_i(j) = \phi_i(j)w(j) \quad [6]$$

where $\phi_i(j)$ is a function of the space coordinates only, and $w(j)$ is a function of spin coordinates.

The systems to be discussed here are closed shells where each space orbital has either no electrons associated with it or else has two electrons associated with it, one with each of the two possible values of the electron spin variable. In this case, without loss of generality, $w(j)$ can be written

$$\hat{S}_z w(j) = \pm \frac{1}{2} w(j) \quad [7]$$

where \hat{S}_z is the operator measuring, in atomic units, the spin component along the z axis. For compactness the following notation can be introduced

$$\begin{aligned} \phi_i(j) &= \phi_i(j)w(+\frac{1}{2}) \\ \bar{\phi}_i(j) &= \phi_i(j)w(-\frac{1}{2}) \end{aligned} \quad [8]$$

The antisymmetrized wavefunction for an N electron system can now be written in the form of a Slater determinant⁽⁶⁾.

$$\psi_n = (N!)^{-1/2} |\phi_1(1) \bar{\phi}_1(2) \dots \phi_{N/2}(N-1) \bar{\phi}_{N/2}(N)| \quad [9]$$

The normalization factor $(N!)^{-1/2}$ arises from the condition that

$$\int \psi^* \psi d\tau = 1 \quad [10]$$

The integration factor $d\tau$ implies integration of all space and spin variables over all of configuration space⁽²⁷⁾.

This wavefunction can now be used to evaluate the electronic energy (assuming normalization)

$$\int \psi_n^* H_{EL} \psi_n d\tau = E_n(R) \quad [11]$$

$$E_n(R) = 2 \sum_i^m H_i^C + \sum_{i,j}^m (2J_{ij} - K_{ij}) + V_{NN} \quad m = N/2 \quad [12]$$

$$\left. \begin{aligned} H_i^C &= \int \phi_i^* (T_E + V_{EN}) \phi_i \, d\tau \\ J_{ij} &= \int \phi_i^*(1) \phi_i(1) |\underline{r}_1 - \underline{r}_2|^{-1} \phi_j^*(2) \phi_j(2) \, d\tau_1 d\tau_2 \\ K_{ij} &= \int \phi_i^*(1) \phi_j(1) |\underline{r}_1 - \underline{r}_2|^{-1} \phi_j^*(2) \phi_i(2) \, d\tau_1 d\tau_2 \end{aligned} \right\} [13]$$

The numerical factors arise from the expansion of the product $\psi_n^* \psi_n$ in terms of the orbitals ϕ_i , and the fact that each ϕ_i occurs twice, associated with different spin functions. J_{ij} , a coulomb integral, is the energy of interaction of the smoothed-out charge distributions $\phi_i^*(1)\phi_i(1)$ and $\phi_j^*(2)\phi_j(2)$ while K_{ij} , an exchange integral, represents the interaction of the overlap densities $\phi_i^*(1)\phi_j(1)$ and $\phi_j^*(2)\phi_i(2)$. K_{ij} is non-zero only between spin orbitals of parallel spin and is a correction for the over counting of repulsions between such electrons.

Orbital energies are given as

$$\epsilon_i = H_{ii} + \sum_j^m (2J_{ij} - K_{ij}) \quad [14]$$

and E_n may be expressed as

$$E_n(\underline{r}, R) = 2 \sum_i^m \epsilon_i - \sum_i^m \sum_j^m (2J_{ij} - K_{ij}) \quad [15]$$

Each orbital ϕ_i can be represented as a linear combination of atomic orbitals (L.C.A.O.), χ_μ ,

$$\phi_i = \sum_\mu C_{i\mu} \chi_\mu \quad [16]$$

where $C_{i\mu}$ is the coefficient of the function χ_μ in the expansion of orbital i . In principle, ϕ_i must be expanded in terms of a complete set⁽³¹⁾;

usually, however, to shorten the calculation a more limited set is used with a corresponding loss of accuracy⁽⁹⁾. The true Hartree-Fock equations have an infinite number of solutions; when the limited basis set is used the number of solutions which can be obtained is reduced to the dimension of the basis set. Choosing a basis set is one of the most difficult and contentious problems in molecular orbital calculations. In simple M.O. theories the most common, and indeed the best choice, is a valence basis set where each orbital in the valence shell of each atom involved is represented by a single Slater function of the appropriate symmetry. This set combines simplicity with balance and represents a good compromise among the various criteria which must be satisfied.

A variational method⁽³⁰⁾ devised by C. C. J. Roothaan^(6,32) can now be used to determine the optimum set of one-electron orbitals, ϕ_i . In this method, using the $C_{i\mu}$ as variational parameters, the energy of the system of electrons is required to be a minimum, subject to the constraint that the set of molecular orbitals be orthogonal and normalized. The resulting equations, Roothaan's equations, are, in matrix form,

$$\underline{F} \underline{C} = \underline{O} \underline{C} \underline{E} \quad [17]$$

\underline{F} is the matrix of the Fock operator, \hat{F} , which is defined by

$$\hat{F} = \hat{H}^C + \hat{G} \quad [18]$$

The matrix elements of \hat{F} are given by

$$\begin{aligned} F_{\mu\nu} &= \int \chi_{\mu}^*(1) \hat{F} \chi_{\nu}(1) d\tau \\ &= \int \chi_{\mu}^*(1) H^C \chi_{\nu}(1) d\tau_1 + \sum_j^{OC} C_{\sigma j}^* C_{\lambda j} \{ 2 \int \chi_{\mu}^*(1) \chi_{\nu}(1) r_{12}^{-1} \chi_{\sigma}^*(2) \chi_{\lambda}(2) d\tau_1 d\tau_2 \\ &\quad - \int \chi_{\mu}^*(1) \chi_{\lambda}(1) r_{12}^{-1} \chi_{\sigma}^*(2) \chi_{\nu}(2) d\tau_1 d\tau_2 \} \end{aligned} \quad [19]$$

$$O_{\mu\nu} = \int \chi_{\mu}^*(1) \chi_{\nu}(1) d\tau \quad [20]$$

is the overlap matrix and \underline{C} is the matrix of coefficients. \underline{E} , the matrix of Lagrange multipliers⁽³¹⁾ needed to implement the variational constraint, is taken to be diagonal; this is strictly valid only when the system of electrons is in a closed shell configuration⁽³³⁾.

This matrix equation, which can also be written as a set of equations

$$F C_i = C_i \epsilon_i \quad [21]$$

has a unique feature, in that the solution of a single operator equation yields all the one-electron orbitals. Using the notation

$$P_{\sigma\lambda} = 2 \sum_{\ell}^{oc} C_{\sigma\ell}^* C_{\lambda\ell} \quad [22]$$

$$M_{\mu\nu} = \int \chi_{\mu}^*(1) \hat{M} \chi_{\nu}(1) d\tau_1 \quad [23]$$

$$\langle \mu\nu | \sigma\lambda \rangle = \int \chi_{\mu}^*(1) \chi_{\nu}(1) r_{12}^{-1} \chi_{\sigma}^*(2) \chi_{\lambda}(2) d\tau_1 d\tau_2$$

the equation for $F_{\mu\nu}$ becomes

$$F_{\mu\nu} = H_{\mu\nu}^C + \sum_{\sigma\lambda} P_{\sigma\lambda} \{ \langle \mu\nu | \sigma\lambda \rangle - \frac{1}{2} \langle \mu\lambda | \sigma\nu \rangle \} \quad [24]$$

Complete Neglect of Differential Overlap⁽⁸⁻¹⁰⁾

This is an approximate form of Hartree-Fock theory in which the Roothaan equations are simplified by systematic approximation of the integrals involved. The modifications can be summarized as follows:

1. A minimal valence basis set is used. One Slater-type atomic orbital is used to represent each atomic orbital in the valence set of each atom in the molecule, e.g., one 1s function for each hydrogen atom, a 2s and 2p_{x,y,z} set for each atom, from Li to F, occurring in the basis.

2. The overlap matrix of the basis functions is replaced by a unit matrix. This is the zero differential overlap (Z.D.O.) approximation^(9,10)

$$\langle \mu | \nu \rangle = \delta_{\mu\nu} = \delta_{\mu\nu} \quad [25]$$

A distinction is made here between two sets of overlap integrals. The Z.D.O. requires that the overlap matrix be diagonal and this matrix is represented by $\underline{0}$ while the actual overlap matrix calculated from the basis functions is designated \underline{S} .

3. Two-electron integrals involving overlap distributions are neglected, thus

$$\langle \mu\nu | \sigma\lambda \rangle = \delta_{\mu\nu} \delta_{\sigma\lambda} \langle \mu\mu | \sigma\sigma \rangle \quad [26]$$

4. The remaining coulomb integrals are reduced to one value per atom pair.

$$\langle \mu\mu | \sigma\sigma \rangle = \gamma_{AB} \quad \chi_{\mu} \text{ on A, } \chi_{\sigma} \text{ on B} \quad [27]$$

The appropriate γ_{AB} 's are evaluated using the valence s orbitals of the atoms A and B.

5. Interaction integrals, involving the cores of other atoms, which depend on overlap distributions are neglected.

$$\langle \mu | \frac{1}{r_B} | \nu \rangle = \delta_{\mu\nu} V_{AB} \quad \chi_{\mu} \text{ on A} \quad [28]$$

6. The interaction integrals, V_{AB} , are approximated by

$$V_{AB} = -Z_B \gamma_{AB} \quad [29]$$

7. Off-diagonal core matrix elements are taken to be proportional to the corresponding calculated overlap integrals

$$H_{\mu\nu} = \beta_{AB}^0 S_{\mu\nu} \quad \chi_{\mu} \text{ on A, } \chi_{\nu} \text{ on B} \quad [30]$$

Diagonal core elements are approximated by

$$\langle \mu | -\frac{1}{2} \nabla^2 - \frac{Z_A}{r_{iA}} | \mu \rangle = U_{\mu\mu} \quad x_{\mu} \text{ on A} \quad [31]$$

$$U_{\mu\mu} = -\frac{1}{2} (I_{\mu} + A_{\mu}) - (Z_A - \frac{1}{2}) \gamma_{AA}$$

I_{μ} and A_{μ} are, respectively, the ionization potential and electron affinity of orbital μ ; these are determined from experimental results. The scaling factor β_{AB}^0 is given by

$$\beta_{AB}^0 = \frac{1}{2} (\beta_A^0 + \beta_B^0) \quad [32]$$

The set of β_A^0 , one for each atom type, is determined by calibrating the theory against detailed calculations on small molecules⁽⁸⁾. The values of all parameters used here are those given in the original paper on CNDO/2^(8c).

Incorporating these approximations, the Roothaan equations reduce to:

$$F_{\mu\mu} = -\frac{1}{2} (I_{\mu} + A_{\mu}) + [(P_{AA} - Z_A) - \frac{1}{2} (P_{\mu\mu} - 1)] \gamma_{AA} + \sum_{B \neq A} (P_{BB} - Z_B) \gamma_{AB} \quad [33]$$

$$F_{\mu\nu} = \beta_{AB}^0 S_{\mu\nu} - \frac{1}{2} P_{\mu\nu} \gamma_{AB} \quad [34]$$

$$H_{\mu\mu} = -\frac{1}{2} (I_{\mu} + A_{\mu}) - \sum_B Z_B \gamma_{AB} + \frac{1}{2} \gamma_{AA} \quad [35]$$

$$H_{\mu\nu} = \beta_{AB}^0 S_{\mu\nu} \quad [36]$$

P_{AA} is the total charge density on atom A and is given by

$$P_{AA} = \sum_{\mu}^{\text{on A}} P_{\mu\mu} \quad [37]$$

The diagonal elements of the density matrix represent electron densities because the use of the Z.D.O. approximation makes the matrix of coefficients,

\underline{C} , unitary. The matrix equation now becomes

$$\underline{F} \underline{C} = \underline{O} \underline{C} \underline{E} = \underline{C} \underline{E} \quad [38]$$

or

$$\underline{F} \underline{C}_i = \epsilon_i \underline{C}_i \quad [39]$$

where \underline{C}_i is vector of coefficients of the expansion of ϕ_i in the basis χ_μ .

The choice of the various approximations used here was based on the criterion that the method should retain the invariance properties of the full Hartree-Fock theory, particularly invariance of the solutions with respect to rotations of the axis system. The neglect of all integrals depending on overlap distributions is internally consistent. Neglect of the quantities $(Z_B \gamma_{AB} - V_{AB})$, known as the penetration integrals, is necessary to improve predicted bond lengths in a wide range of compounds⁽⁹⁾.

One useful feature of CNDO is that the energy can be broken down into atomic and diatomic contributions.

$$\begin{aligned} W_{\text{TOTAL}} &= \frac{1}{2} \sum_{\mu\nu}^{\text{basis}} P_{\mu\nu} (H_{\mu\nu} + E_{\mu\nu}) + \sum_{A<B} Z_A Z_B R_{AB}^{-1} \\ &= \sum_A E_A + \sum_{A<B} E_{AB} \end{aligned} \quad [40]$$

$$E_A = \sum_{\mu}^A U_{\mu\mu} + \frac{1}{2} \sum_{\mu}^A \sum_{\nu}^A (P_{\mu\mu} P_{\nu\nu} - \frac{1}{2} P_{\mu\nu}^2) \gamma_{AA} \quad [41]$$

$$\begin{aligned} E_{AB} &= \sum_{\mu}^A \sum_{\nu}^B (2P_{\mu\nu} H_{\mu\nu} - \frac{1}{2} P_{\mu\nu}^2 \gamma_{AB}) + Z_A Z_B R_{AB}^{-1} \\ &\quad - (P_A Z_B + P_B Z_A) \gamma_{AB} + P_A P_B \gamma_{AB} \end{aligned} \quad [42]$$

The method provides a reasonable account of the ground states of closed-shell and many open-shell molecules. Geometry predictions are

usually close to the observed values. This is true even for such species as the methylene radical, $\text{CH}_2^{(9)}$. CNDO/2 predicted it to be bent while the then current experimental evidence suggested a linear structure. Recent experimental evidence has shown it to be bent. The method is best suited to this kind of calculation, that of finding optimum geometries. Results tabulated by Pople and Beveridge⁽⁹⁾ in their book demonstrate the success of the method in this area.

The gross features of the true charge densities are well reproduced by CNDO. This can be seen by comparison of the charge distribution with that from more detailed calculations, and by comparison of properties calculated from the charge density with the corresponding experimental values. The range of applications of CNDO is remarkable, as is the agreement with experiment achieved by use of this very simple method. A notable exception is the case of force constants, which are reproduced only to an order of magnitude. Virtual orbitals are almost always correctly ordered, though the spacings between levels are not usually quantitatively correct.

Although CNDO does not give a rigorous upper bound to the energy of a system (because of the use of empirical parameters), the quality of the results demonstrated in a wide range of applications is such that a high degree of reliability may be placed on its predictions.

The Infinite Polymer

Equation [5a] determining the electronic wavefunction, ψ_n , of a state n , of a system can be discussed in terms of group theory⁽³⁴⁾. The non-isotropic operator V_n can be shown to have the full symmetry of the nuclear structure. Solutions, ψ_n , also have this symmetry. ψ_n is a product of one-electron

functions and each of these in turn must belong to one of a limited number of symmetry types if ψ_n is to have the correct overall symmetry. The nature and number of independent symmetry types are determined by group theory.

Exceptions to the symmetry rule on ψ_n are known to occur⁽³⁵⁾ in special circumstances where the simple Hamiltonian used here is inadequate. The question of the stability of Hartree-Fock solutions is the subject of current research⁽³⁶⁾.

Each of the one-electron functions is a linear combination of basis functions. Clearly, only linear combinations having the appropriate symmetry can contribute to a given one-electron solution. By converting the original basis functions to symmetrized combinations before beginning the calculation, only those of the correct symmetry need be considered when a particular solution is sought. The potential V_n , however, includes contributions from all occupied orbitals (equation [5a]) and, therefore, from many different symmetry types. In this indirect way the orbitals of different symmetry are coupled.

A perfect crystal is infinite in extent and consists of clusters of atoms bearing a fixed relationship to each other and to points in space defined by the vectors⁽³⁷⁾

$$\underline{R}_p = n_1 \underline{a}_1 + n_2 \underline{a}_2 + n_3 \underline{a}_3 \quad [43]$$

The n_i are integers and the basic vectors, \underline{a}_i , are called the primitive translations of the lattice, or set of points so defined. Depending on whether the number of linearly independent \underline{a}_i 's is one, two or three, the structure described is a polymer, surface or solid. An operation which converts a structure into an identical structure, differing at most by the artificial numbering of the atoms, is called a symmetry operation. The set

of all such operations for a crystal is called a space group and can be shown to conform to the algebra of groups⁽³⁴⁾. Such a space group has an invariant subgroup which consists of all lattice translations as defined by Equation [43]. The different symmetry types, the irreducible representations, of an invariant subgroup can be converted into those of the full space group⁽³⁸⁾. For present purposes the translational subgroup is usually adequate and it is on this subgroup that the discussion will be centred.

Let the set $\{T_n\}$ be translation operators defined in a linear lattice with basic vector \underline{a} by

$$T_n \phi_i(\underline{r}) = \phi_i(\underline{r} + n\underline{a}) \quad [44]$$

where $\phi_i(\underline{r})$ is a one-electron solution of the equation

$$H\phi_i(\underline{r}) = \left[-\frac{\hbar^2}{2m} \nabla^2 + V(\underline{r})\right] \phi_i(\underline{r}) = E_i \phi_i(\underline{r}) \quad [45]$$

The effect of two translations is independent of the order in which they are performed.

$$T_n T_m \phi_i(\underline{r}) = T_m T_n \phi_i(\underline{r}) = \phi_i(\underline{r} + n\underline{a} + m\underline{a}) \quad [46]$$

This is equivalent to saying the operators T_n commute. Similarly, T_n and H commute because $V(\underline{r})$ has the symmetry of the lattice and satisfies the equation

$$V(\underline{r}) = V(\underline{r} + m\underline{a}) \quad [47]$$

For any integer m , consequently, the subgroup $\{T_n\}$ and H can have simultaneous eigen functions, that is, a set $\{\phi_i(\underline{r})\}$ can be found to satisfy

$$(H - E_i) \phi_i(\underline{r}) = 0 \quad [48]$$

$$(T_n - t_{ni}) \phi_i(\underline{r}) = 0 \quad [49]$$

Since $\phi_i(\underline{r})$ must remain normalized, T_n must be unitary⁽³⁴⁾; therefore

$$|t_{ni}|^2 = 1 . \quad [50]$$

T_n is not Hermitian; therefore, its eigenvalues are complex.

In an infinite lattice, the translation group has an infinite number of operations and symmetry types. Difficulties arising from this can be circumvented by an artifact introduced by Born and von Karman⁽³⁹⁾. The full crystal is divided into segments, each consisting of an integral number of unit cells. By using one such segment as a model crystal, that is, by requiring that the wavefunctions match at the segment boundaries and that they be normalized within the segment, the problem is reduced to one of finite dimensions. The order of the translation group, which is isomorphic to a cyclic group of the same order, is equal to the number of cells in the segment^(2,34). Problems concerning normalization and counting of states are also solved by use of this approximation.

In this model translation by a full segment of N unit cells is equivalent to a zero translation; hence

$$t_N = (t_1)^N = 1 \quad [51]$$

A general solution of this equation is

$$\left. \begin{aligned} t_n &= e^{2\pi i(m/N)n} & 0 \leq m, n \leq N-1 \\ &= e^{2\pi i k n} & 0 \leq k \leq \frac{N-1}{N} \end{aligned} \right\} \quad [52]$$

$$i = \sqrt{-1}$$

The quantity k , called the wave vector, is the label of a translational symmetry type. Restriction of n to the range 0 to $N-1$ merely reflects the reduction of the crystal to a finite segment. k is restricted to the range

of discrete values of the form m/N , where m is less than N . The phase waves characterized by a k value have a physical significance only at the nuclear positions. Waves, characterized by a wave vector, k' , corresponding to an m value outside this range, will have further oscillations between nuclei, but the values of the wave at the nuclear positions will be the same as a wave corresponding to one of this set of k 's. The k to which k' is equivalent is given by

$$k = m/N \qquad m' = m + jN; j \text{ is an integer} \qquad [53]$$

because $e^{2\pi i(m'/N)r} = e^{2\pi i(m/N)r} e^{2\pi i(jN/N)r} = e^{2\pi i(m/N)r}$.

All k values of this form can be reduced in this way to the set defined above, usually called the first Brillouin zone.⁽⁷⁾ When N becomes infinite, k becomes continuous and the first Brillouin zone is the range of k values from 0 to 1.

Use of the Born-von Karman boundary conditions is equivalent to sampling k space (reciprocal space) at a discrete set of points.⁽⁴⁰⁾ It is important, therefore, to ensure that the set is sufficiently dense to represent properly the behaviour of the energy in reciprocal space. This is achieved by choosing N large enough to ensure that a further increase in N does not give rise to a change in the calculated results.

Because of the way in which wave vectors are equivalent, the range of values chosen is somewhat arbitrary. The convention used here is that N is chosen to be odd and the range of k values is

$$-\frac{N-1}{2N} \leq k \leq \frac{N-1}{2N} \qquad [54]$$

Let the set $\{\chi_{\mu}(\underline{r} - \underline{R}_{\mu})\}$ be the basis functions in the lattice. μ is an atomic orbital label (s , p_x , etc.) and \underline{R}_{μ} the position vector of the nucleus on which it is centred. \underline{R}_{μ} is defined with respect to some origin

chosen in the lattice.

$$\underline{R}_\mu = \underline{R} + \underline{r}_\mu = \underline{ra} + \underline{r}_\mu \quad [55a]$$

\underline{R} is a vector connecting the origin to an equivalent point in another unit cell, the r^{th} one, and \underline{r}_μ is the position vector of the appropriate nucleus within the unit cell.

Bloch's method⁽³⁴⁾ for constructing symmetry functions can be used to transform this basis set to symmetrized combinations having the translational symmetry of the lattice. Thus,

$$\eta_\mu(k) = \sqrt{\frac{1}{N}} \sum_{\underline{R}} e^{2\pi i k \underline{R}} \chi_\mu(\underline{r} - \underline{R}_\mu) \quad [55b]$$

There are N such complex functions corresponding to the N values of k . Assuming the basis functions to be real, an alternative definition of a symmetrized set consisting of real functions is given by (∂k is defined below)

$$\left. \begin{aligned} \phi_\mu(k) &= \sqrt{\frac{2-\delta k}{N}} \sum_S \chi_\mu^S \cos 2\pi k S = (2)^{-1/2} [\eta_\mu(k) + \eta_\mu(-k)] \\ \psi_\mu(k) &= \sqrt{\frac{2-\delta k}{N}} \sum_S \chi_\mu^S \sin 2\pi k S = -i(2^{-1/2}) [\eta_\mu(k) - \eta_\mu(-k)] \end{aligned} \right\} \quad [56]$$

Here the sum is over all unit cells in the Born-von Karman segment

$$\chi_\mu^S = \chi_\mu(\underline{r} - \underline{S}_\mu) = \chi_\mu(\underline{r} - \underline{sa} - \underline{r}_\mu) \quad [57]$$

a is the unit-cell length or lattice constant and \underline{a} is a vector of magnitude a parallel to the translation axis of the polymer. There are $\frac{N+1}{2}$ cosine functions, one for each of the k values; there are $\frac{N-1}{2}$ sine functions, since $k=0$ is excluded. These functions are not individually eigen functions of the translation operators. Translational symmetry couples the two functions

belonging to any non-zero k value as follows:

$$\begin{aligned} T_n \phi_\mu(k) &= \cos n\pi k \phi_\mu(k) - \sin n\pi k \psi_\mu(k) \\ T_n \psi_\mu(k) &= \sin n\pi k \phi_\mu(k) + \cos n\pi k \psi_\mu(k) \end{aligned} \quad [58]$$

Matrix elements over this new basis set are readily evaluated. The procedure necessary to do this demonstrates that totally symmetric one-electron operators cannot have matrix elements between basis functions having different k values. Examples of such operators include those essential to the theory, namely the overlap, core-Hamiltonian, and Fock operators. Although a one-electron operator, the Fock operator is a sum of two-electron operators so that it is necessary to evaluate matrix elements involving such operators. A limited number of examples are worked here and a list of all necessary two electron matrix elements is given in Table 1.

A result, essential to the procedure, is given by the well-known mathematical theorem^(2,34)

$$\begin{aligned} \sum_P \cos 2\pi k p &= N \delta k \\ \sum_P \sin 2\pi k p &= 0 \end{aligned} \quad [59]$$

$$\begin{aligned} \delta k &= 1 && \text{if } k \text{ is an integer or zero;} \\ &= 0 && \text{if } k \text{ is not an integer.} \end{aligned} \quad [60]$$

The sum is made over all unit cells in the lattice used to define the set of k values. δk will be called the lattice delta function. It derives from the Dirac delta function⁽³¹⁾, differing from it only in the fact that it is satisfied by any integer value of the argument. The theorem will be referred to as the lattice theorem.

Consider the matrix element for the one-electron operator H between Bloch functions $\phi_\mu(k_1)$ and $\phi_\nu(k_2)$ when neither k_1 nor k_2 is zero.

$$\langle \phi_\mu(k_1) | H | \phi_\nu(k_2) \rangle = w \sum_{\mathbf{r}} \sum_{\mathbf{s}} \cos 2\pi k_1 \mathbf{r} \cos 2\pi k_2 \mathbf{s} H_{\mu\nu}(\mathbf{r}, \mathbf{s}) \quad [61]$$

$$H_{\mu\nu}(\mathbf{r}, \mathbf{s}) = \langle \chi_\mu^{\mathbf{r}} | H | \chi_\nu^{\mathbf{s}} \rangle \quad [62]$$

$$w = \sqrt{2-\delta k_1} \sqrt{2-\delta k_2} / N \quad [63]$$

When $\mathbf{p} = \mathbf{s} - \mathbf{r}$, $H_{\mu\nu}(\mathbf{r}, \mathbf{s})$ can be written as $H_{\mu\nu}(\mathbf{p})$ because in a perfect lattice the integral depends only on the separation between the cells \mathbf{r} , \mathbf{s} and not on their absolute positions. A further convention is introduced here: in the evaluation of the matrix element over single site functions $\chi_{\mathbf{r}}$ is assumed to be the origin unit cell containing χ_μ . The right hand side of the equation can now be written:

$$\sum_{\mathbf{r}} \sum_{\mathbf{p}} \cos 2\pi k_1 \mathbf{r} \cos 2\pi k_2 (\mathbf{p} + \mathbf{r}) H_{\mu\nu}(\mathbf{p}) \quad [64]$$

$$= \frac{1}{2} \sum_{\mathbf{r}} \sum_{\mathbf{p}} \{ \cos 2\pi k_2 \mathbf{p} [\cos 2\pi (k_1 + k_2) \mathbf{r} + \cos 2\pi (k_2 - k_1) \mathbf{r}] \\ - \sin 2\pi k_2 \mathbf{p} [\sin 2\pi (k_1 + k_2) \mathbf{r} + \sin 2\pi (k_2 - k_1) \mathbf{r}] \} H_{\mu\nu}(\mathbf{p}) \quad [65]$$

Using the lattice theorem, this becomes

$$= \frac{N}{2} \sum_{\mathbf{p}} \cos 2\pi k_2 \mathbf{p} [\partial(k_1 + k_2) + \partial(k_2 - k_1)] H_{\mu\nu}(\mathbf{p}) \quad [66]$$

By the definition of the range of k values (equations [54] and [56]) and that of ∂k , $\partial(k_1 + k_2)$ can never be satisfied; hence

$$\langle \phi_\mu(k_1) | H | \phi_\nu(k_2) \rangle = w \frac{\partial(k_2 - k_1)N}{2} \sum_{\mathbf{p}} \cos 2\pi k_2 \mathbf{p} H_{\mu\nu}(\mathbf{p}) \quad [67] \\ = w \frac{\partial_{12}N}{2} \sum_{\mathbf{p}} \cos 2\pi k_2 \mathbf{p} H_{\mu\nu}(\mathbf{p}) \quad \partial_{12} = \partial(k_2 - k_1)$$

$$= \partial_{12} \sum_p \cos 2\pi k_2 p H_{\mu\nu}(p) \quad [68]$$

This result has two important consequences. First, the delta function establishes that the overlap and Fock matrices are reduced to block diagonal form in this basis set. Matrix elements can only occur between functions having the same k value; by arranging the basis set so that all functions of a particular k occur together, the full matrix is reduced to a set of smaller blocks. If n is the number of basis functions in a unit cell and there are N unit cells in the Born-von Karman unit, the full matrix is of dimension $(nN) \times (nN)$. When reduced, it becomes one $n \times n$ block ($k=0$) and $\frac{N-1}{2N}$ blocks of dimension $2n \times 2n$ (all non-zero k values). Second, the matrix elements may be represented in terms of lattice sums involving a single summation. In the CNDO/2 approximation only four types of lattice sum occur and these are defined below.

Using this result the normalization of the basis set in the Born-von Karman unit can be demonstrated. In CNDO/2 the overlap $O_{\mu\nu}(p)$ between atomic basis functions χ_μ, χ_ν p unit cells apart is given by

$$O_{\mu\nu}(p) = \delta_{\mu,\nu} \delta_{p,0} + \delta_{\mu\nu} \delta_{p0} \quad [69]$$

therefore,

$$\langle \phi_\mu(k_1) | \phi_\nu(k_2) \rangle = \delta_{1,2} \delta_{\mu,\nu} + \delta_{12} \delta_{\mu\nu} \quad [70]$$

Another convention must be introduced to simplify the notation. When writing matrix elements μ_1 signifies $\phi_\mu(k_1)$ while $\bar{\nu}_2$ signifies $\psi_\nu(k_2)$; thus for example

$$\langle \mu_1 \bar{\nu}_2 | \nu_3 \nu_4 \rangle = \langle \phi_\mu(k_1) \psi_\nu(k_2) | r_{12}^{-1} | \phi_\nu(k_3) \phi_\nu(k_4) \rangle \quad [71]$$

This notation is used throughout the following discussion.

CNDO uses the approximation $\mu \neq \nu$

$$H_{\mu\nu}^C(p) = \beta_{AB} S_{\mu\nu}(p) = \beta_{AB} \langle \chi_\mu(0) | \chi_\nu(p) \rangle \quad [72]$$

S is used here to represent the true overlap integral while O is the Z.D.O. value occurring in the theory (see equation [25] and accompanying note).

Lattice integrals for the operator H^C can be written

$$\begin{aligned} R_{\mu\nu}(k) &= \beta_{AB} \sum_p \cos 2\pi kp S_{\mu\nu}(p) \\ Q_{\mu\nu}(k) &= \beta_{AB} \sum_p \sin 2\pi kp S_{\mu\nu}(p) \end{aligned} \quad [73]$$

Diagonal matrix elements such as $H_{\mu\mu}^C(k)$ require special attention since $H_{\mu\mu}^C(p=0)$ is approximated by $U_{\mu\mu}$ (equation [35]). The term in the lattice sum for $H_{\mu\mu}^C(k)$ corresponding to $H_{\mu\mu}^C(p=0)$ is omitted and the appropriate $U_{\mu\mu}$ entered instead. $R_{\mu\mu}(k)$ is defined accordingly

$$R_{\mu\mu}(k) = \beta_A^O \sum_{p=0} \cos 2\pi kp S_{\mu\nu}(p) \quad [74]$$

Matrix elements $S_{\mu\nu}(p)$ go to zero rapidly as p increases; hence the lattice sums are strongly convergent.

The matrix elements of the corresponding two electron operators are expanded in the same way. By using the CNDO approximations for coulomb and exchange integrals it can be shown that only a very limited number of two electron integrals are non-zero in this basis. Further, since the density matrix \underline{P} is also block diagonal in this basis, not all the surviving integrals need be evaluated. A complete list of those necessary, together with their representations in terms of lattice sums is given in Table 1. Again only two kinds of lattice sum are necessary to represent all the requisite two-electron integrals. They are

TABLE 1

A complete list of CNDO electron repulsion integrals
for the polymer are given below:

Type 1: Coulomb in character:

$$\langle \mu_1^2 | v_2^2 \rangle = N^{-1} [\Gamma_{AB}(0) + \frac{1}{2} \omega \Gamma_{AB}(2k_1)],$$

$$\langle \mu_1^2 | \bar{v}_2^2 \rangle = N^{-1} [\Gamma_{AB}(0) - \frac{1}{2} \omega \Gamma_{AB}(2k_1)],$$

$$\langle \bar{\mu}_1^2 | \bar{v}_2^2 \rangle = N^{-1} [\Gamma_{AB}(0) + \frac{1}{2} \omega \Gamma_{AB}(2k_1)].$$

Type 2: Essentially exchange in character:

$$\langle \mu_1 \bar{\mu}_1 | v_2 v_2 \rangle = -(\omega/2N) \Delta_{AB}(2k_1),$$

$$\langle \mu_1 \bar{\mu}_1 | v_2 \bar{v}_2 \rangle = (\delta_{12}/2N) \Gamma_{AB}(2k_1),$$

$$\langle \mu_1 \bar{\mu}_1 | \bar{v}_2 \bar{v}_2 \rangle = -(\omega/2N) \Delta_{AB}(2k_1).$$

Type 3: Exchange in character:

$$\langle \mu_1 \mu_2 | v_1 v_2 \rangle = (2N)^{-1} [\Gamma_{AB}(k_1+k_2) + \Gamma_{AB}(k_2-k_1) + \omega \Gamma_{AB}(0)],$$

$$\langle \mu_1 \bar{\mu}_2 | v_1 v_2 \rangle = -(2N)^{-1} [\Delta_{AB}(k_1+k_2) + \Delta_{AB}(k_2-k_1)],$$

$$\langle \mu_1 \bar{\mu}_2 | \bar{v}_1 v_2 \rangle = (2N)^{-1} [\Gamma_{AB}(k_1+k_2) - \Gamma_{AB}(k_2-k_1) + \omega \Gamma_{AB}(0)],$$

$$\langle \mu_1 \bar{\mu}_2 | v_1 \bar{v}_2 \rangle = (2N)^{-1} [\Gamma_{AB}(k_1+k_2) + \Gamma_{AB}(k_2-k_1) - \omega \Gamma_{AB}(0)],$$

$$\langle \bar{\mu}_1 \bar{\mu}_2 | \bar{v}_1 \bar{v}_2 \rangle = (2N)^{-1} [\Gamma_{AB}(k_1+k_2) + \Gamma_{AB}(k_2-k_1) + \omega \Gamma_{AB}(0)],$$

$$\langle \bar{\mu}_1 \mu_2 | \bar{v}_1 \bar{v}_2 \rangle = (2N)^{-1} [\Delta_{AB}(k_1+k_2) + \Delta_{AB}(k_2-k_1)],$$

$$\langle \mu_1 \mu_2 | \bar{v}_1 \bar{v}_2 \rangle = -(2N)^{-1} [\Gamma_{AB}(k_1+k_2) - \Gamma_{AB}(k_2-k_1) - \omega \Gamma_{AB}(0)],$$

where $\mu_1 = \phi_{\mu}(k_1)$, $\bar{\mu}_1 = \psi_{\mu}(k_1)$, $\delta_{12} = \delta_{k_1 k_2}$, and $\omega = [1 - \delta(k_1)] \delta_{12}$. μ is centered on atom A at the origin and v on atom type B which is summed over the lattice. Lattice sums involving sine functions vanish when the appropriate $k = 0$.

$$\Gamma_{AB}(k) = \sum_p \cos 2\pi k \cdot q \cdot \gamma_{AB}(p) \quad [75]$$

$$\Delta_{AB}(k) = \sum_p \sin 2\pi k \cdot q \cdot \gamma_{AB}(p)$$

$\gamma_{AB}(q)$ is the coulomb integral between atom A in the origin unit cell and atom B, p unit cells away. The summations extend over the whole lattice including the origin cell. For purposes of calculation they are truncated at some point which is chosen to ensure convergence.

Coulomb lattice sums of this kind illustrate the advantages and difficulties of this formulation of the theory. Their compactness and the relatively small number necessary simplify the calculations immensely. On the other hand, the convergence problems inherent in this formalism are most strikingly demonstrated by these sums. Sine and cosine coulomb lattice sums for non-zero k are conditionally convergent; they are alternating series of monotonically decreasing terms. Cosine coulomb sums are divergent for k = 0. The coulomb integrals over single site functions, $\langle x_{\mu}^r x_{\mu}^r | r_{12}^{-1} | x_{\nu}^s x_{\nu}^s \rangle$, behave like $|\underline{R}_{\mu} - \underline{S}_{\nu}|^{-1}$ when s-r is large. At this range $|\underline{R}_{\mu} - \underline{S}_{\nu}|$ can be approximated by $a^{-1}|s-r|^{-1}$, hence

$$\begin{aligned} \Gamma_{AB}(0) &= a^{-1} \sum_s^{\text{lattice}} |s-r|^{-1} - f_{AB} \\ &= a^{-1} \sum_{n=-\infty}^{\infty} \frac{1}{n} - f_{AB} = \infty \end{aligned} \quad [76]$$

f_{AB} is a short-range correction for the difference between $\gamma_{AB}(r,s)$ and $a^{-1}|s-r|^{-1}$.

Although the k=0 lattice sums are divergent the total energy should be convergent. The electron-electron repulsion terms and the nuclear-nuclear repulsion terms are balanced by the electron-nuclear attraction terms.

All of these terms contain singularities but their sum should be convergent^(40,41). The expression for the total energy illustrates this point. Let θ_A be the total electron charge on atom A and Z_A the nuclear charge. Long range contributions to E, E_{LR} , can be evaluated by omitting from the energy summation the terms arising from overlap and exchange effects and all coulomb terms arising from cells less than some arbitrary distance apart, say m cells; this last omission is indicated by primed summations.

$$\begin{aligned}
 E_{LR} &= \sum_A \sum'_B \theta_A \theta_B R_{AB}^{-1} + \sum_A \sum'_B Z_A Z_B R_{AB}^{-1} - \sum_A \sum'_B (\theta_A Z_B + Z_A \theta_B) R_{AB}^{-1} \\
 &= \sum_A \sum'_B (\theta_A - Z_A) (\theta_B - Z_B) R_{AB}^{-1} \\
 &= \sum_A \sum'_B \sum_{\text{cell lattice}} \sum'_r \sum'_s (\theta_A - Z_A) (\theta_B - Z_B) R_{AB}^{-1}(r,s) \quad [77]
 \end{aligned}$$

Because each unit cell must be neutral

$$\sum_A^{\text{cell}} (\theta_A - Z_A) = 0 \quad [78]$$

At long range, small separations within the unit cell become negligible and for suitably large choice of m, E_{LR} becomes zero.

A very elegant method designed to utilize this fact was developed by P. P. Ewald⁽⁴²⁾. It has been used to evaluate crystal energies by separating the lattice contributions into a convergent local field and a set of divergent but cancelling terms arising from the long-range field. A modification of this method to deal with the unusual characteristics associated with one dimensional periodicity is described in Appendix 1. Results obtained by use of the method are presented in the section dealing with convergence. The excellent agreement between the results obtained in

this way and those obtained by use of suitably truncated lattice sums justifies the use of the latter. Appendix 2 contains tabulated convergence data.

Final Formulae and Computational Details

Using the basis functions of equation [54], Roothaan's equations take the form

$$F(k) \theta(k) = \theta(k) E(k) \quad [79]$$

$$F(k) = G(k) + H(k) \quad [80]$$

where F , H^c , G have the usual meanings, $\theta(k)$ is the matrix of one-electron solutions and $E(k)$ the matrix of corresponding eigenvalues.

The form of $H^c(k)$ has already been discussed. Elements of $G(k)$ can be evaluated from the general relationship

$$G_{\mu\nu} = \sum_{\ell}^{oc} \sum_{\sigma,\lambda} C_{\sigma\ell}^* C_{\lambda\ell} \{2\langle\mu\nu|\sigma\lambda\rangle - \langle\mu\lambda|\sigma\nu\rangle\}$$

when $\mu \neq \nu$

$$G_{\mu\nu}(k_1) = -\frac{N}{2} \sum_{k_2} \{P_{\mu\nu}(k_2) \langle\mu_1\mu_2|\nu_2\nu_1\rangle + P_{\mu\bar{\nu}}(k_2) \langle\mu_1\mu_2|\bar{\nu}_2\nu_1\rangle \\ + P_{\bar{\mu}\nu}(k_2) \langle\mu_1\bar{\mu}_2|\nu_2\nu_1\rangle + P_{\bar{\mu}\bar{\nu}}(k_2) \langle\mu_1\bar{\mu}_2|\bar{\nu}_2\nu_1\rangle\} \quad [81]$$

This derivation employs a number of relationships (Table 2) involving the elements of the reciprocal space density matrix, $P_{\mu\nu}(k)$, which are defined by

$$P_{\mu\nu}(k) = \frac{2}{N} \sum_{\ell}^{oc} C_{\mu\ell}(k) C_{\nu\ell}(k) \quad [82]$$

$$P_{\mu\bar{\nu}}(k) = \frac{2}{N} \sum_{\ell}^{oc} C_{\mu\ell}(k) C_{\bar{\nu}\ell}(k)$$

Using the reduction formulae for the integrals (Table 1) and cancelling terms where possible, $G_{\mu\nu}(k_1)$ may be written ($\mu \neq \nu$)

TABLE 2

Relationships among the Matrix Elements in the Basis
Translational-Symmetry Functions

$k = 0$

$$M_{\mu\nu}(k=0) = M_{\nu\mu}(k=0)$$

$$M_{\mu\nu}(k=0) = M_{\nu\mu}(k=0) = M_{\mu\nu}(k=0) = M_{\nu\mu}(k=0) = 0$$

$k \neq 0$

$$M_{\mu\nu}(k) = M_{\nu\mu}(k) = M_{\mu\nu}(k) = M_{\nu\mu}(k)$$

$$M_{\mu\nu}(k) = M_{\nu\mu}(k) = -M_{\mu\nu}(k) = -M_{\nu\mu}(k)$$

These relationships hold for the symmetric operators \hat{H}^c , \hat{G} , \hat{F} , \hat{P} , defined in the text and for the overlap operator. They are valid for \hat{G} , \hat{F} and \hat{P} only when the system under consideration is a closed shell.

$$G_{\mu\nu}(k_1) = -\frac{1}{4} \sum_k [P_{\mu\nu}(k_2) + P_{\mu\nu}^-(k_2)] [\Gamma_{AB}(k_1+k_2) + \Gamma_{AB}(k_2-k_1)] \\ + [P_{\mu\nu}^-(k_2) - P_{\mu\nu}(k_2)] [\Delta_{AB}(k_1+k_2) + \Delta_{AB}(k_2-k_1)] \quad [83]$$

Similar expressions may be found for all necessary matrix elements and the final formulae for elements of $F(k)$ are given in Table 3.

The real space density matrix may be written as

$$\rho_{\mu\nu}(q) = \sum_k [P_{\mu\nu}(k) \cos 2\pi kq + P_{\mu\nu}^-(k) \sin 2\pi kq] [2 - \delta(k)] \quad [84]$$

This is simply the Fourier transform^(7,31) of the density matrix in reciprocal, or k , space. An alternative formulation of the matrix elements of $F(k)$ is given by the Fourier series

$$F_{\mu\nu}(k) = \sum_p \cos 2\pi kp F_{\mu\nu}(p) \quad [85]$$

When a converged solution of the standard formalism has been found, the eigenvalues and eigenvectors at points of special interest in k space not included in the original set can be found by first evaluating the appropriate $F(k)$ matrices in this way.

The electronic energy per unit cell is given by

$$W_e = \frac{1}{2} \sum_{\mu} \sum_{\nu} \sum_k P_{\mu\nu}(k) [H_{\mu\nu}(k) + F_{\mu\nu}(k)] \quad [86]$$

and total energy per unit cell, including nuclear repulsion, by

$$W_t = W_e + \frac{1}{2} \sum_A^{\text{cell}} Z_A^2 \sum_p^{\text{lattice}'} 1/R_{AA}(p) + \sum_{A>B}^{\text{cell}} Z_A Z_B \sum_p^{\text{lattice}} 1/R_{AB}(p) \quad [87]$$

The prime on the lattice summation indicates the omission of $p = 0$. The first nuclear repulsion term is for translationally equivalent atoms, the second for translationally inequivalent atoms. As mentioned above the

TABLE 3

Matrix Elements of the Fock Operator in the Basis
of Translational-Symmetry Functions

The various quantities appearing in the equations are defined in the text. Use has been made of the identities given in Table 2 to achieve these compact forms.

- (1) Diagonal cosine-cosine terms $F_{\mu\mu}$,

$$F_{\mu\mu}(k_1) = \frac{1}{2}(1 + A)_{\mu\mu} + 0.5\gamma_{AA} + R_{\mu\mu}(k_1) \\ + \sum_B (P_B - Z_B)\Gamma_{AB}(0) - \frac{1}{4} \sum_{k_2} [P_{\mu\mu}(k_2) + P_{\bar{\mu}\bar{\mu}}(k_2)] \\ \times [\Gamma_{AA}(k_1 + k_2) + \Gamma_{AA}(k_1 - k_2)],$$

where P_B is the total electron density on atoms of type B.

- (2) Corresponding sine elements,

$$F_{\mu\bar{\mu}}(k_1) = F_{\mu\mu}(k_1) [1 - \delta(k_1)].$$

- (3) Off-diagonal elements,

$$F_{\mu\bar{\nu}}(k_1) = 0, \quad \text{all } k_1,$$

$$F_{\bar{\mu}\bar{\nu}}(k_1) = F_{\mu\nu}(k_1) [1 - \delta(k_1)],$$

$$F_{\mu\nu}(k_1) = R_{\mu\nu}(k_1) - \frac{1}{4} \sum_{k_2} [P_{\mu\nu}(k_2) + P_{\bar{\mu}\bar{\nu}}(k_2)] \\ \times [\Gamma_{AB}(k_1 + k_2) + \Gamma_{AB}(k_1 - k_2) - \frac{1}{4} \sum_{k_2} [P_{\mu\bar{\nu}}(k_2) - P_{\bar{\mu}\nu}(k_2)]] \\ \times [\Gamma_{AB}(k_1 + k_2) + \Delta_{AB}(k_2 - k_1)],$$

$$F_{\bar{\mu}\bar{\nu}}(k_1) = Q_{\mu\nu}(k_1) - \frac{1}{4} \sum_{k_2} [P_{\mu\nu}(k_2) + P_{\bar{\mu}\bar{\nu}}(k_2)] \\ \times [\Delta_{AB}(k_1 + k_2) - \Delta_{AB}(k_2 - k_1)] - \frac{1}{4} \sum_{k_2} [P_{\mu\bar{\nu}}(k_2) - P_{\bar{\mu}\nu}(k_2)] \\ \times [\Gamma_{AB}(k_1 - k_2) - \Gamma_{AB}(k_1 + k_2)].$$

In the above equations the summations over k_2 include all N values of the wave vector allowed by the cyclic boundary conditions.

divergent terms inherent in this equation should cancel to give W_t a finite value.

Factorization of the energy is possible in this case as it was in the molecular problem. Individual atom-atom energies can be found by using in equations [39] and [40] the direct-space matrix elements derived from the converged solution in k-space. Interaction energies between unit cells can be defined on the basis of the atom-atom energies involved. Individual contributions to each of the above energies arising from specific terms such as one-electron, coulomb and exchange can also be identified. The separation of the last two terms is somewhat arbitrary but useful nonetheless.

These, then, are the main features of the method. The results will demonstrate its usefulness. Important features will be discussed as they arise. The discussion will centre on the main features of the results and dwell on numerical detail only when necessary. This approach is taken for two reasons. First, the inherent limitations of an approximate method such as this must be recognized and care taken not to overinterpret its results. Second, too much emphasis on detail tends to obscure the overall pattern of results, particularly where the detail cannot be verified by comparison with independent methods. The emphasis will centre on the physical aspects of the results. Unfortunately, comparison of calculated parameters with those resulting from experiment is even more difficult in the case of polymers than it is for small molecules. This is due largely to the fact that the calculations refer to polymers which are perfect, and are assumed to be in a non-interacting environment. Experimentally no such thing exists. In the gas and liquid phases the polymer's conformation is usually random and in the crystalline state, where crystals can be obtained, the crystal forces modify

the results obtained for the appropriate experimental quantities. Therefore, spectra and physical constants are not readily available and where they are comparison with theoretical results must be made carefully.

Computational Details

A Fortran computer program was written to implement the present scheme. This program, POLYM1, is capable of handling polymers composed of hydrogen and first-row atoms. Unit cells containing up to twelve hydrogen and six first-row atoms can be handled with ease by machines comparable to the CDC 6400.

As mentioned before the full $nN \times nN$ Fock matrix is reduced in this basis to one $n \times n$ matrix and $\frac{N-1}{2}$ matrices of dimension $2n \times 2n$. Each of the latter can be divided into four sub-matrices which are related in pairs, $F_{\mu\nu}(k)$ and $F_{\bar{\mu}\bar{\nu}}(k)$, $F_{\mu\bar{\nu}}(k)$ and $F_{\bar{\mu}\nu}(k)$. $F_{\mu\nu}(k)$ and $F_{\bar{\mu}\bar{\nu}}(k)$ are symmetric and identical ($k \neq 0$), while $F_{\mu\bar{\nu}}(k)$ and $F_{\bar{\mu}\nu}(k)$ are skew symmetric and $F_{\bar{\mu}\nu}(k)$ is the transpose of $F_{\mu\bar{\nu}}(k)$, the diagonals being zero. Out of a total of $4n^2$ elements there are at most n^2 distinct elements and only these need be stored. In this way the overlap, density and Fock matrices require little more than a quarter of the expected computer storage space. The largest polymer calculation attempted in this laboratory--a single calculation on a dimethyl-beryllium chain undertaken to test the feasibility of doing large systems--required only 50000₈ words of core storage and less than 500 seconds of central processor time to execute. A single conformation of polyethylene requires less than 40000₈ words of core storage and only 64 seconds of central processor time. Clearly, on a relatively modest budget, extensive investigations of simple systems is possible at this level of approximation or at any comparable level, e.g., INDO, MINDO^(9,23).

CHAPTER 2

RESULTS OF THE ZERO ORDER THEORY

The Hydrogen Chain

The simplest closed-shell polymer is a chain of hydrogen molecules. Although it does not occur in reality it serves as a useful model on which to test the method, and to illustrate its strengths and weaknesses.

In the CNDO/2 approximation the optimum theoretical bond-length of an hydrogen molecule is 0.748 \AA . The most stable linear chain is one in which the molecular bond-length is unchanged and the centres of neighbouring molecules are separated by 2.500 \AA . The stabilization energy per molecule in the chain is $6.33 \cdot 10^{-1} \text{ kcal.m}^{-1}$ ($1.01 \cdot 10^{-3} \text{ a.u.}$) with respect to the isolated molecule. This suggests a very weak inter-molecular interaction, consistent with the experimental evidence concerning the hydrogen crystal⁽⁴³⁾.

The theory shows the system to be molecular rather than atomic; it does not consist of a chain of equally spaced atoms but of diatomic molecules comparatively widely separated. This can be explained in the following way. A chain of equally spaced atoms may be considered from two different viewpoints. The simpler is to consider it as a lattice on a monatomic basis. Because there is only one basis function per atom, there is only one band in the Brillouin zone (Fig. 1). Each atom contributes one electron to the crystal, and so, allowing for spin pairing, the band is half full, making the crystal metallic. Alternatively, the chain may be treated as one with a diatomic basis. Doubling the unit cell in real space causes the Brillouin zone to be halved (Fig. 1), while the number of bands in the new zone is double

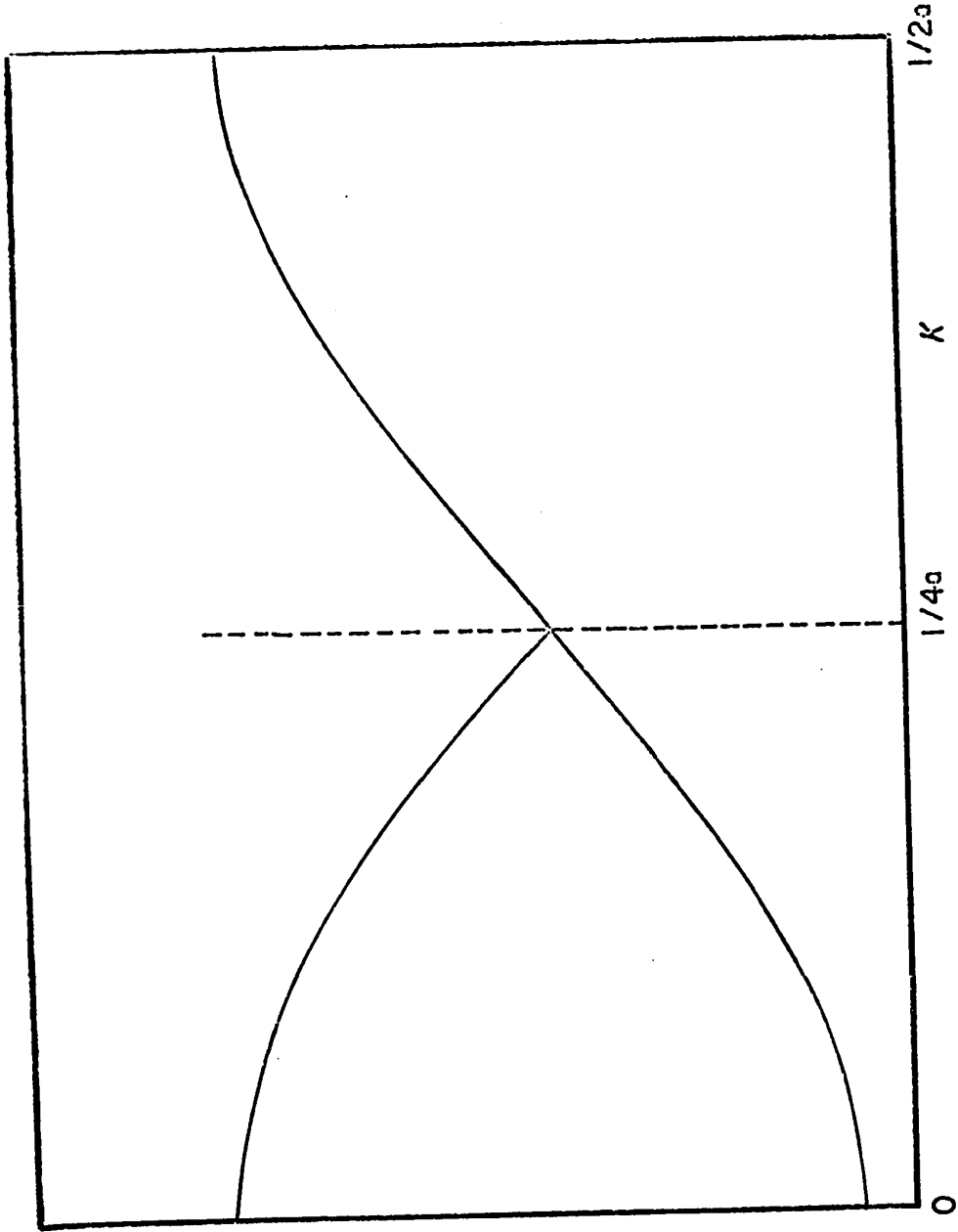


Fig. 1. Schematic representation of the effect, on the band structure, of doubling the unit cell in the direct lattice. The dependence of the units in k -space on a is shown explicitly.

that in the old one. Because each unit cell now contributes two electrons the lower band is filled. However, it touches the other, vacant band at the $k = 1/2$ zone boundary and so again a degeneracy results. Any distortion, such as that leading to the molecular structure, which causes a band gap to open at this boundary will lead to a stabilization of the system. This result is related to the Hume-Rothery theory of alloys⁽⁴⁴⁾ and the Jahn-Teller effect^(37,45) in molecules.

Mathematically, the interaction integrals between nearest neighbours are equal in the symmetric configuration. When considered as a diatomic lattice, the atoms can be split into two sets, say X and Y, on the basis of translational equivalence. These sets are related to one another by other symmetry elements. At the $k = 1/2$ edge of the Brillouin zone the phase factors are such that the sine functions vanish and for the cosine functions a complete change of phase occurs between successive unit cells. When the interaction elements between the two different translational sets are calculated, they consist of equal contributions with opposite phases, and hence they vanish. Let

$$F_{XY}(k) = \langle \phi_X(k) | F | \phi_Y(k) \rangle; \quad F_{XY}(P) = \langle X_X^0 | F | X_Y^P \rangle .$$

By symmetry

$$F_{XY}(0) = F_{XY}(-1); \quad F_{XY}(1) = F_{XY}(-2), \text{ etc.}$$

$$F_{XY}(k) = \sum_P \cos 2\pi k p F_{XY}(P)$$

$$\text{but at } k = 1/2 \quad \cos 2\pi k p = (-1)^P$$

therefore

$$\begin{aligned} F_{XY}(k) &= F_{XY}(0) - F_{XY}(-1) + F_{XY}(1) - F_{XY}(-2) + \dots & [88] \\ &= 0 \end{aligned}$$

The two cosine functions give rise to four matrix elements. Two of these are zero by this analysis and the remaining two, the diagonal elements of the interaction matrix, are equal. These identical elements become the eigenvalues. Vanishing conditions for the off-diagonal cosine-cosine elements depend on the equalities leading to equation [88]. Only when all lattice spacings are equal and the matrix elements are symmetric with respect to the symmetry element which would be destroyed by the distortion does this occur. (See the discussion of the infinite polyene for a further example of this behaviour.) It should be mentioned that the degeneracy may occur only at this level of approximation. Configuration interaction^(2,6) might resolve the degeneracy. Even if it did, the gain in stabilization in going to the molecular structure is so substantial in this case (68.42 kcal/m of diatoms) that a pseudo-Jahn-Teller⁽¹⁵⁾ effect would likely occur, leading to the same overall result.

When, in an infinite linear array of hydrogen molecules, the intermolecular separation is so large that no interaction occurs the energy levels of all of the molecules are identical. When the molecules are brought together interaction between them causes the infinite degeneracy to be lifted. The sharp molecular energy levels become bands⁽⁷⁾ of very closely spaced polymer energy levels. In the case of the hydrogen chain, because the interaction is weak, the bands remain quite narrow; the plots of band energy against wave vector show little dispersion (Fig. 2). Just as a given number of basis functions in a molecule give rise to an equal number of molecular orbitals in the final result, so the number of basis functions in the unit cell equals the number of bands in the Brillouin zone. A lattice with a molecular basis has a band for each molecular orbital in the unit cell.

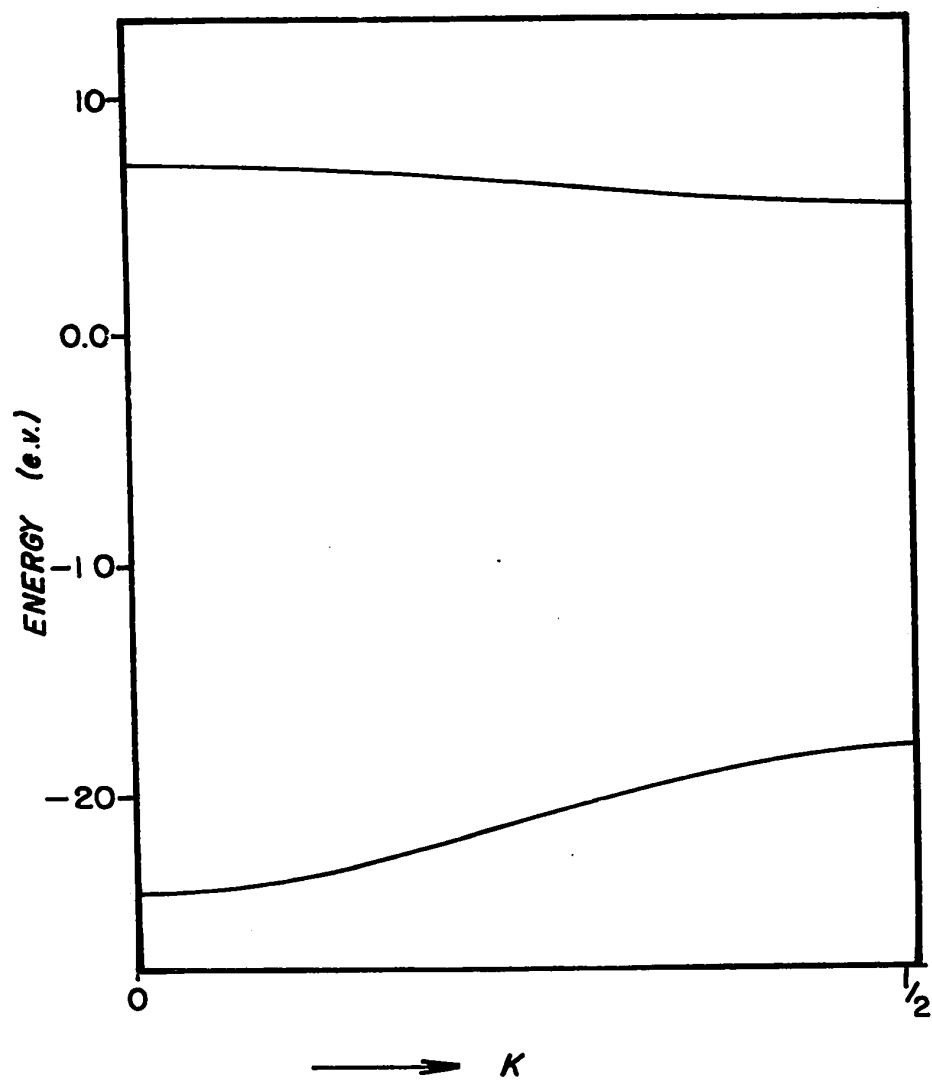


Fig. 2. The band structure of the optimum linear lattice of H₂ molecules.

Hence in the present case there are two bands.

For the free molecule the calculated (CNDO) singlet and triplet excitation energies are respectively 14.684 eV and 9.446 eV. The difference between these energies, 5.238 eV, is due to the exchange stabilization of the triplet, and is given by $2K_{ij}$ ⁽³²⁾. K_{ij} is the exchange integral between the orbital i , from which excitation occurs, and the orbital j to which the electron is transferred. This integral gets smaller as the dimensions of the system under consideration increase⁽¹⁸⁾, so that for the infinite polymer the singlet-triplet splitting is apparently zero. To illustrate this, consider a linear lattice with a monatomic basis. The coulomb integral J_{ij} between orbitals $\theta_i(k)$ and $\theta_j(k)$ is given by

$$J_{ij} = \sum_{\mu\nu\sigma\lambda} C_{\mu i}^*(k) C_{\nu i}(k) C_{\sigma j}^*(k) C_{\lambda j}(k) \int \phi_{\mu}(k) \phi_{\nu}(k) |r_{12}^{-1}| \phi_{\sigma}(k) \phi_{\lambda}(k) d\tau \quad [89]$$

The matrix C is unitary (so that $|C_{\mu i}| < 1$) and the integral over Bloch basis functions has been shown (Table 1) to be

$$\sum_{\mu\nu} \sum_{\sigma\lambda} \Gamma_{AB}(0)/N$$

But

$$\Gamma_{AB}(0) = \sum_p \gamma_{AB}(p) < \gamma_{AB}(0) + \sum_{p \neq 0} \frac{1}{|R(p)|} = \gamma_{AB}(0) + \frac{1}{a} \sum_{n \neq 0} \frac{1}{n} \quad [90]$$

As N , the dimension of the lattice, increases sum increases logarithmically.

Therefore

$$\lim_{N \rightarrow \infty} \frac{\Gamma_{AB}(0)}{N} = 0 \quad [91]$$

Hence J_{ij} , and likewise K_{ij} , is zero. This argument can easily be generalized to demonstrate this result even where the coulomb integrals are not approximated in this way.

However, the consequent suggestion that no singlet-triplet splitting occurs in polymers is not correct. The model giving rise to the usual expressions for the excitation energy and singlet-triplet splitting in molecules

$$\begin{aligned}
 E_{ij}^{(1\rightarrow1)} &= \epsilon_j - \epsilon_i + J_{ij} + 2K_{ij} \\
 E_{ij}^{(1\rightarrow3)} &= \epsilon_j - \epsilon_i - J_{ij} \\
 E_{ij}^{(1\rightarrow1)} - E_{ij}^{(1\rightarrow3)} &= 2K_{ij}
 \end{aligned}
 \tag{92}$$

is not applicable to polymers (or crystals). Polymer orbitals are delocalized over the whole structure and the excitation process described by the process leading to the above equations refers to an infinitely delocalized excitation. It ignores the strong coupling between the excited electron and the vacancy left in the polymer bands⁽⁴⁷⁾. Configuration interaction or other many-body methods⁽⁴⁸⁾ can be used to construct the correct localized representation of the excitation process. A promising approach to this problem has recently been suggested in this laboratory⁽⁴⁶⁾. At present, the differences between band energies can serve only as upper bounds to the true spectra.

Although unable to account for many-electron effects, such as dispersive forces⁽⁴⁹⁾, or to represent the effects of higher electrical multipoles⁽⁴³⁾ (because of the small basis set), the method gives a physically reasonable structure for the H_2 chain. The binding is shown to be weak, as it is in the true three-dimensional crystal, and the system is shown to be molecular in character.

The Infinite Polyene $(CH)_{2N}$

Conjugated polyenes, both linear and cyclic, were among the first

molecules to be the subject of theoretical investigation⁽¹¹⁻¹⁶⁾. The earliest molecular orbital method, the Hückel method^(6,9,10), is applicable only to π electron systems and so its application is restricted to polyenic systems. Hückel's method, which is based on a parameterized hamiltonian similar to the one-electron part of the present calculations, was used extensively to study a wide range of polyenes, including the infinite polyene. The structure of this fictitious molecule has since been the subject of considerable controversy which will be reviewed later in this section.

In the all-transconfiguration the infinite polyene has a planar skeleton with a unit cell consisting of two CH groups. These groups are disposed so that the centre of the carbon-carbon bond is a centre of symmetry (Fig. 3). For convenience, one CH group, and all those translationally equivalent to it, will be labelled I, while the other and its translationally equivalent CH groups will be labelled II. Two distinct configurations are possible, the regular polyene where all carbon-carbon bond lengths are equal, and the alternant polyene where alternate carbon-carbon bonds are long and short.

For the regular or symmetric polyene two methods of calculation were employed. The standard program, POLYM 1, represents one method; the other method involves a special symmetry-adapted program, SYMPOL, which was written to deal with this specific problem. The symmetry-adapted basis functions used in SYMPOL are defined as follows:

$$\begin{aligned}\phi_{\mu}^{\pm}(k) &= (2)^{-1/2} [\phi_{\mu}^I(k) \pm \{\phi_{\mu}^{II}(k)\cos\pi k - \psi_{\mu}^{II}(k)\sin\pi k\}] \\ \psi_{\mu}^{\pm}(k) &= (2)^{-1/2} [\psi_{\mu}^I(k) \pm \{\phi_{\mu}^{II}(k)\sin\pi k + \psi_{\mu}^{II}(k)\cos\pi k\}]\end{aligned}\tag{93}$$

where the functions $\phi_{\mu}^I(k)$ are the usual Bloch functions, labelled here to

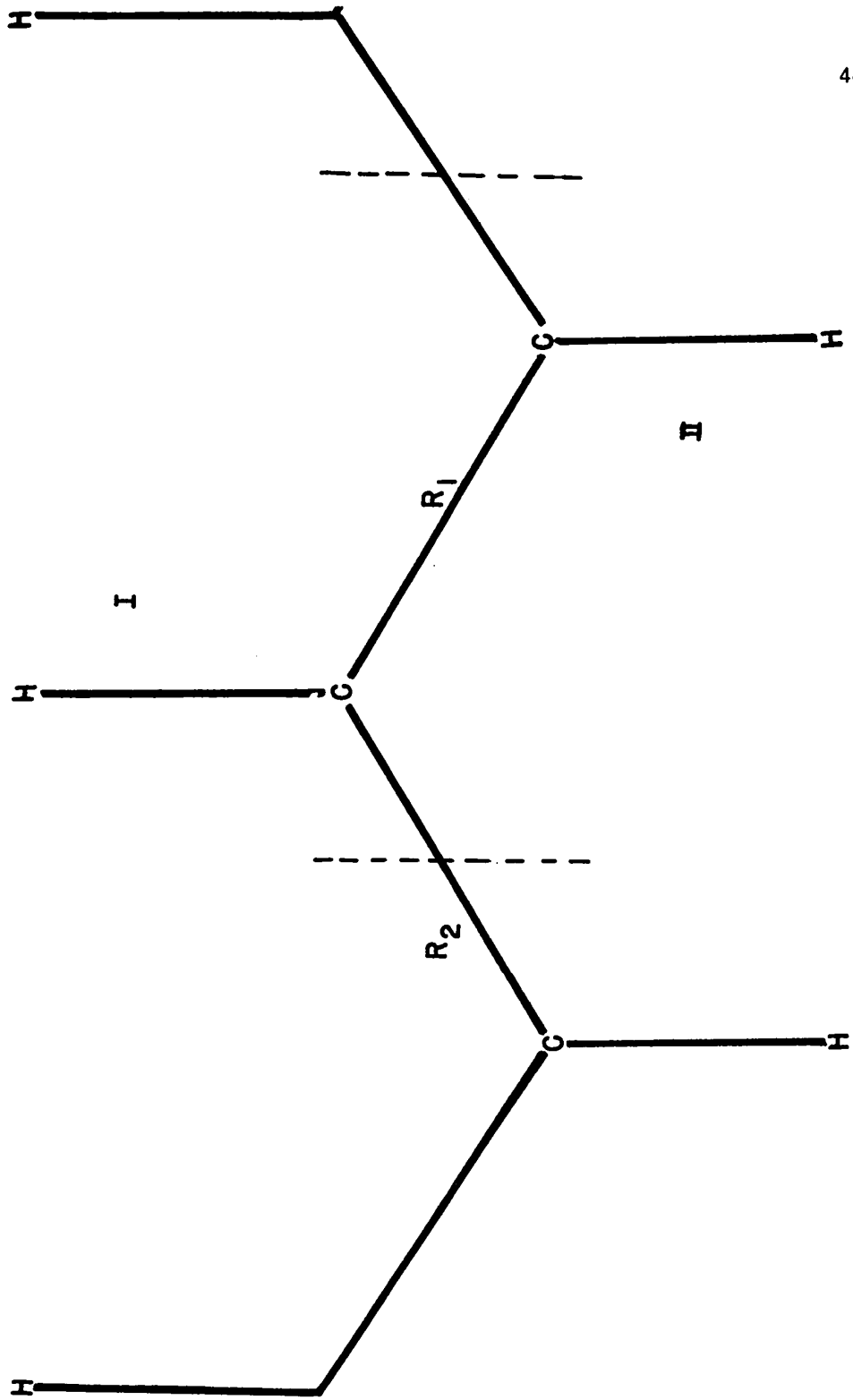


Fig. 3. Diagram of the polyene unit cell.

7

identify the CH group in which they are centred. Transformations such as these may be found by inspection or by the method of Winston and Halford⁽⁵⁰⁾.

All lattice integrals in SYMPOL are based on these symmetry functions, which utilize the glide plane (parallel to the translation axis) and symmetry plane (perpendicular to both the translation axis and the molecular plane) occurring in the regular polyene but not in the alternant one. Under this transformation the Fock matrix, for general non-zero wavevector k , is reduced from a 20×20 matrix to four 5×5 matrices. This set of four consists of two pairs of identical matrices, thus

$$F(k) = \begin{bmatrix} A & & & 0 \\ & A & & \\ & & B & \\ 0 & & & B \end{bmatrix}$$

All details of the calculation parallel those of the usual method, except that only the two distinct 5×5 matrices need be solved. Application of the inverse transformation to the solutions obtained by use of SYMPOL gives results which are directly comparable to those of the usual method. The results of both methods are identical.

The convention of choosing N to be odd proved inconvenient here as it excludes the point $k = 1/2$ from the sample set. When the band structure of the symmetric polyene is plotted on the basis of the results of either method it appears as though a non-zero band gap exists. Use of the Fourier synthesis to find the orbitals and their energies at $k = 1/2$, the point at which the band gap is a minimum, shows that it is zero. At points k' close to $k = 1/2$, the band gap is linear in $|1/2 - k'|$. Because of the degeneracy at $k = 1/2$ the wavefunction obtained in the usual way is inadequate; it is necessary to have recourse to a higher order approximation, such as configuration interaction,

to find the correct wavefunction.

The alternant form can be generated from the regular form by lengthening one C-C bond length in the unit cell (R_1) and shortening the other (R_2). This process can be studied by using a parameter δ , defined as

$$\delta = \frac{1}{2} |2R_0 - R_1 - R_2| \quad [94]$$

where R_0 is the bond length in the regular polyene. It was found that, by using the wavefunction for a small non-zero value of δ to start the iterative method of solution for the case $\delta = 0$, a wavefunction with alternant symmetry could be found for the symmetric structure. There are, of course, two such solutions related to one another by the plane of symmetry. Because they have the alternant symmetry they exhibit a band gap, and other characteristics of the alternant form which will be described later. Their common energy can be taken as an upper bound to the energy of the correct wavefunction for the symmetric structure.

Calculations on the alternant structure proper give well-behaved solutions. The geometry of the unit cell for the most stable alternant form is as follows: the carbon-carbon bond lengths are 1.350 Å and 1.432 Å; the carbon-hydrogen bond length is 1.115 Å and the $\angle C-CC$ is 125° . This result compares very favourably with bond lengths of the central C-C bonds in 1:8 diphenyl 1:3:5:7 octatetraene as determined by X-ray analysis of the crystalline solid⁽⁵¹⁾. The central C_2H_2 unit of this molecule has the following structure: carbon-carbon bond lengths of 1.35 Å and 1.44 Å (± 0.01 Å), carbon-hydrogen bond length of 1.08 Å (assumed) and $\angle CCC$ of 124.8° . All calculated parameters agree with the experimental results except the CH bond length which is slightly too long, a characteristic of CNDO calculations^(9,10). In this configuration the calculations show the atoms to be almost neutral,

the net charge on each hydrogen atom being -0.006. The carbon atoms, with a net charge of +0.006, are strongly polarized along the chain axis. Table 4 gives some typical density matrix elements between functions in the zeroth unit cell. π density matrix elements between translationally equivalent atoms are zero in accordance with the theory of alternant hydrocarbons⁽⁵²⁾. Density matrix elements between the translationally inequivalent π basis functions are non-zero; they do not converge as rapidly with increasing separations of the basis functions as do the other density matrix elements (Table 5). Long range density-matrix elements are the sums of strongly alternating series. Although the total energy may converge for small values of N , it is necessary to use much larger values of N to ensure convergence of these matrix elements. The stronger convergence of the energy is due to its dependence on $P_{\mu\nu}^2$, by which small values of $P_{\mu\nu}$ do not appreciably affect the value of E .

The band gap at $k = 1/2$ is calculated to be 7.75 eV, three times greater than the estimated value of 2.23 eV (18000 cm^{-1}), for the first excitation energy of an infinite polyene. This estimate is based on experimental results for shorter polyenic systems⁽¹⁵⁾. This discrepancy is the result of two factors: first, the energy difference between two crystal orbital energy levels does not provide a good estimate to the corresponding excitation energy; second, although the ordering of virtual orbitals given by CNDO is almost always correct, the spacings between the energy levels are not usually quantitatively correct^(9,10). The latter, in turn, is due to two factors: first, the use of the zero differential overlap approximation; second, the use of the S.C.F. method, which optimizes the occupied orbitals at the expense of the virtual orbitals.

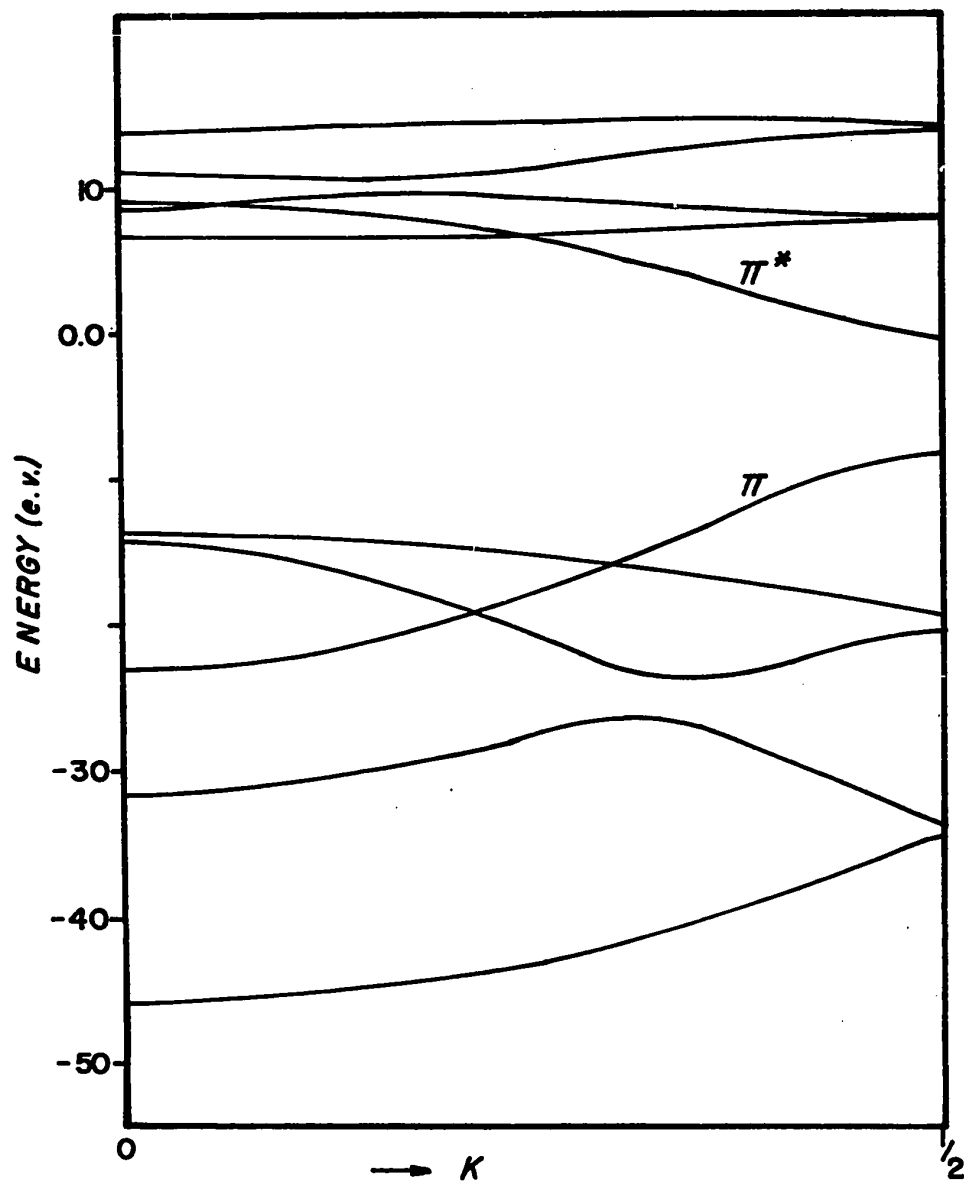


Fig. 4. The band structure of the optimum alternant polyene.

TABLE 4

Density Matrix Elements within the Origin Unit Cell
of the Optimum Alternant Polyene (see text)

	H^I	C_S^I	C_x^I	C_y^I	C_z^I
H^I	1.005677	.510760	-.000000	-.829301	.000696
C_S^I	.510760	1.012321	.000000	-.018741	.004022
C_x^I	-.000000	.000000	1.000000	.000000	.000000
C_y^I	-.829301	-.018741	.000000	.968534	-.008129
C_z^I	.000696	.004022	.000000	-.008129	1.013468
	H^{II}	C_S^{II}	C_x^{II}	C_y^{II}	C_z^{II}
H^I	0.153141	-.012973	0.0	0.009871	0.008172
C_S^I	-.012973	0.351371	0.0	-.247961	0.440361
C_x^I	0.0	0.0	0.860687	0.0	0.0
C_y^I	-.004160	0.247961	0.0	0.035138	0.321889
C_z^I	0.001828	-.440361	0.0	0.321889	-.423945

TABLE 5

Comparison of Density Matrix Elements for the Symmetric and Alternant Polyenes

Because the polyene is an alternant hydrocarbon, the π density matrix elements between translationally equivalent atoms are zero. The minus sign indicates a cell to the left of the origin and R1 is taken to be the short bond (Fig. 3). Results for the optimum alternant polyene (see text) are compared with those for the symmetric polyene having R1 = R2 = 1.389 Å, RCH = 1.115 Å, $\theta = 125^\circ$.

<u>Alternant Polyene</u>										
cell index	-5	-3	-2	-1	0	1	2	3	5	
$C_S^I-C_S^I$	-0.0001	-0.0017	-0.0052	0.0081	1.0123	0.0081	-0.0052	-0.0017	-0.0001	
$C_S^I-C_S^{II}$	0.0	0.0009	0.0393	0.3262	0.3514	0.0343	0.0030	0.0006	0.0	
$C_X^I-C_X^{II}$	-0.0023	-0.0093	-0.0643	0.3801	0.8607	-0.2836	0.1414	-0.0788	-0.0279	
<u>Symmetric Polyene</u>										
cell index	-5	-3	-2	-1	0	1	2	3	5	
$C_S^I-C_S^I$	0.0	-0.0004	-0.0026	0.0115	1.0059	0.0115	-0.0026	-0.0004	0.0	
$C_S^I-C_S^{II}$	0.0001	0.0037	0.0368	0.3390	0.3390	0.0368	0.0037	0.0007	0.0	
$C_X^I-C_X^{II}$	0.0725	0.1283	-0.2128	0.6368	0.6368	-0.2128	0.1283	-0.0923	-0.0600	

The lowest vacant orbital, the π^* band at $k = 1/2$, has an orbital energy of -0.475 ev. This suggests that the anion of the system is stable. Further variational calculations to optimize the orbitals of the anion can only lead to stabilization of that system. (Stability of this anion could not be predicted by Hückel theory.)

In summary, then, the present method shows the infinite alternant polyene to be a closed shell molecule, with a structure very similar to that of the central portion of long finite polyenes. The symmetric polyene is shown to be an open shell molecule at this level of approximation.

As mentioned in the introduction, early Hückel calculations predicted that the bond alternation observed in short open-chain conjugated polyenes would decrease as the chain length is increased. The infinite polyene was predicted to have the equality of bond lengths characteristic of small cyclic polyenes⁽¹¹⁻¹³⁾. Furthermore, the lowest excitation energy was predicted to decrease linearly with increasing chain length giving a zero excitation energy when the chain length becomes infinite. These results were challenged by Kuhn⁽¹⁴⁾ who pointed out that the experimental evidence showed that the decrease of excitation energy with increasing chain length deviates from linearity and seems to approach asymptotically to a finite limit of 2.23 ev ($18,000$ cm^{-1})⁽¹⁵⁾. He demonstrated using the free-electron model that bond alternation would resolve this problem. Further studies using a variety of methods followed. Salem and Longuet-Higgins⁽⁵³⁾, using a π -electron model, proved that bond alternation is a characteristic of the system. The proof, which is claimed to be independent of numerical approximation, has recently been challenged⁽⁵⁷⁾ but later vindicated⁽⁵⁸⁾. Nearly all the studies mentioned involve the use of either the F.E.M., or a π -electron molecular-

orbital method with nearest-neighbour interactions only. Because the literature on this subject is so extensive, it is not possible to review it exhaustively. Adequate reviews are provided in references 11 to 16 and 52 to 56.

More recently there have been some very interesting developments. Unrestricted Hartree theory⁽⁵⁷⁾, employing a simple product wavefunction with different orbitals for electrons with different spins, has been applied to the problem. The purpose of this study was to investigate the possibility of either spin-density waves (SDW) or charge-density waves (CDW) being the ground state of the large polyenic systems. No evidence in favour of the latter was found but SDW solutions were found which give significantly greater lowering of the energy than does bond alternation. However, the method involves extensive use of parameters and treats only nearest-neighbour interactions. While every effort was made to allow for parameterization, the latter approximation, in the light of the present work, seems to be very severe. The latest experimental evidence⁽⁵⁶⁾ suggests that the 18-annulene molecule exhibits bond alternation in the gas phase, though not in the solid.

Another recent development has been the application, by André and Leroy⁽⁵⁹⁾, of the full ab initio S.C.F. method to this problem, using Born-von Karman boundary conditions. In this case the results suggest that the symmetric structure is the more stable. Two features of these results are disquieting. The first is the fact that the energy of stabilization is found to be -115.8 kcal/m, an unacceptably large value in view of the small change in geometry involved. The second and more fundamental point is the prediction of a non-zero band gap for the symmetric structure. Symmetry considerations suggest that this result is not correct.

When using the nearest-neighbour approximation the symmetry of the lattice sums is automatically ensured. For example, when evaluating the Fock matrix element $F_{X_I X_{II}}^{C C}$ ($k=1/2$) for the symmetric polyene, the Fourier series is

$$F_{X_I X_{II}}^{C C} (k=1/2) = F_{X_I X_{II}} (q=0) + \cos\pi(F_{X_I X_{II}} (q=1) + F_{X_I X_{II}} (q=-1)) + \dots$$

But $\cos n\pi = (-1)^n$

and $F_{X_I X_{II}} (q=0) = F_{X_I X_{II}} (q=-1)$; $F_{X_I X_{II}} (q=1) = F_{X_I X_{II}} (q=-2)$, etc.

because of the X-Y plane of symmetry through each C-H group (Fig. 3). Hence, as in the case of equation [88], the series consists of pairs of equal contributions with opposite signs, and so the matrix element is zero. This result is valid for the present method and for normal solutions - those with the full symmetry of the lattice - of more elaborate one-electron methods. At $k = 1/2$ all sine-type functions vanish and the off-diagonal cosine I-cosine II matrix elements vanish as shown above. The submatrix corresponding to functions of π symmetry is, therefore, further reduced to two identical blocks consisting of I-I cosine interactions. Because of this reduction and the fact that π basis functions are symmetry distinct from all other basis functions in the infinite polyene, the solution of the Fock matrix leads to a degeneracy. Use of the nearest neighbour approximation automatically leads to this result, because only the matched interactions, $F_{X_I X_{II}} (q=0)$ and $F_{X_I X_{II}} (q=-1)$, are included in the sum. When longer lattice sums are used care must be taken to ensure that the symmetry is not violated. Using a five-cell segment while treating non-nearest-neighbours, for example, suggests that the I-II elements for $q = 0, \pm 1, \pm 2$ should be included in the lattice sum. If so, the cancelling partner

of $F_{X_I X_{II}}$ ($q=2$), which is $F_{X_I X_{II}}$ ($q=-3$) is omitted and the resulting incorrect lattice sums lead to a spurious band gap in the solution (Table 6).

Because the results of André and Leroy do not show the correct symmetry behaviour they must be treated with some caution. Their results show one promising feature, however. Their band gap for the symmetric polyene is 4.10 eV while the value quoted for the alternant structure is 6.12 eV. Adjusting the lattice sums will reduce the latter by approximately 3 eV giving a band gap of ~3 eV for the alternant structure, a value close to the experimental estimate of 2.23 eV for the excitation energy limit.

In a recent publication⁽⁶⁰⁾ Tric has attempted to calculate the vibrational spectrum of long polyenes. Certain features of the spectrum arising from skeletal vibrations were attributed to the existence of long-range π - π interactions. Gavin and Rice⁽⁶¹⁾, for different reasons, comes to a similar conclusion. These careful analyses show, as predicted here (Table 5), that even in alternant structures, as finite open-chain polyenes are, significant π density-matrix elements persist at long range.

What then is the structure of the infinite polyene? Calculations on the alternant form suggest that it is the more stable, but without a solution for the symmetric structure no definitive statement is possible. Using results obtained for small δ to estimate an upper bound for energy of the symmetric structure shows that the barrier between equivalent alternant structures is no more than 3 kcal/m. This suggests that a dynamic interconversion process between equivalent alternant forms may be occurring. The most recent experimental evidence is consistent with this picture of the gas-phase polyene. Interactions between polyenes in crystals are known to be large⁽⁷⁵⁾ and will have to be accounted for before detailed discussion of

TABLE 6

The Effect of Truncation of Lattice Sums in the Polyene Calculation

N_c is the number of unit cells included in the coulomb lattice sums. The terms "balanced" and "unbalanced" are discussed in the text.

N_c	5		37	
	Balanced	Unbalanced	Balanced	Unbalanced
E_{cell} (a.u.)	-15.6693	-15.6725	-15.6719	-15.6717
Band gap (e.v.)	0.0	3.7	0.0	0.27

the structures of polyenic crystals is possible. One final comment is in order. It may well be that polyenes are unstable with respect to singlet (CDW) or triplet (SDW) instabilities in the ground state but this remains to be proven both theoretically and experimentally.

Polyethylene

This is the simplest saturated chemically well-defined polymer. Calculations^(17,20,21,23,62) have been done on the all-trans and regular helical configurations. The basic features of the electronic structure of the molecule in these configurations are now clear although differences in detail occur between different methods⁽⁶³⁾.

Helical configurations of all polymers have been of interest to many since the biological significance of such configurations was discovered⁽³⁻⁵⁾. In the case of polypeptides the obvious stabilizing feature is the hydrogen-bonded network within the coiled chain. Speculation about other forms of stabilization can only be resolved by detailed theory or experiment. Scheraga and other workers⁽⁶⁴⁾ have been studying conformational problems of large molecules for some time. Their methods usually involve empirical potential functions with terms for each of the important contributing factors. The values of the constants used are determined from experiment and, more recently, by calibration against detailed S.C.F. calculations. The quality of this work has been shown by the high degree of correlation between their predictions and the observed results. As with all empirical methods, the separation of various effects is necessary but this is clearly an approximation, sometimes a severe one. This is particularly true where the possibility exists of unusual features in the binding. In general these methods can be expected to provide quite accurate predictions of preferred

conformations but the interpretative aspects of the method must be handled carefully. Their major weakness is that they give no account of the electron states in the polymer.

Helical configurations of the polyethylene molecule can be described in terms of the usual bond lengths and angles together with two helix parameters, w and h (Fig. 6). The helical angle w is the angle of rotation about the helical axis subtended, in a plane perpendicular to the axis, by successive carbon atoms. The pitch, h , is the distance along the helical axis between successive carbon atoms. Equations relating the standard bond lengths and angles to these helix parameters were derived by Shimanouchi and Mizushima⁽⁶⁵⁾. When $w = 180^\circ$ the configuration is all-trans or staggered (Fig. 5); when $w = 135^\circ$ the configuration is eclipsed; and when $w = 90^\circ$ the configuration is all gauche.

Extended Hückel^(17,21), CNDO/2^(20,21) and ab initio S.C.F.⁽⁶²⁾ calculations have given band structures for the all-trans configuration which agree as to the general features of the valence bands (Fig. 7). Results for the conduction bands are very sensitive to the approximations used. Both the extended Hückel and ab initio methods give broad conduction bands⁽⁶³⁾ while the CNDO method gives very narrow ones. This discrepancy arises from the Z.D.O. and S.C.F. approximations discussed earlier. Estimates of the band-gap vary with the method used to calculate it. The Hückel calculation gives a significantly lower value than do the CNDO and ab initio calculations. As this parameter is not simply related to the excitation energy this difference is not necessarily significant (see the final discussion for further comment). Furthermore, the calculations employed in this comparison probably include the same error in the lattice

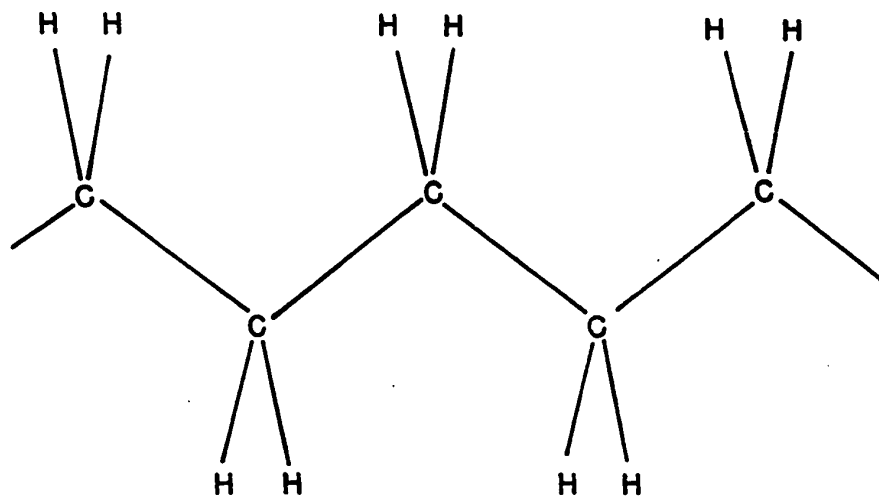


Fig. 5. Diagram of the polyethylene molecule.

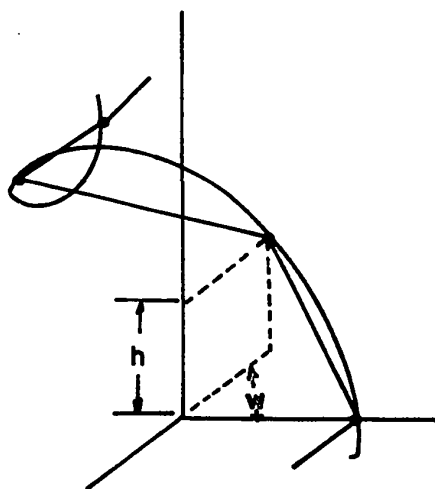


Fig. 6. Diagram of the helix parameters.

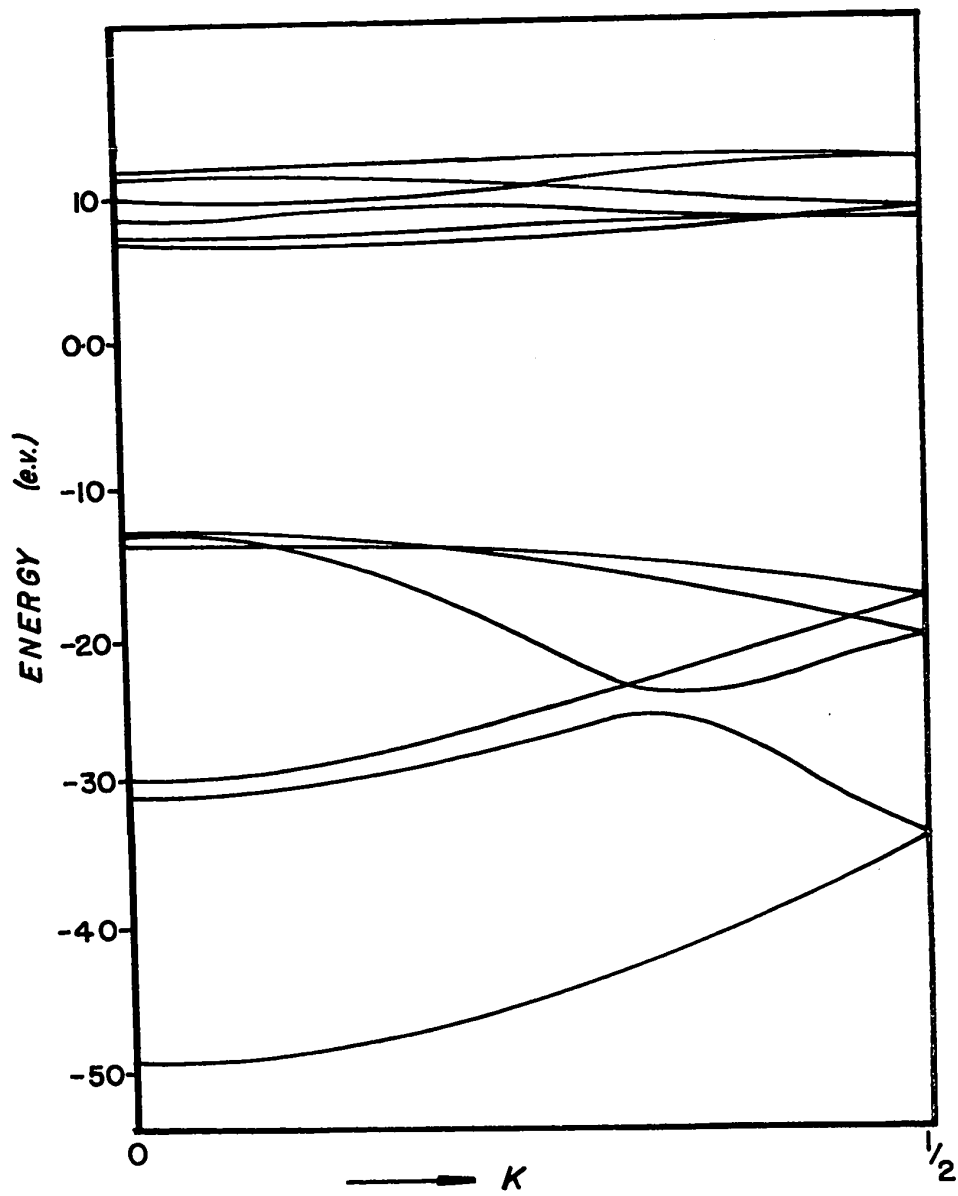


Fig. 7. The band structure of polyethylene.

sums that appeared in the polyene calculations done in the same laboratory. This error would exaggerate the band gap in both CNDO and ab initio results. It was not possible to check this because details of the calculation, such as geometry and parameterization, were not provided.

There are three occupied valence bands, two of which are symmetric in the plane of the carbon skeleton while the third is antisymmetric. These symmetric bands cannot cross⁽⁶⁶⁾; recent papers contain incorrectly drawn band structures as a result of neglecting this symmetry. The Fermi level occurs at $k = 0$, the highest occupied level being part of a symmetric band (Fig. 7).

Both Extended Hückel and CNDO have been used to study the energy of the helix coiled in configurations corresponding to the range of w values from 180° to 60° . Each method shows the all-trans form to be the more stable, and further predicts a double minimum close to the all-gauche ($w = 90^\circ$) configuration. In these calculations a standard set of bond lengths and angles was assumed. Apart from a limited investigation of the dependence of the helix energy on the CCC skeletal angle in the E.H. calculations⁽²¹⁾, no attempt was made to optimize the geometry of the unit cell. Since the energy difference between the all-trans and all-gauche forms is as little as 0.5 kcal/m, this is a serious oversight.

Partial optimization of the unit cell geometry in the all-trans configuration gives disappointing results. The calculated carbon-carbon bond length (1.4875 Å) is shorter than the experimental figure⁽⁶⁷⁾ (1.54 Å), the skeletal angle too large (116.25° vs 109.45°), but, because the previous two effects tend to cancel one another, the unit cell length is approximately correct. When this new unit-cell geometry is used in the helix calculations,

two changes occur in the overall pattern of the results. Where there was a double minimum in the E_{cell} vs w curve before ($w \sim 60^\circ$, $w \sim 80^\circ$), there is now a single minimum at $w = 60^\circ$, with a slight shoulder at $w = 65^\circ$ (Fig. 8). The double minimum, also appearing in the results of calculations employing empirical potentials, may be a spurious result, caused by the use of unoptimized geometries. A still more interesting result is the fact that the all-gauche form has been stabilized relative to the all-trans form. It is true that the CNDO method enhances gauche interactions⁽²⁰⁾, making the gauche form of butane more stable than the trans form. As Imamura points out, however, the results obtained by using different lengths of lattice sum suggest very strongly that the long-range interactions in polyethylene stabilize the gauche form. Moreover, optimization of the unit cell geometry in helix configurations close to $w = 60$ must lead to a further enhancement of the relative stability of these configurations. Although the absolute energy difference involved is quite small and the result not beyond criticism, it raises an interesting point.

Polyethylene consists of all-trans chains packed in a lattice with lattice constants $a = 7.49 \text{ \AA}$ and $b = 4.96 \text{ \AA}$; c is the fiber axis. Recent papers⁽²⁰⁾ suggest that to be consistent with these experimental results, the theory must show the all-trans configuration to be more stable than the all-gauche. This is not necessarily so; it is probably sufficient that the gauche form be no more than about 1 kcal/m more stable than the trans form. Crystals such as polyethylene are bound by Van der Waal's forces. Salem⁽⁷¹⁾ showed that, for finite polyethylene chains, the force of attraction between chains in the all-trans configuration is given, to a good approximation, by

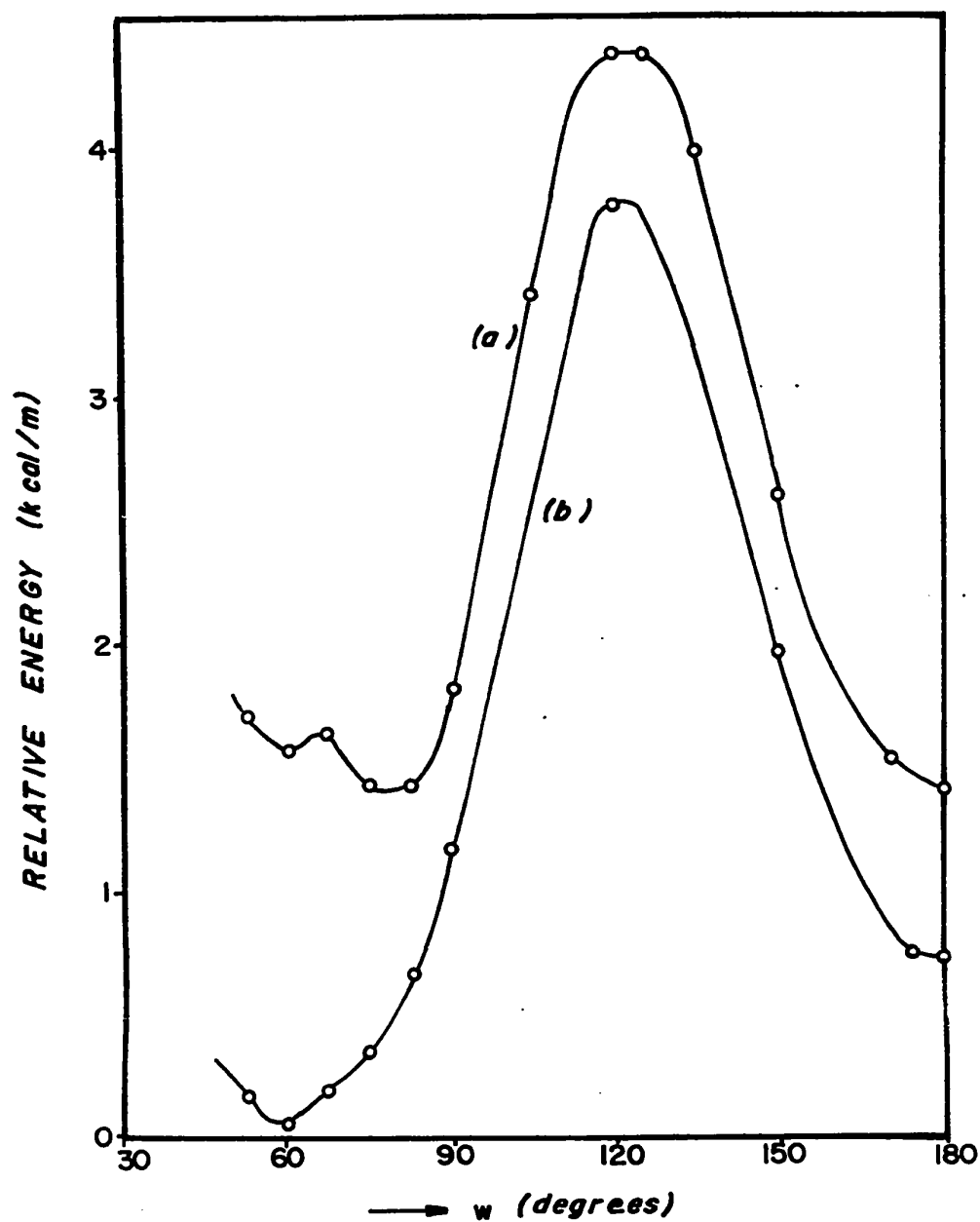


Fig. 8. Plot of E_{cell} against the helix parameter w for polyethylene. (a) is the standard geometry; (b) is the optimized geometry (see text). Curve (b) has been shifted up the scale for convenience. The actual separation at $w = 180^\circ$ is 5.23 kcal/m.

$$\Delta E = - \frac{3\pi}{8} \frac{c}{a} \frac{N}{D^2} \quad [95]$$

c is a constant to be determined (Salem's value is $1340 \text{ (\AA)}^6 \text{ kcal/mole}$); D is the separation between chains of N units with a lattice spacing a . This is valid only for $D \gg a$. Sparnaay⁽⁷¹⁾ found a similar result for the interaction of cylindrical molecules, with further correction terms proportional to $\frac{1}{D^5}(r/D)^2$ where r is the radius of the cylinder.

With such a high order dependence on the intermolecular separation packing considerations become very important⁽⁶⁸⁾. In normal polyethylene crystals the chain axes are approximately 4.5 \AA apart, giving a stabilization energy of the order of -2.0 kcal/m . Increasing this distance to 5.5 \AA causes the stabilization to drop to -0.75 kcal/m , a net loss of 1.25 kcal/m . Packing of the bulky helical coils must lead to larger average chain separations. At this range these formulae cannot be used to make quantitative estimates of the energy loss. However, it is clear that conformational energies and crystal packing energies are of similar magnitudes and small conformational gains may be off-set by the loss of packing energies. The relationship between free molecule conformations and those of molecules packed in crystals cannot, therefore, be assumed. Cases where structural features provide particularly high stabilization in the free molecule, such as the α -helix of polypeptides or the planar structure of polyenes, are possible exceptions to this.

The polyene and hydrogen chains, in their respective symmetric configurations, have vacant orbitals which are degenerate or near-degenerate with the highest filled orbital. That this feature has striking effects on both of these chains has already been seen. In polymers where the gap between the filled and vacant levels is much greater what effect, if any, do the vacant orbitals

have on the polymer structure, and how is it manifested? This question can be answered by a well-established theory⁽⁶⁹⁾ originally developed in the study of small molecules. In this method the change in the molecular wavefunction accompanying a vibration is represented by the usual spectral expansion of first-order perturbation theory⁽³⁰⁾.

$$\psi_0^{(1)} = \sum_{n \neq 0} \langle \psi_n | V | \psi_0 \rangle [E_n - E_0]^{-1} \psi_n \quad [96]$$

The sum is taken over all excited states of the molecule. Two features become immediately apparent. Only those states having the same symmetry as V are coupled to the totally symmetric ψ_0 by the perturbation. Since V can be shown to have the symmetry of the vibration causing the perturbation, the excited states involved are, to first order, those with the same as the vibration. Further, the denominator $[E_n - E_0]$ dictates that the largest contribution to the change in wavefunction comes from the lowest state of this symmetry.

Polyethylene has a large band gap and the question arises as to whether or not the lowest vacant orbital influences the structure. The present calculations, using a unit cell consisting of two CH_2 units, show the highest occupied and lowest vacant orbitals to belong to the $k = 0$ representations. The group of $k = 0$ is the factor group D_{2h} ⁽⁶⁶⁾. Under this group the highest occupied level is classified as a b_{3g} orbital while the lowest vacant is b_{3u} . Less than 1 eV higher than this there is a b_{2u} virtual orbital. The transition density from b_{3g} to b_{3u} is of A_u symmetry while that from b_{3g} to b_{2u} is B_{1u} .

Optical-transition selection rules show the $b_{3g} \rightarrow b_{2u}$ transition to be allowed and polarized along the chain (z) axis; the $b_{3g} \rightarrow b_{3u}$ transition

is optically forbidden but mixing could occur during a suitable vibration. Inspection shows that there is no mode of suitable a_u symmetry having a zero wave-vector, q . Conservation of momentum requires that

$$k + k' + q = \text{integer} \quad [97]$$

for the process where a vibrational mode of vector q mixes one-electron states having wave vectors k and k' . Hence no such process can occur here.

The b_{3g} and b_{2u} orbitals can be mixed by a mode having b_{1u} symmetry. Without solving the dynamical equations it is impossible to determine what the form of this mode should be. A reasonable guess would be the skeletal vibration shown here



which would cause alternation. The large excitation energy, $E_n - E_0$, required suggests the mixing process would not be efficient; at most it should only soften the b_{1u} vibration without causing alternation.

A set of distortions of the type described in equation [94], where

$$\partial = |R_1 - R_0| = |R_2 - R_0| = |2R_0 - R_1 - R_2|$$

were introduced and the energies of the resulting structures calculated. The variation E with ∂ was fitted to a curve. An estimate of the force-constant was made by evaluating the second derivative of E with respect to ∂ , at the point $\partial = 0$. A similar procedure was used to find the second derivative of the E versus ∂ curve for a uniform expansion of all bonds. The respective values are $3.79 \cdot 10^6$ and $3.33 \cdot 10^6$ dynes/cm. The similarity is striking, showing that the "softening" effect of the virtual orbital mixed into the ground state is probably minimal.

One point must be emphasized. The distortions used here are not vibrational modes of the chain. While it is likely that a mode exists having the characteristics of the alternating distortion no vibrational mode can behave like the uniform stretching motion. Because the distortion is cumulative such a motion, even for a long finite chain, would result in the terminal atoms travelling physically unreasonable distances.

The effect of the distortion on the band structure is to stabilize the majority of the occupied orbitals giving a net change in the electronic energy of -0.003309 a.u./cell, when $\delta = 0.005 \text{ \AA}$. Increased nuclear repulsion, by 0.003418 a.u./cell, causes an overall loss of stabilization of $6.33 \cdot 10^{-2}$ kcal/m ($1.09 \cdot 10^{-4}$ a.u./cell).

A further note on the relationship between the band structures obtained by using different unit cells can be made at this point. The orbitals at $k = 0$ using the large cell can be classified under the group D_{2h} ; three transform as A_g , two as B_{1g} , and one as B_{3g} ; three transform as B_{2u} , two as B_{3u} and one as B_{1u} . Those which are antisymmetric under inversion, labelled 'u', would in a calculation based on the small unit cell appear at $k = 1/2$. This can be seen by considering the phase factors: at $k = 1/2$ the phase corresponds to a change of sign between every consecutive pair of cells; in this way the two small cells which constitute the large cell will always have site basis-function coefficients which are opposite in sign and hence antisymmetric under inversion. The band structure for the all-trans structure, based on the large cell, is given in Fig. 8.

The results of calculations on polyethylene have recently received very valuable experimental verification⁽⁷⁰⁾. X-ray photo-electron spectra of polyethylene have shown excellent correlation with both ab initio and

semi-empirical band structures. In the latter case the possibility exists of using such spectra to provide data for recalibration of the theory where necessary.

The results of these calculations suggest that the present method provides a good description of compounds of low polarity. Comparison with both experimental results and ab initio calculations demonstrate that the method reproduces the general features of the band structure properly. Conformational calculations, as far as can be verified, give the correct overall behaviour.

The Carbon Chain

Polyenes, which were discussed previously, are representative of a particular type of molecule, another example of which is the carbon chain. At low molecular weights chains consisting of carbon atoms alone are seen to exist in two distinct forms, the cumulene and the polyynes. The former has a carbon skeleton with equal bond lengths while the latter exhibits marked bond alternation. Electronic spectra resulting from the two forms are quite different⁽⁷²⁾. When the lowest excitation energy of each form is plotted against the number of carbon atoms in the chain a straight line is obtained in each case; a little evidence of curvature is observed for the polyynes at the high molecular weight limit (Fig. 9).

These spectra raise the possibility of there being two stable forms of the infinite carbon chain. Symmetry considerations, similar to those used in the polyene and hydrogen chains, suggest that the infinite cumulene is electronically degenerate, or near-degenerate, and possibly unstable with respect to a distortion. Detailed calculations show that this instability does

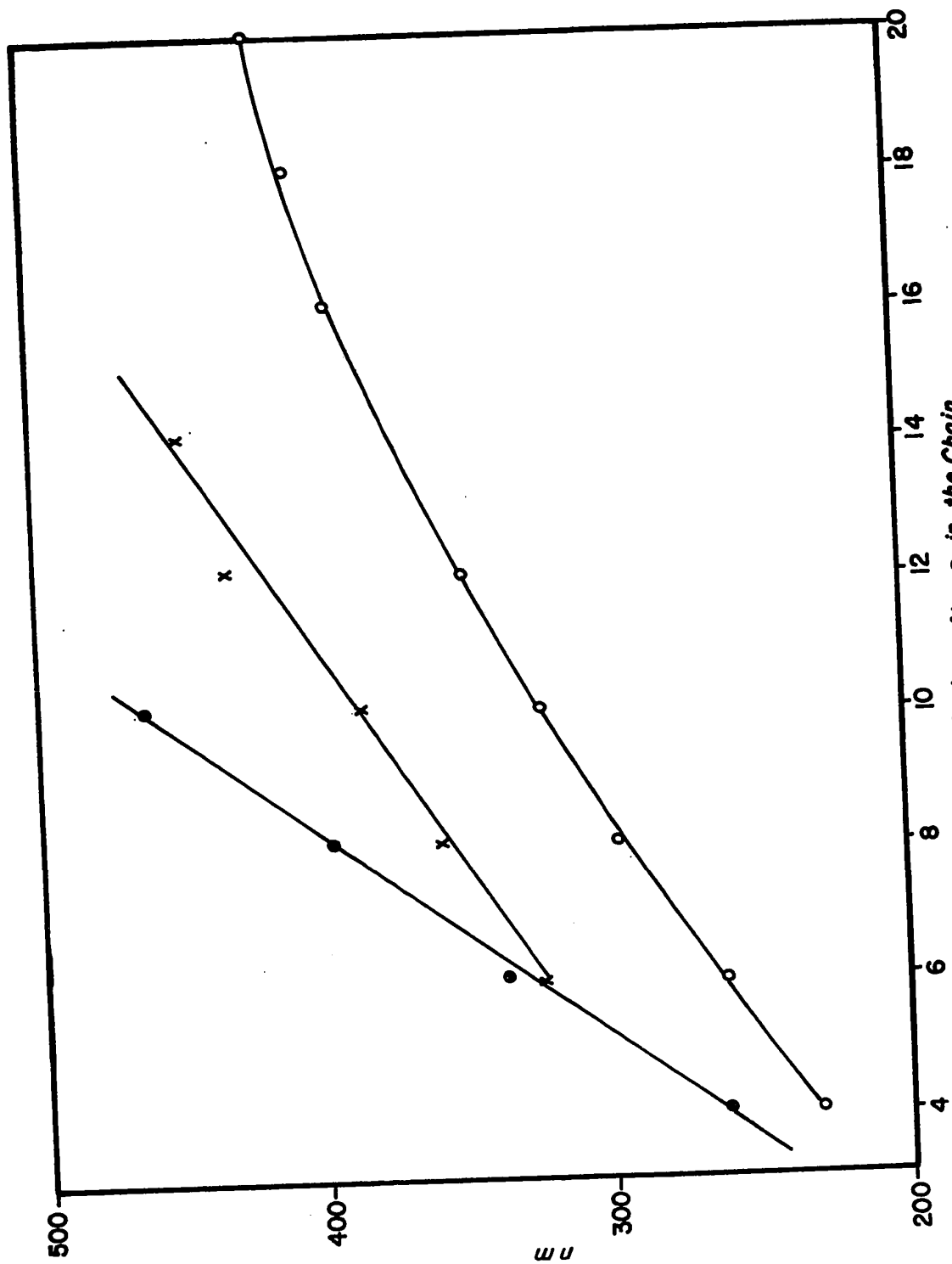


Fig. 9. Experimental results for the effect of increasing chain length on the first excitation energy of polyenes (o), cumulenes (●) and polyyne (x).

occur. The calculated optimum structure of the carbon chain is a linear acetylene-like structure with alternating bond-lengths of 1.224 Å and 1.387 Å. Acetylene has been shown, by X-ray analysis of the solid⁽⁷³⁾, to have a bond length of 1.2087 Å while diacetylene⁽⁷⁴⁾ has carbon-carbon bond lengths of 1.19 ± 0.03 Å and 1.36 ± 0.03 Å. When a "triple" bond length of 1.205 Å is assumed, the "single" bond length is estimated as 1.379 ± 0.001 Å. Clearly the calculated bond lengths for the polymer show an increase over the bond lengths for the shorter members of the series (CNDO/2 gives a bond length 1.200 Å for acetylene). The difference between the long and short bonds in the polyene is also much greater than in the polyene (0.163 Å compared with 0.082 Å, almost exactly a factor of two different).

An upper bound to stabilization energy arising from alternation can be found by subtracting from the energy of the alternant form the energy of the most stable symmetric form as calculated by the polymer program. In the latter case, as in the case of the symmetric polyene, the energy found in this way is at best an upper bound to the energy of the symmetric structure. The stabilization is found to be 7.41 kcal/m (0.0118 a.u./unit cell) compared with a value of 4.81 kcal/m for the polyene. In view of the fact that in the polyene case the number of π electrons being stabilized by the alternation is twice that in the polyene the above results are much as might be expected. The band gap is 10.8 e.v., again larger than that of the polyene.

Long-range π - π interactions which are evident in the polyenes also occur in the acetylenic chain. The convergence is more rapid in this case (Table 7), a reflection, perhaps, of the more strongly alternating nature of the lattice potential. Even the σ density-matrix elements are slightly more rapidly convergent, in spite of the shorter bond lengths. The cell-cell

TABLE 7

Density Matrix Elements for the Optimum Carbon Chain

The intracell bond is taken to be the short bond (1.224 Å) and the intercell bond is taken to be the long bond (1.387 Å). A negative cell index refers to a cell to the left of the origin cell. Because the chain is an alternant hydrocarbon the density matrix elements between translationally equivalent π orbitals are zero.

Cell Index	-3	-2	-1	0	1	2	3
$C_S^I-C_S^I$	-0.0009	-0.0061	-0.0102	1.0346	-0.0102	-0.0061	-0.0009
$C_S^I-C_S^{II}$	0.0030	0.0272	0.4438	0.5042	0.0191	0.0019	0.0003
$C_X^I-C_X^{II}$	0.0141	-0.0475	0.3246	0.8974	-0.2629	0.1156	-0.0566

energies are significant for about six cells on either side of the origin cell; the long-range exchange through the π density-matrix is the only non-zero energy term beyond the third nearest-neighbours.

The experimental excitation energies⁽⁷²⁾ (Fig. 10) for the smaller polyynes show a remarkable linearity but there is some evidence of curvature at the high molecular weight limit. Cumulene results, however, show no such tendency and seem to be consistent with the predicted zero band-gap for the infinite cumulene. The persistence of the separate forms of carbon chain even to ten or twelve atom chains suggests an energy barrier to interconversion of the different forms. The cumulene has the general formula $C_{2n}H_4$ while the polyyne formula is $C_{2N}H_2$. For some critical value of N the cumulene becomes unstable with respect to the polyyne and a hydrogen molecule. Calculation of this value of N would pose a rather interesting problem much as does the calculation of the critical ring size for the onset of bond alternation in cyclic polyenes.

In summary, the carbon chain is predicted to be acetylenic with bond lengths of 1.387 Å and 1.224 Å. A band gap is predicted which is greater than that predicted for the polyene.

Beryllium

The ground state of an isolated Be atom is 1S_0 , arising from the configuration $1s^2 2s^2$. Slater⁽²⁾ points out that the conductivity of the metal depends on the overlap of the energy bands arising from the 2s and 2p atomic functions. It is not clear from first principles whether or not the 2s and 2p bands are broadened enough to overlap in the case of a one-dimensional lattice. Calculations were undertaken for this system to

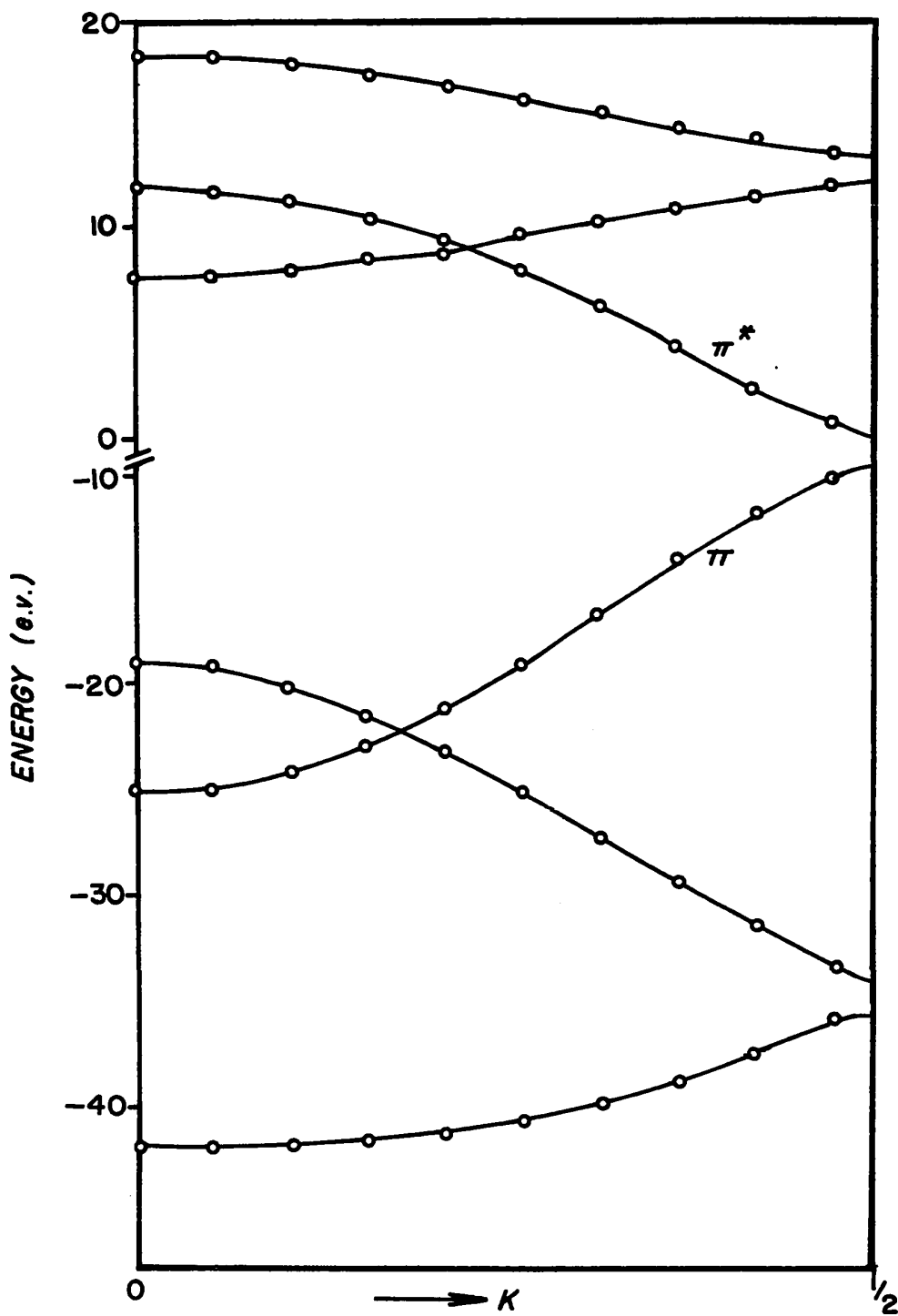


Fig. 10. Band structure of the optimum carbon chain.

determine the ground state and resolve this problem.

Linear symmetric, linear alternant and non-linear zig-zag chains were considered. The calculations indicate that both linear structures are insulators while the zig-zag chain is metallic. Of the two linear structures the symmetric one is predicted to be the more stable having an energy minimum when the lattice constant is 1.9633 Å. Because metallic or non-metallic behaviour is determined by band overlap, a quantity which is quite sensitive to the lattice constant, it should be possible by reducing the lattice constant to convert the chain to a metal. Metallic behaviour begins when the nearest-neighbour distance is 1.8875 Å, the point at which the band gap has fallen to zero. An energy barrier of 3.40 kcal/m. exists between the equilibrium configuration and the onset of metallic behaviour. Above 1.8875 Å the band gap is almost linear with respect to the lattice constant (Fig. 11) having a value of 1.80 eV at the equilibrium separation. Just above 1.8875 Å the system is an intrinsic semiconductor because the band gap is of the order of kT . The highest occupied band (Fig. 12) is a σ band and the lowest vacant one is a π band. CNDO is known to over-stabilize π orbitals⁽¹⁰⁾ and in the present case this may offset the poor model used to calculate the excitation energy; the band-gap is, therefore, probably closer to the true value than the predicted band-gaps of other systems. Furthermore, since CNDO predicts a closed shell structure in spite of this over-stabilization of the lowest conduction band, it is very likely that more elaborate methods will give the same result.

The band structure of the Be chain is quite simple (Fig. 12). It has one interesting feature however. The band gap is between a σ band which changes phase from one atom to the next (it would appear at $k = 1/2$ if the

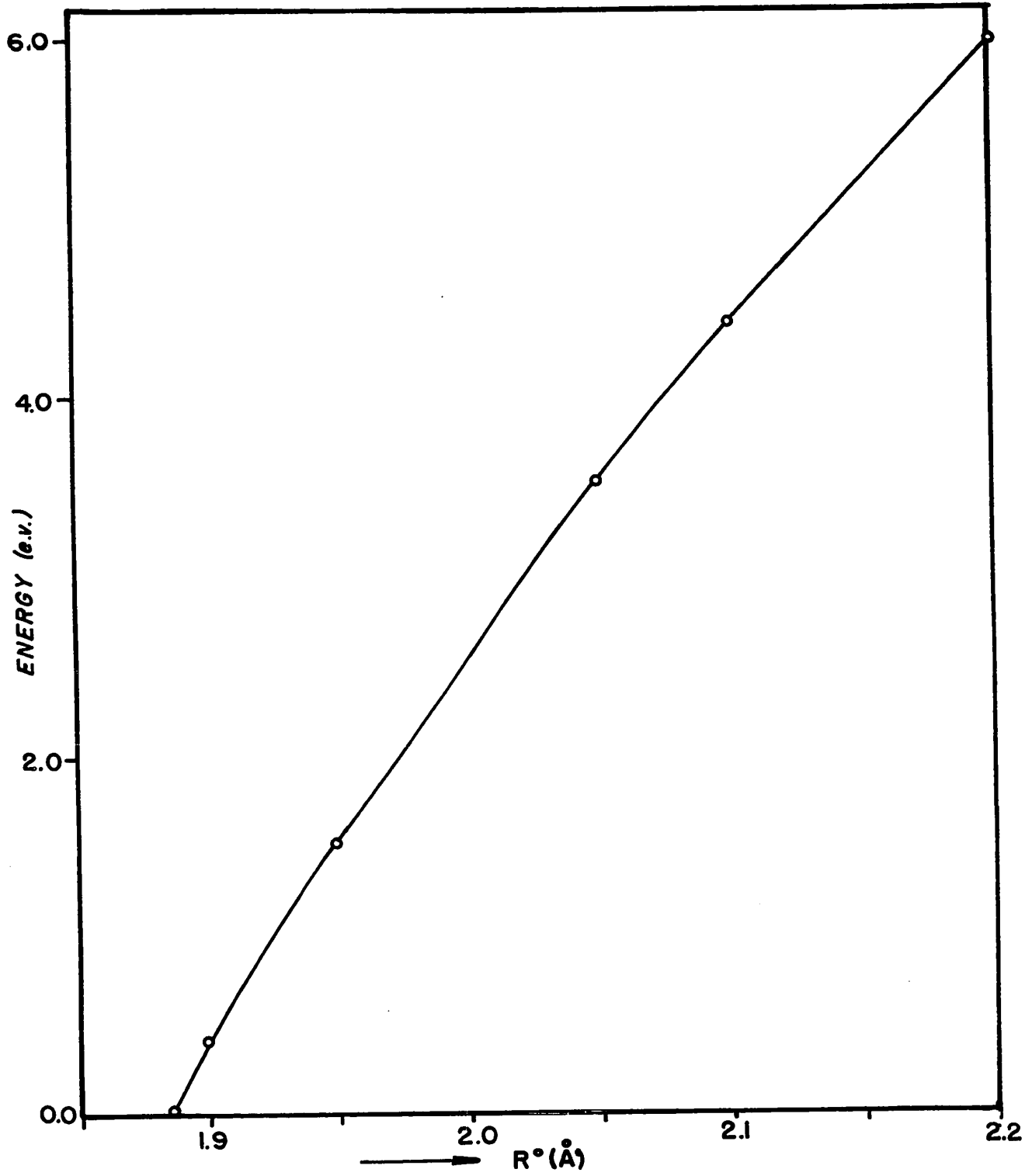


Fig. 11. The band gap of the beryllium chain as a function of the lattice constant.

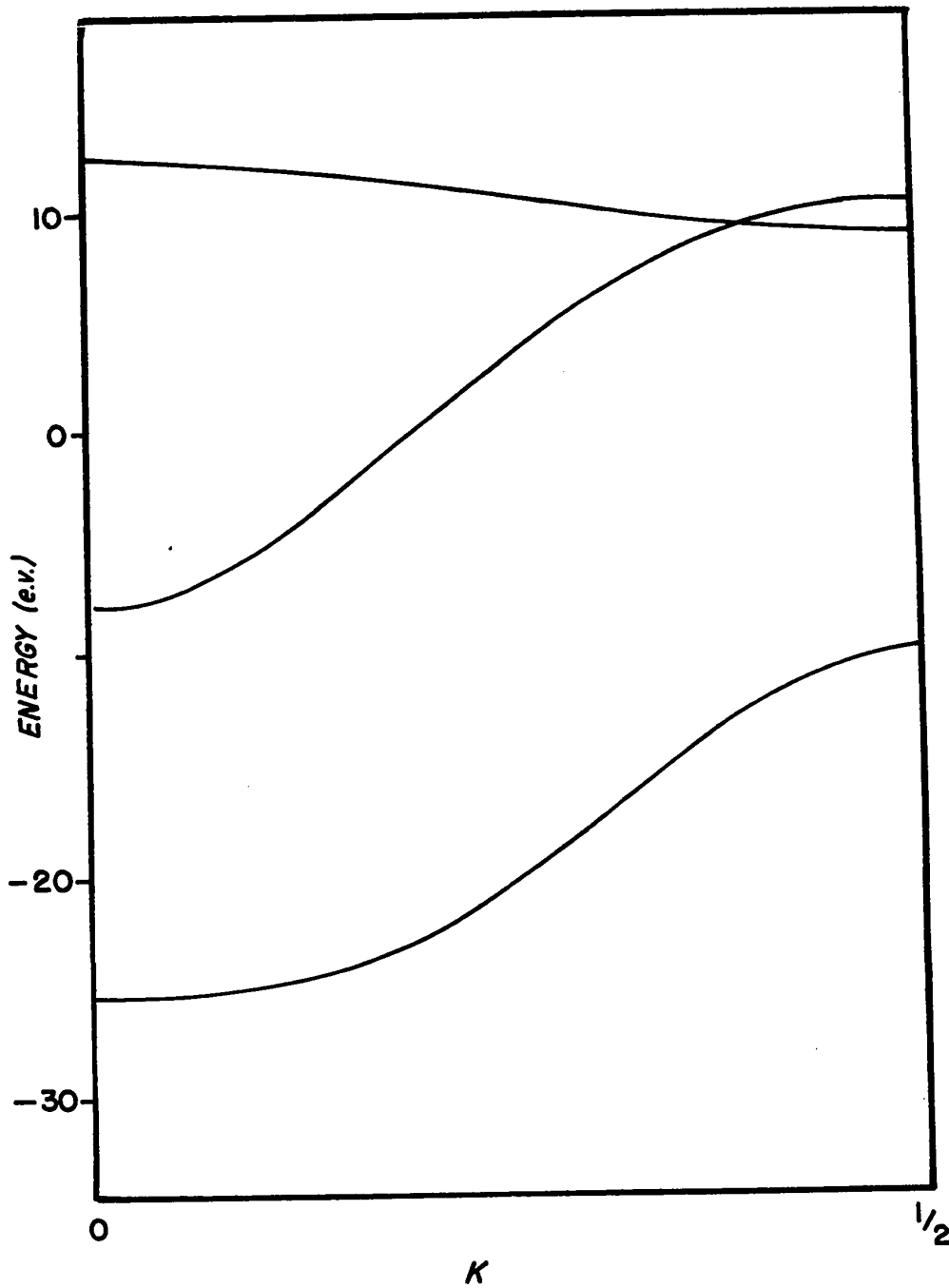


Fig. 12. The band structure of the beryllium chain based on a monatomic cell.

band structure were based on a monatomic cell) and a translationally symmetric π band. Optical transitions between these levels are forbidden but out of plane vibrations with wave vector $q = 1/2$ should cause mixing of the two. The fact that the zig-zag chain is metallic supports this.

Inspection of the real space density matrix and cell-cell energies shows that the linear chain electrons are very tightly bound. The energy of interaction of the origin cell with the third cell away is only $-3.0 \cdot 10^{-7}$ a.u. Binding results primarily from one-electron contributions, e.g., of the -265.8 kcal/m contributed to the electronic binding energy by nearest neighbour interactions, 99% is due to one-electron terms. Even in this case the nearest-neighbour approximation is not totally reliable. Second nearest-neighbour interactions, which amount to -3.87 kcal/m at 1.9633 \AA , drop to -5.44 kcal/m at 1.900 \AA , a 40% increase in stabilization, while the overall energy per unit cell increases by 1.15 kcal/m. Clearly the lattice constant calculated in the nearest neighbour approximation will be larger than that obtained from the more elaborate calculation.

Because it is not possible to calculate the energy of the metallic form of the chain by the present method the ground state of the molecule cannot be definitely assigned. The present results suggest, however, that it is a non-metal as predicted by Peierls⁽⁷⁶⁾.

LiF Chains

Lithium fluoride was chosen, for two reasons, to form the basis for model calculations on ionic linear chains. Crystalline LiF has a lattice energy of -240.1 kcal mole⁻¹⁽⁷⁷⁾, a high value for a lattice composed of monovalent ions. Because all the atoms involved are from the first row of the periodic table they are convenient from the point of view of computation.

Although CNDO is generally very successful in reproducing experimental bond lengths it is unusually inaccurate in the case of LiF, giving a calculated optimum bond length of 2.161 Å compared with an experimental value of 1.51 Å⁽⁹⁾. The CNDO predicted value of the dipole moment is -7.90 debye while the experimental value is -6.6 debye⁽⁹⁾. In view of these discrepancies, it is necessary to be particularly circumspect in the interpretation of the results for the LiF chain.

In the calculations both linear and skewed chains were considered. The linear structure was optimized and the possibility of bond alternation investigated. The optimum symmetric chain has a lithium-fluorine separation of 2.255 Å, an increase of 0.094 Å from the calculated molecular bond length. The lattice stabilization at the optimum symmetric chain geometry is -55.2 kcal m⁻¹, significantly lower than that for the three-dimensional crystal but sizeable nonetheless. No evidence of bond alternation could be found. Skewed chains were shown to be more stable than linear ones, but no energy minimum could be found. Results of skewed-chain calculations seem to indicate that the system is trying to stabilize itself by going to a two- or three-dimensional structure.

At the calculated equilibrium molecular separation the net charge on Li is +0.563 while in optimum linear chain structure the net charge on Li is +0.523. Comparison of results for the LiF molecule at a separation 2.11 Å and a symmetric linear chain with the same separation shows that the net charge on Li in the chain (+0.479) is substantially reduced from that in the free molecule (+0.556). These results are certainly contrary to what one would expect in going from the molecule to the three-dimensional crystal; whether the effect is due to a qualitative difference between the chain structure and the three-dimensional structure, or is due to some limitation in the method, or

both, is not clear. Results on H-F systems, to be presented later, suggest that the latter is the more likely.

The band structure of the chain (Fig. 13) is much as expected. The bands are narrow with little curvature. It is, however, one of the few cases where the vacant, or conduction, bands are shown by CNDO to be wider than the valence bands. The band widths, in order of decreasing stability, are 3.03 ev, 0.988 ev, 0.57 ev, 4.28 ev, 3.27 ev, and 3.63 ev. These bands can be labelled according to the dominant atomic-orbital components which are, respectively, F_s , F_π , F_z , Li_s , Li_π , Li_z . The band gap is 12.53 ev showing that, as expected, the linear chain is a good insulator. An interesting possibility is indicated by the band structure: the lowest vacant level is at $k = 0$ in the Li_s band, having an orbital energy of -1.13 ev. This suggests the possibility of a stable anion of the chain. Recent limited CNDO calculations on solid LiF show a similar feature in the three-dimensional band structure. Detailed comparison of the present results with those of recently reported⁽⁷⁹⁾ calculations of the band-structure of the three-dimensional LiF crystal is not possible because of the lack of detail provided. The general features of the results of both calculations are quite similar.

Analysis of the real space density matrix elements and the cell-cell energies shows that the binding in the chain has many of the characteristics of an ionic structure. At three cells separation all density matrix elements are less than 1.10^{-3} . Nearest-neighbour coulomb interactions are actually destabilizing but all subsequent coulomb interactions are stabilizing. Of the second-nearest-neighbour interaction only 8% is due to non-coulombic effects, such as overlap and exchange. At greater separations these effects are negligible; all subsequent interactions are simply those of a set of point

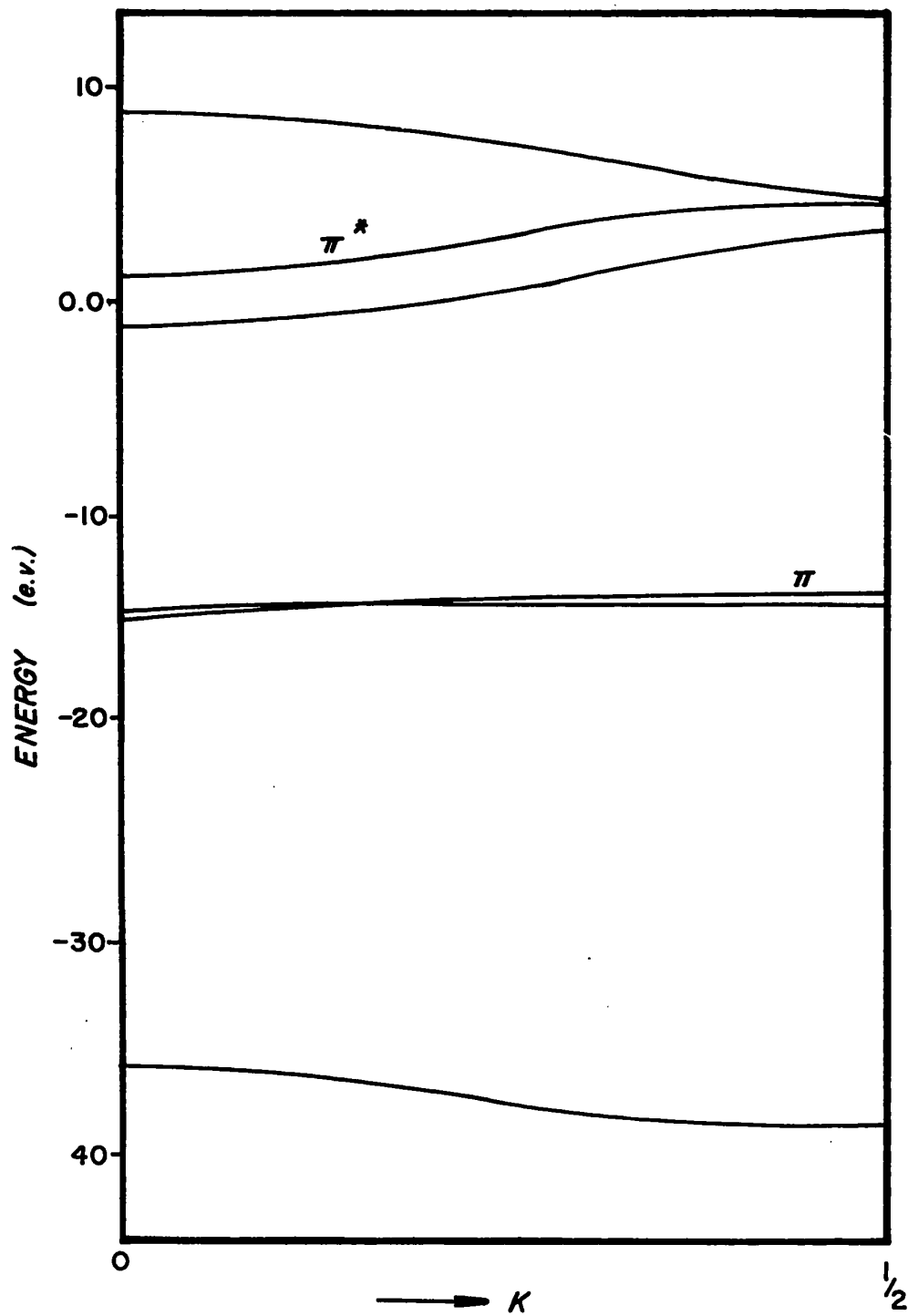


Fig. 13. The band structure of the lithium fluoride chain in the optimum linear configuration.

charges in the different unit cells interacting. The lattice sums are included up to 19 cells on each side of the origin. In order to estimate the long-range, or far-field, correction due to the remainder of the lattice a simple model was developed.

The effect at a distance of the net charges in the unit-cell can be shown to be equivalent to that of a point-dipole of the appropriate magnitude⁽⁷⁸⁾. Classical electrostatics gives the energy of interaction of two parallel dipoles $\bar{\mu}$, of equal magnitude μ , connected by the vector \underline{R} to be⁽⁷⁸⁾

$$E = \frac{\bar{\mu} \cdot \bar{\mu}}{|\underline{R}|^3} - 3 \frac{(\bar{\mu} \cdot \bar{R})}{|\underline{R}|^5} = \frac{\mu^2}{|\underline{R}|^3} (1 - 3 \cos^2 \theta) \quad [98]$$

where θ is the angle between $\bar{\mu}$ and \bar{R} . Since all unit cells are equivalent, the point dipole is at the same position in each, whence $|\bar{R}| = na$ for some integer n and where a is the lattice constant.

$$E_{F.F.} = \sum_{\underline{R}} \frac{\mu^2}{|\underline{R}|^3} (1-3\cos^2\theta) = \frac{\mu^2}{a^3} (1-3\cos^2\theta) \left\{ \sum_{n=-\infty}^{-n_H} \frac{1}{|n|^3} + \sum_{n=n_H}^{\infty} \frac{1}{n^3} \right\} \quad [99]$$

The sum, which is clearly convergent, is independent of detail of the lattice and need be evaluated only once. Its value is $2.9197102 \cdot 10^{-3}$ for $n_H = 19$. Typical values of E_{FF} are less than 10^{-4} . However, the significant part of E_{FF} in determining the configuration of the chain is its variation with changes in the geometry of the unit cell. When a is increased, μ also increases, so that the quantity μ^2/a^3 varies quite slowly; the variation for reasonable changes in a is an order of magnitude less than E_{FF} itself. The angular dependence is significant only for non-linear structures for which no stable minimum can be found anyway, and so it is reasonable to neglect E_{FF} in determining the optimum geometry of the linear chain.

It seems quite likely that the long LiF bond length and the repulsive coulombic terms in the nearest-neighbour interaction are due, in part at least, to the use of the approximation [equation 29]

$$V_{AB} = -Z_B \gamma_{AB}$$

The interaction of two diffuse densities is smaller than the interaction of one diffuse density with a point charge. Li, having the smallest valence shell orbital exponent of any atom in the first row and hence very diffuse orbitals, is the atom for which this approximation is poorest. As the separation between the atoms decreases this approximation becomes consistently worse and the destabilization increases. This approximation should therefore make Li bond lengths long; the error should be a maximum when the charge separation, the quantity multiplying V_{AB} , is greatest, that is, LiF. This effect is known as the neglect of penetration⁽⁹⁾.

The effect of this neglect of the penetration integral can be seen in detail in the coulomb contributions to the total energy per unit cell (-27.939047 au per cell). The sum of all coulomb contributions in a 39 cell segment at the calculated optimum linear geometry is -22.888218 au per cell. Of this total -23.013322 au per cell is due to the intra-cell coulomb energy of the origin unit cell. This contribution arises mainly from the fluorine and lithium self-energies (coulomb) since the lithium-fluorine coulomb interaction is repulsive in this approximation (+0.0422 au per cell). Clearly the coulomb interaction of the origin cell with the lattice is repulsive, to the order of 0.1251045 au per cell. However, the contribution of the nearest-neighbour terms to this is 0.1284658 au per cell, so that the remaining non-nearest-neighbour contributions are stabilizing (-0.003613 au per cell).

In the region where the neglect of penetration is important the coulomb terms are much more repulsive than one would otherwise expect, leading to the long calculated bond lengths. Another convergence problem of considerable importance is that of the electron density. Truncation of the lattice sums might lead to an incorrect value of the polarizing field and hence to structures of incorrect polarity. Calculations using the modified Ewald transformation (Appendix 1) were used to check this. Comparison (Table 8) of the resulting density matrices with those from the direct lattice summation shows the results to be identical. This, together with the results given in Appendix 2, suggests that the use of reasonable lattice-sum ranges gives the correct result and that convergence problems are not significant in this case.

Inspection of the highest filled σ band, which is only marginally (0.3 eV) below the highest filled π band, shows that this $k = 1/2$ level has a dominant F_z component. The lowest vacant σ orbital is at $k = 0$ and is mainly Li_s in character. Distortion would remove a plane of symmetry and allow s-z mixing at the zone boundaries. This suggests that the lattice-vibration which destroys this plane of symmetry might be quite soft. Using the curve fitting method discussed previously, the breathing mode, which retains the plane of symmetry, is found to have a larger force constant than the alternating mode. The absolute values of these force constants, $2.96 \cdot 10^4$ dyne/cm and $2.42 \cdot 10^4$ dyne/cm respectively, are not likely to be correct but the ordering is significant. Again the "breathing mode" cannot be a true mode of the system.

In view of the foregoing results it is difficult to say whether or not a linear chain potential is sufficient to sustain a truly ionic structure.

TABLE 8

Comparison of the density matrices resulting from a calculation
using truncated lattice sums and one using lattice summations
obtained by use of the Ewald transformation

The results given here are for the density matrix elements in the origin
unit cell of a linear LiF lattice having a lattice constant of 2.0 Å.

Direct Calculation

	F_S	F_X	F_Y	F_Z
Li _S	0.3105	0.0	0.0	-.1758
Li _X	0.0	0.2982	0.0	0.0
Li _Y	0.0	0.0	0.2982	0.0
Li _Z	0.2932	0.0	0.0	-.2053

Ewald Transformation

	F_S	F_X	F_Y	F_Z
Li _S	0.3105	0.0	0.0	-.1758
Li _X	0.0	0.2982	0.0	0.0
Li _Y	0.0	0.0	0.2982	0.0
Li _Z	0.3932	0.0	0.0	-.2053

The system has many characteristics of an ionic lattice, narrow valence-band structure, very tight charge distributions, large coulomb interactions at long range, very short-range non-coulombic interactions and equal bond lengths throughout. On the other hand, the net charges are considerably smaller than might be expected and, more important, decrease on going from the molecule to the chain. It is difficult to judge whether this is an effect of the parameterization or whether it is a genuine effect. It seems more likely that in this particular case the approximations are unduly severe and that the parameterization for lithium may not be very good. These results show that care is necessary in the interpretation of semi-empirical results, but also, given this care, that useful results can be obtained by these methods.

Hydrogen Fluoride

Hydrogen bonded systems have been of considerable interest to chemists since the phenomenon was first identified; the discovery of the crucial role played by these bonds in biological systems⁽⁸¹⁾ heightened this interest. Discussion of the nature of this weak bonding has continued unabated for many years^(81,82). A number of studies on dimers, small polymers and solids in which hydrogen bonding is the main binding force have been published⁽⁸²⁾ recently. Both semi-empirical and ab initio S.C.F. methods have been used in these investigations; in this way, they provide a basis for the assessment of the applicability of semi-empirical methods to these systems. Both ab initio and semi-empirical methods provide results which are qualitative and, at best, semi-quantitative. Experimental results show that ab initio calculations using large basis sets provide better results than the semi-empirical methods. Nevertheless, the latter do provide good qualitative and adequate quantitative

results⁽⁸²⁾.

Hydrogen fluoride is the most striking example of a hydrogen-bonded system. Solid hydrogen fluoride consists of "infinitely" long, zig-zag (Fig. 14) chains (in which the binding is by means of hydrogen bonds) stacked together to form a three-dimensional structure⁽⁸³⁾. Liquid hydrogen fluoride is also believed to be extensively hydrogen-bonded. Even in the gas phase this behaviour persists, with considerable evidence for the existence of short polymers, notably $(\text{HF})_6$, which persist even at room temperature⁽⁸⁴⁾. In view of this, HF seems to be a particularly suitable system on which to test the method.

Calculations were performed on HF polymers in both the linear and zig-zag configurations. The latter are clearly the more stable but the potential surface is unusually flat. Optimization of the chain geometry is very difficult because of this, and because of the sensitivity of the geometrical parameters to one another. The approximate optimum calculated structure is one in which the fluorine-fluorine nearest-neighbour distance is 2.2625 \AA with an F-F-F angle of 128° . The system is predicted to be molecular, with a bond length of 1.064 \AA .

A definite value for the H-F bond length in crystalline HF is not yet available. Experimental difficulties make this a particularly elusive parameter, and to date the best estimate is that derived from wide-line nuclear magnetic resonance experiments⁽⁸⁵⁾. The raw data suggest a value of $1.02 \pm 0.03 \text{ \AA}$, but it may be as low as $0.95 \pm 0.03 \text{ \AA}$. Either way, the result clearly indicates a substantial increase in the bond length from the free molecule value of 0.917 \AA ⁽⁸⁶⁾. CNDO predicts the molecular bond length to be 1.000 \AA ⁽⁹⁾, and so the present calculations give an increase of 0.064 \AA

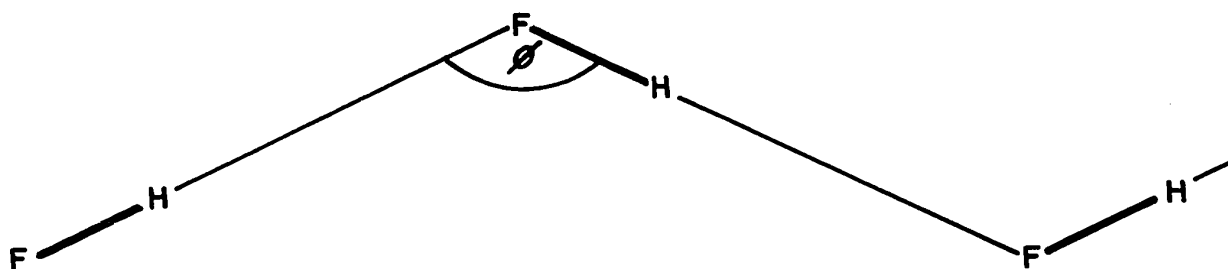


Fig. 14. Diagram of the unit cell of the zig-zag hydrogen fluoride chain.

on formation of the chain, in qualitative agreement with the experimental result.

X-ray analysis of crystalline HF⁽⁸³⁾ gives a value of $2.49 \pm 0.01 \text{ \AA}$ for the shortest fluorine-fluorine distance in the chain and an F-F-F angle of 120.1° . The calculated values of 2.2625 \AA and 128° , respectively, deviate considerably from these. Of the two the F-F bond length discrepancy is the more striking. Calculations on dimers, and on short polymers, show that CNDO consistently underestimates the F-F distance; the CNDO result for the dimer is 2.45 \AA compared with a value of 2.88 \AA obtained by ab initio methods and an experimental value of $\sim 2.8 \text{ \AA}$ ⁽⁸²⁾.

Both ab initio and semi-empirical methods give very flat potential surfaces for small aggregates of HF molecules. Kollman and Allen, in their ab initio calculations, found that a decrease of 0.25 \AA in the F-F distance from the equilibrium value of 2.88 \AA to 2.63 \AA corresponds to an energy change of only 0.94 kcal/m . A comparable decrease from the equilibrium value of 3.00 \AA to 2.76 \AA in the hydrogen bond length of the linear water dimer gives rise to an energy change of 0.75 kcal/m .

Recent experimental evidence regarding the hexamer⁽⁸⁴⁾ and the dimer⁽⁸³⁾ in the gas phase suggests that they are very flexible. The evidence to date points to the fact that the hydrogen bonds of HF aggregates are not as sensitive to structural detail as was previously believed.

It might be thought from this that the energy of stabilization with respect to the monomer is small. This does not seem to be the case. CNDO gives a dimerization energy of $\sim -9 \text{ kcal/m}$, while ab initio calculations⁽⁸²⁾ predict a value of -4.6 kcal/m . The chain stabilization energy calculated here, possibly a similar overestimate, is -16.7 kcal/m . Recent CNDO calculations by Bacon and Santry⁽⁸⁷⁾ on HF aggregates (using a different

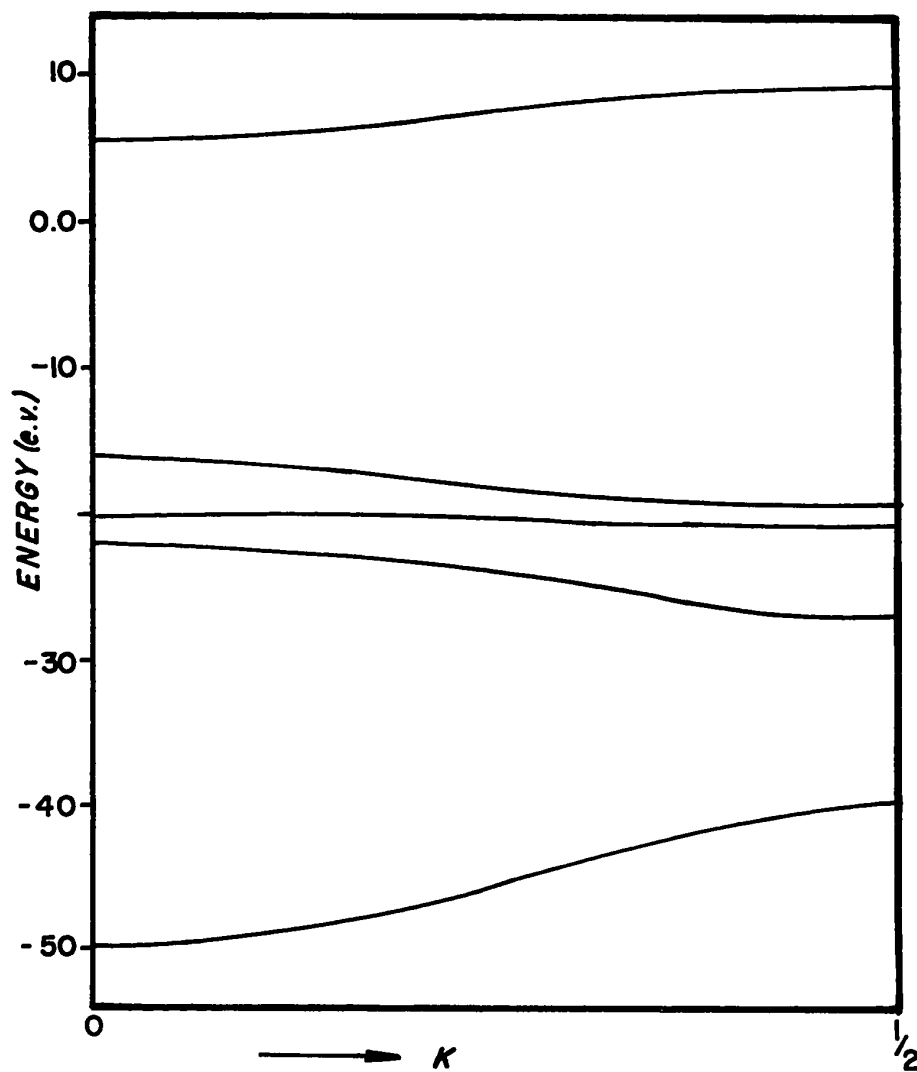


Fig. 15. The band structure of the zig-zag hydrogen fluoride chain.

approach) give the chain stabilization energy to be -12.77 kcal/m and the crystal stabilization energy to be -13.09 kcal/m. These calculations also show an increase in the curvature of the potential surface in going from the chain to the crystal.

What overall conclusions can be drawn from these results? A substantial stabilization is achieved when HF molecules form clusters or solids; the resulting structures are reasonably flexible, the energy required to distort them being quite small. Calculations both semi-empirical and ab initio which reflect an essentially static approach to the problem may not be appropriate for the discussion of small aggregates of HF molecules. The results for the HF polymer suggest that the detailed structure of the chain is as much a property of the three-dimensional stacking of the chains as it is of the chains themselves.

CHAPTER 3

A PERTURBATION THEORY OF MOLECULAR DISTORTIONS

The theory presented in the previous chapters assumes that the polymer has perfect translational symmetry. This, of course, is an approximation and presumably a rather severe one. When studying the stability of small molecules one ideally varies all the geometrical parameters until an absolute energy minimum is found. The polymer theory permits only the parameters within one unit cell to be varied; all other cells are then taken to be identical with this one. Clearly such an optimization procedure produces a structure which corresponds to an energy minimum with respect to homogeneous deformations only⁽⁴⁰⁾. While it might seem likely that the structure is an energy minimum with respect to all deformations there is no guarantee that this is the case. Indeed there is evidence that some structures are stabilized by disorder and that some of this stabilization results from energetic, as well as entropy, considerations⁽⁸⁸⁾. Therefore, a theory capable of handling non-homogeneous deformations would be useful in the discussion of stability. Such a theory would also be useful for the calculation of force constants.

This chapter introduces a possible method for handling these problems. The method is developed in the formalism appropriate to small-molecule calculations. Its accuracy is tested by detailed comparison against direct S.C.F. calculations on a number of representative molecules.

The intention here is to develop a method of finding a wavefunction for some nuclear configuration, given a wavefunction for a neighbouring configuration. In order to limit the labour involved certain criteria must be satisfied:

- (1) Matrix diagonalization must not be a necessary part of the method.
- (2) The method must employ only the normal types of integrals used in S.C.F. theory.
- (3) The method must not employ a greater number of integrals than the normal S.C.F. method.

By choosing a suitable definition of the perturbation operator, a method satisfying these criteria can be found. The method, which is described below, assumes the CNDO approximations. Extension of the method to deal with non-orthogonal basis sets modifies the algebra but not the overall scheme. The main additional feature in the application of the method to general basis sets is the need to include corrections to the ortho-normalization of the basis functions⁽⁸⁹⁾, a problem which does not arise in the Z.D.O. approximation.

The following scheme is proposed. The superscript D refers to the molecular configuration considered to be "distorted", while the superscript (0) refers to the configuration taken as zero order, for which solutions of self-consistent field equations

$$\underline{FC} = \underline{OCE} \quad [17]$$

exist. The superscript (n) refers to the nth order term in the expansion of any quantity in terms of a power series in the perturbation parameter λ (to be set to units, finally). Equation [100A] defines the corrections to the basic molecular integrals

$$\lambda T_{\mu\nu}^{(1)} = T_{\mu\nu}^D - T_{\mu\nu}^{(0)} \quad [100A]$$

$$\lambda U_{\mu\nu}^{(1)} = U_{\mu\nu}^D - U_{\mu\nu}^{(0)} \quad [100B]$$

$$\lambda \langle \mu\nu | \sigma\lambda \rangle^{(1)} = \langle \mu\nu | \sigma\lambda \rangle^D - \langle \mu\nu | \sigma\lambda \rangle^{(0)} \quad [100C]$$

where

$$T_{\mu\nu} = \int \chi_{\mu}^*(1) \left[-\frac{1}{2} \nabla^2\right] \chi_{\nu}(1) d\tau_1 \quad [101A]$$

$$U_{\mu\nu} = \int \chi_{\mu}^*(1) \left[-\sum_A V_A(\mathbf{r})\right] \chi_{\nu}(1) d\tau_1 \quad [101B]$$

$$\langle \mu\nu | \sigma\lambda \rangle = \iint \chi_{\mu}^*(1) \chi_{\nu}(1) \frac{1}{r_{12}} \chi_{\sigma}^*(2) \chi_{\lambda}(2) d\tau_1 d\tau_2 \quad [101C]$$

In keeping with the approximate M.O. method the basis set of functions, χ_{μ} , is assumed to be orthonormal. In terms of these integrals, it immediately follows for the one electron Hamiltonian, H, that

$$H^D = H^{(0)} + \lambda H^{(1)} \quad [102]$$

Only first order corrections to the one electron Hamiltonian occur. E, the electronic energy, F, the Fock matrix, P, the bond order matrix. and G, the electron repulsion matrix may also be expanded in terms of λ , thus

$$\begin{aligned} E^D &= E^{(0)} + \lambda E^{(1)} + \lambda^2 E^{(2)} + \dots \\ F^D &= F^{(0)} + \lambda F^{(1)} + \lambda^2 F^{(2)} + \dots \\ P^D &= P^{(0)} + \lambda P^{(1)} + \lambda^2 P^{(2)} + \dots \\ G^D &= G^{(0)} + \lambda G^{(1)} + \lambda^2 G^{(2)} + \dots \end{aligned} \quad [103]$$

The self-consistent field equations for G may be written

$$G_{\mu\nu} = \sum_{\sigma\lambda} P_{\sigma\lambda} \left\{ \langle \mu\nu | \sigma\lambda \rangle - \frac{1}{2} \langle \mu\lambda | \sigma\nu \rangle \right\} \quad [104]$$

Expanding the various factors in terms of powers of λ and collecting terms of the appropriate orders together gives

$$G_{\mu\nu}^{(n)} = \sum_{\sigma\lambda} \left[P_{\sigma\lambda}^{(n-1)} \left\{ \langle \mu\nu | \sigma\lambda \rangle^{(1)} - \frac{1}{2} \langle \mu\lambda | \sigma\nu \rangle^{(1)} \right\} + P_{\sigma\lambda}^{(n)} \left\{ \langle \mu\nu | \sigma\lambda \rangle^{(0)} - \frac{1}{2} \langle \mu\lambda | \sigma\nu \rangle^{(0)} \right\} \right] \quad [105]$$

Since, from the choice of perturbation, $\langle \mu\nu | \sigma\lambda \rangle^{(2)} \equiv 0$, $p^{(n)}$ does not appear in any equation for G beyond $(n+1)^{\text{th}}$ order. It is also clear that

$$\begin{aligned} \underline{F}^{(n)} &= \underline{H}^{(n)} + \underline{G}^{(n)} \\ &= \underline{G}^{(n)} \quad n > 1 \end{aligned} \quad [106]$$

The perturbation equations

$$\underline{F}^{(0)}\underline{C}^{(1)} + \underline{F}^{(1)}\underline{C}^{(0)} = \underline{C}^{(0)}\underline{E}^{(1)} + \underline{C}^{(1)}\underline{E}^{(0)} \quad [107]$$

$$\underline{F}^{(0)}\underline{C}^{(2)} + \underline{F}^{(1)}\underline{C}^{(1)} + \underline{F}^{(2)}\underline{C}^{(0)} = \underline{C}^{(0)}\underline{E}^{(2)} + \underline{C}^{(1)}\underline{E}^{(1)} + \underline{C}^{(2)}\underline{E}^{(0)} \quad [108]$$

etc. are solved by method of self-consistent field perturbation theory⁽⁹⁰⁾.

The corrections to the coefficient matrix are represented by linear combinations of the zero-order wavefunctions⁽⁸⁷⁾, in matrix notation

$$\begin{aligned} \underline{C}^{(1)} &= \underline{C}^{(0)}\underline{A} \\ \underline{C}^{(2)} &= \underline{C}^{(0)}\underline{B} \end{aligned} \quad [109]$$

Applying the orthonormality conditions ($\underline{1}$ = unit matrix)

$$\begin{aligned} \tilde{\underline{C}}^{(0)}\underline{C}^{(0)} &= \underline{1} \\ \tilde{\underline{C}}^{(0)}\underline{C}^{(1)} + \tilde{\underline{C}}^{(1)}\underline{C}^{(0)} &= 0, \text{ etc.} \end{aligned} \quad [110]$$

the elements of A can be shown to be

$$A_{ij} = \frac{F_{ij}^{(1)}}{\epsilon_j^{(0)} - \epsilon_i^{(0)}} = \frac{\sum_{\mu\nu} F_{\mu\nu}^{(1)} C_{\mu i}^{(0)} C_{\nu j}^{(0)}}{\epsilon_j^{(0)} - \epsilon_i^{(0)}} \quad [111]$$

$\tilde{\underline{C}}$ is the transpose of \underline{C} ; since \underline{C} is an orthogonal matrix $\tilde{\underline{C}}$ is \underline{C}^{-1} . $\epsilon_i^{(0)}$ is the zero-order orbital energy of orbital "i". From equation [109]

$$C_{\mu i}^{(1)} = \sum_j C_{\mu j}^{(0)} A_{ji} \quad [109A]$$

The summation runs over all orbitals. The first-order correction to the density matrix is given by

$$P_{\mu\nu}^{(1)} = 2 \sum_{\lambda}^{\text{oc}} [C_{\mu\lambda}^{(0)} C_{\nu\lambda}^{(1)} + C_{\mu\lambda}^{(1)} C_{\nu\lambda}^{(0)}] \quad [112]$$

Substituting from equation [109A] into equation [112] and using the fact that A_{ij} is skew symmetric (equation [111]), it can be shown that when expanding $C^{(1)}$, the correction to the μ^{th} component of occupied orbital " λ ",

$$C_{\mu\lambda}^{(1)} = \sum_m^{\text{vac}} C_{\lambda m} A_{m\lambda} \quad [109B]$$

only contributions from vacant orbitals need be included. The apparent singularity in A_{ii} is thus avoided. Similar formulae can be obtained for the elements of the matrix B occurring in the second-order equations⁽⁸⁷⁾.

Cases where the orbital occupancy changes when the perturbation is introduced cannot be handled in this way. A different formalism must be developed to deal with such changes.

The scheme of calculation is the following: a first estimate of $F^{(1)}$ (e.g., $H^{(1)}$) is used to calculate $P^{(1)}$; $P^{(1)}$ is used to calculate a new $F^{(1)}$ and this cycle is repeated until $P^{(1)}$ is constant to within some preset limit. Higher order equations can be solved in a similar manner; explicit expressions and procedures are given in reference 87. The total energy (and orbital energies) to any order may be found in the usual way, e.g., for first order

$$E_{\text{EL}} = \frac{1}{2} \sum_{\mu\nu} P_{\mu\nu} (H_{\mu\nu} + F_{\mu\nu}) \quad [40]$$

$$\rightarrow E_{\text{EL}}^{(1)} = \frac{1}{2} \sum_{\mu\nu} P_{\mu\nu}^{(0)} [H_{\mu\nu}^{(1)} + F_{\mu\nu}^{(1)}] + P_{\mu\nu}^{(1)} [H_{\mu\nu}^{(0)} + F_{\mu\nu}^{(0)}] \quad [113]$$

$$\underline{\underline{\text{CFC}}} = \text{diag}(\epsilon_1, \epsilon_2, \dots, \epsilon_n) \quad [114]$$

$$\rightarrow \underline{C}^{(0)} \underline{F}^{(1)} \underline{C}^{(0)} = \underline{C}^{(0)} \underline{F}^{(0)} \underline{C}^{(1)} + \underline{C}^{(1)} \underline{F}^{(0)} \underline{C}^{(0)} = \text{diag}[\epsilon_1^{(1)}, \epsilon_2^{(1)}, \dots, \epsilon_n^{(1)}] \quad [115]$$

The orthogonality properties and properties of the solutions of $F^{(0)}$ can be used to simplify these equations for certain orders.

Results

The scheme has been implemented to second order in the CNDO/2 approximation. A number of representative molecules have been studied and the results are summarized below.

Geometry changes, including bond length and bond angle variations, were used to test the method and the results are compared with the results of direct S.C.F. calculations. The molecules studied, ethylene, carbon dioxide, and methanol, include single and double bonds, polar and non-polar bonds. The quantities computed include the total energies, orbital energies, density matrices and, for methanol, the dipole moment components.

For "reasonable" changes in geometry (5%-10% of the value of a given parameter) the relative error in the energy change is less than 1%. Relative errors in the changes in density matrix elements are of the order of 1-2%. That the overall reproduction of the S.C.F. results is good is most readily shown by the graphs (Figs. 16 and 17) and Tables 9 and 10 below.

Discussion

The second order theory is capable of predicting potential curves quite accurately over reasonable ranges of the geometrical parameters. This is true even when the starting, zero-order, configuration does not correspond to the energy minimum.

First order results are qualitatively correct. Quantitatively it is

TABLE 9
Comparison of P.T. and S.C.F. Results for Geometry Variations
in Ethylene

Geometrical parameters:

R = C-C bond length

θ = CCH bond angle

ϕ is the angle between the planes containing the CH₂ groups.

The configuration R = 1.34 Å

θ = 120°

ϕ = 0

is taken as the zero-order geometry. All energies are in atomic units.

Variation in R

ΔR	ΔE (S.C.F.)	ΔE (P.T.)	% Relative Error
+0.05 Å	0.006651	0.006656	0.072
+0.10 Å	0.024953	0.024993	0.16
+0.15 Å	0.052683	0.052820	0.26

Relative errors in the changes in the density matrix elements are all less than 2.4% or, in absolute terms, 1.10^{-5} .

Variation in θ

The matrix of relative errors (the change in the total energy) given here assumes the θ value in the column at the left to be the zero-order value.

θ =	116	118	120	122	124
116					2.14
118	0.07			0.50	1.61
120	0.28	$9.5 \cdot 10^{-4}$		0.35	1.47

The calculated optimum θ value is $\sim 122^\circ$ and so the $116^\circ \rightarrow 124^\circ$, etc., involve passing the minimum. Although the results are not as good as when both points are on the same side of the minimum they are still acceptable, the absolute error for $116^\circ \rightarrow 124^\circ$ being $2.75 \cdot 10^{-4}$. In this case the largest relative error in the density matrix is 0.23%.

Variation in ϕ

See the discussion for details of this case.

	Relative Errors	
	E	P
$\phi = 0 \rightarrow \phi = 6^\circ$ (applied symmetrically)	0.032%	0.25%
$\phi = 0 \rightarrow \phi = 4^\circ$ (unsymmetric)	0.25%	all errors in $P \leq 2 \cdot 10^{-6}$

TABLE 10
Results for Carbon Dioxide

Geometrical Parameters: R1 and R2 are the carbon-oxygen bond lengths and θ is the OCO bond angle.

The zero order configuration is R1 = R2 = 1.615 Å, with $\theta = 180^\circ$.

	R1	R2	θ	Error in E	ρ_C	ρ_{O_1}	ρ_{O_2}		$\Delta\rho_{\max}$
(i)	1.645	1.645	180	0.088%	3.5179	6.2410	6.2410	SCF	0.2%
				5.10^{-5} au	3.5179	6.2411	6.2411	PT	$1.3.10^{-4}$
(ii)	1.584	1.645	180	0.55%	3.5182	6.2396	6.2422	SCF	0.8%
				$1.4.10^{-5}$ au	3.5183	6.2396	6.2421	PT	7.10^{-4}
(iii)	1.615	1.615	170	6.93%	3.5178	6.2411	6.2411	SCF	4%
				4.10^{-5} au	3.5177	6.2411	6.2411	PT	4.10^{-3}

Comparison of First and Second Order Results

	$100E^{(1)}/\Delta E$	$100[E^{(1)}+E^{(2)}]/\Delta E$
(i)	66.8	100.1
(ii)	38.1	100.5
(iii)	199.0	106.9

Systematic variation in R_{CO} is shown in Fig. 16 .

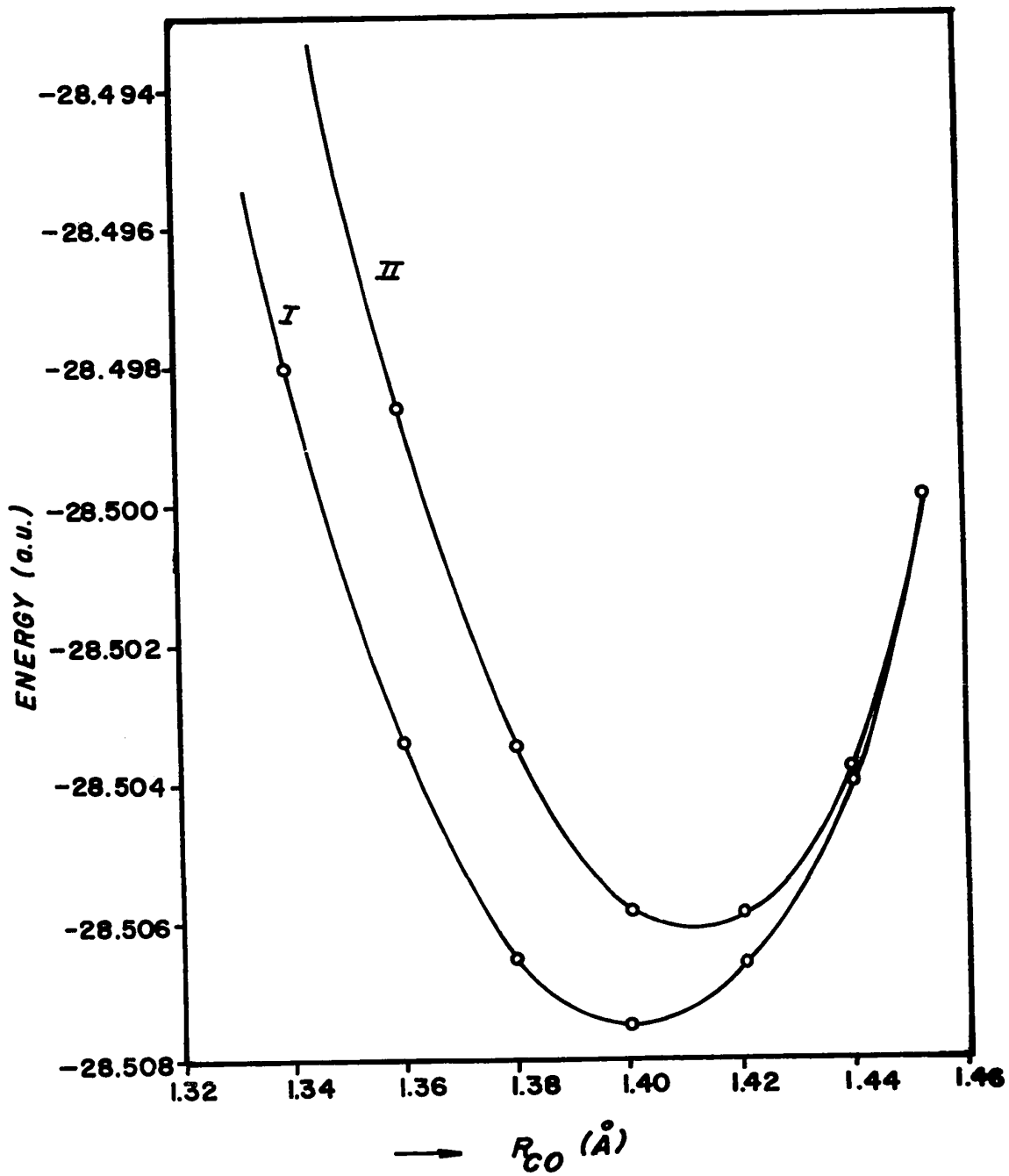


Fig. 16. The P.T. and S.C.F. results for the variation in the energy of the methanol molecule with carbon-oxygen bond length. I is the first order P.T. result. II is the S.C.F. and second order P.T. result; they cannot be distinguished on this scale.

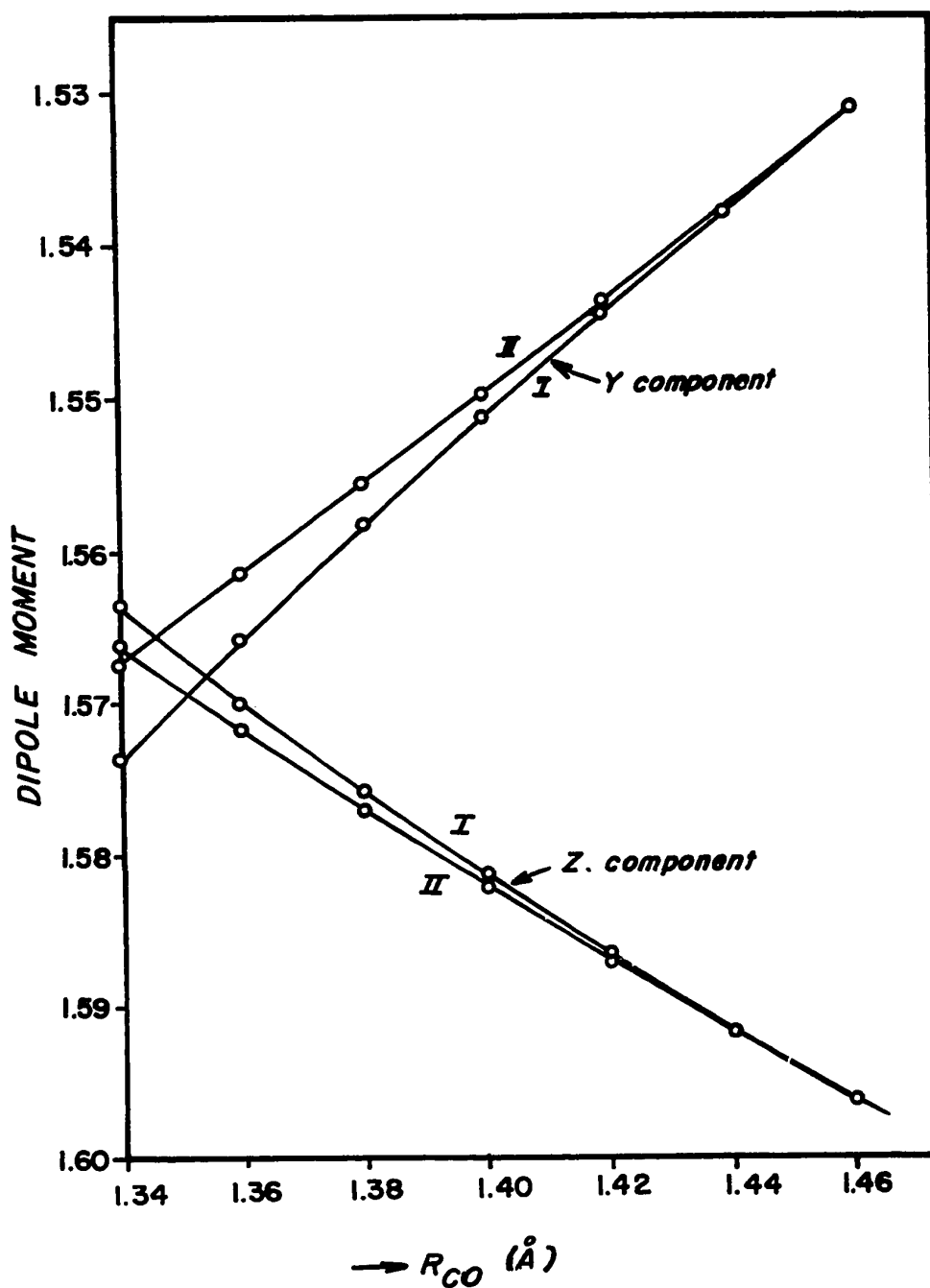


Fig. 17. P.T. and S.C.F. results for the variation of component of the dipole moment of methanol with carbon-oxygen bond length. I is the first order P.T. result; II is the S.C.F. and second order P.T. result.

not completely reliable, particularly when the configuration being computed is on the other side of the energy minimum from the zero-order configuration. Predictions of the first order theory may be qualitatively wrong when the zero-order configuration represents an extremum of the density matrix with respect to the geometrical parameter being varied. The planar configuration of ethylene and the linear configuration of carbon dioxide correspond to extrema of the density matrix; the first order predictions for the energy and density matrix variations accompanying the out-of-plane twist in ethylene and the out-of-line bend in carbon dioxide are very inaccurate. The method represents a finite perturbation theory; if it were an infinitesimal perturbation theory, the first-order theory would predict no change in P for these distortions since $(\partial P/\partial \lambda)_{\lambda=0} = 0$. As it is $(\partial P/\partial \lambda)$ is a still small quantity and not very useful for predictive purposes.

As formulated here the theory, order by order, is not invariant to rotations of the axis system, but the sum of all orders is invariant. This is a limitation but not necessarily one so severe that it invalidates the theory. For small changes, such as those for which the theory has been developed, the sum of the first two orders is very close to invariant to rotations of the axis system. For example, an artificial perturbation is introduced into the ethylene calculations by rotating the axis system out of plane by 4° . The first order energy is calculated to be $3.29087 \cdot 10^{-3}$ au while the second order energy is $-3.28692 \cdot 10^{-3}$ au, giving a net result of $3.95 \cdot 10^{-6}$ au. This order of absolute error is acceptable. However, it indicates that care is necessary in the use of the method if such errors are to be minimized when only a few terms in the perturbation series are used.

Related methods developed for the purpose of studying force constants

have recently been published⁽⁸⁹⁾. Because of the need to express the variation in molecular energy in terms of the variation in geometrical parameters these methods are necessarily more complicated. They involve particularly such quantities as the derivatives of multicentre integrals with respect to geometrical parameters, leading to a substantial increase in computational effort. While the present method can be adapted to the study of force constants, it has been developed specifically for a simpler problem, that of calculating the wavefunction and energy of a molecule in a given nuclear configuration, starting from the wavefunction for a neighbouring configuration.

CHAPTER 4

PERTURBATION THEORY OF POLYMER DISTORTIONS

The formalism developed in Chapter 1 for the regular polymer must now be revised to deal with the generalization to distorted lattices. This is readily achieved by systematically examining the individual equations involved, and modifying them where necessary. Where the formalism for the regular polymer is complicated that for the distorted polymer is doubly so. Before providing any detail, a general discussion is desirable in the interests of clarity.

Translational symmetry transformations, the Fourier transformations introduced in Chapter 1, reduce the operator matrices of S.C.F. theory to block-diagonal form. The overall Fock matrix, for example, can be considered to be constructed from submatrices, each of which consists of the block of matrix elements between the set of functions belonging to a particular k value and those belonging to another k value. When the polymer is regular the reduction is exact and all off-diagonal submatrices are null; when it is slightly irregular the reduction is not exact, and small elements remain in the off-diagonal submatrices. In the latter case, it is no longer possible to solve the equations by diagonalizing submatrices⁽³⁴⁾. Because the full crystal matrix is very large, it is not feasible to diagonalize it directly. When the irregularities are small the method developed in the last chapter can be used, together with the usual symmetry transformations, to find approximate solutions. The transformations provide convenient zero-order solutions and by converting the equations for the distorted lattice to near

block-diagonal form reduce the perturbation equations to a convenient form.

Certain features are particularly useful. The zero-order matrices are block-diagonal and this simplifies certain matrix products occurring in the perturbation theory. It also reduces the number of integrals needed when the perturbation series is to be truncated at first order. Most important of all, it provides a convenient method of blocking the polymer Fock matrix so that the blocks can be handled one at a time. This will be more clearly seen when the equations are given explicitly. One further reason for employing the symmetry transformations is that the momentum-space representation is intimately connected with the theory of scattering from lattices⁽⁷⁶⁾. Retention of the k-space formalism leaves open the possibility of an interpretation of the results based on scattering of electron waves by phonons (vibrational waves).

Theory

The basis functions for the calculations are the atomic functions $\chi_{\mu}(\underline{r} - \underline{R}_{\mu})$ and lattice symmetry functions $\phi_{\mu}(k)$, $\psi_{\mu}(k)$ similar to those used in the zero order theory.

$$\begin{aligned}\phi_{\mu}(k) &= \frac{2-\partial_k}{N} \sum_{\underline{R}} \text{Cos}2\pi k \underline{R} \chi_{\mu}(\underline{r}-\underline{R}_{\mu}) \\ \psi_{\mu}(k) &= \frac{2-\partial_k}{N} \sum_{\underline{R}} \text{Sin}2\pi k \underline{R} \chi_{\mu}(\underline{r}-\underline{R}_{\mu})\end{aligned}\tag{56}$$

These functions will be labelled with superscripts (0) and (D) according as they refer to the atomic functions $\chi_{\mu}(\underline{r})$ in their zero-order lattice positions or distorted lattice positions.

Matrix Elements and Lattice Integrals

These can be defined as before.

$$M_{\mu\nu}^{(0)}(k_1 k_2) = \langle \phi_{\mu}^{(0)}(k_1) | \hat{M} | \phi_{\nu}^{(0)}(k_2) \rangle = \partial k_1 k_2 M_{\mu\nu}^{(0)}(k_1) \quad [67]$$

where \hat{M} is a totally symmetric one-electron operator.

$$M_{\mu\nu}^D(k_1 k_2) = \langle \phi_{\mu}^D(k_1) | \hat{M} | \phi_{\nu}^D(k_2) \rangle \\ = \frac{\sqrt{(2-\partial k_1)(2-\partial k_2)}}{N} \sum_R \sum_S \text{Cos} 2\pi k_1 R \text{Cos} 2\pi k_2 S M_{\mu\nu}^D(R, S) \quad [116]$$

and

$$M_{\mu\nu}^D(R, S) = \int \chi_{\mu}^*[\underline{r}-\underline{R}-\underline{U}_{\mu}(R)] \hat{M} \chi_{\nu}[\underline{r}-\underline{S}-\underline{U}_{\nu}(S)] d\tau \quad [117]$$

$\underline{U}_{\mu}(R)$ is the displacement, in cell R , of the nucleus on which is centred the atomic function χ_{μ} . $M_{\mu\nu}^D(R, S)$ is then the matrix element between the displaced function χ_{μ} in cell R and the displaced function χ_{ν} in cell S . Because of these displacements this matrix element now depends on the absolute values of R and S (see discussion below), not as was the case in the regular lattice on the difference between them. The resulting lattice integral $M_{\mu\nu}^D(k_1 k_2)$ must be evaluated by performing the full double summation.

In the case of the two electron integrals a similar situation pertains and lattice integrals such as $\langle \mu_1 \mu_2 | \nu_3 \nu_4 \rangle^D$, defined below,

$$\langle \mu_1 \mu_2 | \nu_3 \nu_4 \rangle = \frac{\sqrt{(2-\partial k_1)(2-\partial k_2)(2-\partial k_3)(2-\partial k_4)}}{N^2} \sum_R \sum_S \sum_L \sum_M \text{Cos} 2\pi k_1 R \text{Cos} 2\pi k_2 R \text{Cos} 2\pi k_3 L \text{Cos} 2\pi k_4 M [\gamma^D(\mu_R, \mu_S, \nu_L, \nu_M)] \quad [118]$$

must be evaluated by performing all the lattice sums directly.

Perturbation Equations

The perturbing quantities are defined by the equations

$$\begin{aligned}\lambda H_{\mu\nu}^{(1)}(k_1 k_2) &= H_{\mu\nu}^D(k_1, k_2) - H_{\mu\nu}^{(0)}(k_1, k_2) \\ &= H_{\mu\nu}^D(k_1, k_2) - a_{k_1 k_2} H_{\mu\nu}^{(0)}(k_1, k_2)\end{aligned}\quad [119]$$

$$\text{and } \lambda \langle \mu_1 \mu_2 | \nu_3 \nu_4 \rangle^{(1)} = \langle \mu_1 \mu_2 | \nu_3 \nu_4 \rangle^D - \langle \mu_1 \mu_2 | \nu_3 \nu_4 \rangle^{(0)} \quad [120]$$

The formal matrix equations may be taken from the discussion of the molecular problem

$$\underline{F}^{(0)} \underline{C}^{(0)} = \underline{C}^{(0)} \underline{E}^{(0)} \quad [17]$$

$$\underline{F}^{(1)} \underline{C}^{(0)} + \underline{F}^{(0)} \underline{C}^{(1)} = \underline{C}^{(1)} \underline{E}^{(0)} + \underline{C}^{(0)} \underline{E}^{(1)} \quad [107]$$

$$\text{subject to } \tilde{\underline{C}}^{(0)} \underline{C}^{(0)} = \underline{1} \quad [110]$$

$$\tilde{\underline{C}}^{(0)} \underline{C}^{(1)} + \underline{C}^{(1)} \underline{C}^{(0)} = \underline{0}$$

$\underline{C}^{(1)}$ is to be expressed as

$$\underline{C}^{(1)} = \underline{C}^{(0)} \underline{A} \quad [109]$$

For the regular polymer the symmetry transformation converts the zero-order equation to the form

$$\tilde{\underline{C}}^{(0)}(k_1) \underline{F}^{(0)}(k_1) \underline{C}^{(0)}(k_1) = \underline{E}^{(0)}(k_1) \quad k = 0, \dots, \frac{N-1}{2N} \quad [79]$$

which is a shorthand notation for

$$\tilde{\underline{C}}^{(0)}(k_1 k_1) \underline{F}^{(0)}(k_1 k_1) \underline{C}^{(0)}(k_1 k_1) = \underline{E}^{(0)}(k_1 k_1) \quad [121]$$

This equation expresses more clearly the fact that $\underline{F}^{(0)}(k_1 k_1)$ represents the block of matrix elements between the set of basis functions characterized by k_1 and the same basis functions characterized by k_1 . In the non-regular lattice the reduction to block-diagonal form is not complete and the sub-

matrices $F(k_1k_2)$ where $k_1 \neq k_2$ are not in general null. In this case the first-order equations become, using the block-diagonal nature of the zero-order matrices to simplify the result,

$$\tilde{C}^{(0)} \underline{F}^{(1)} \underline{C}^{(0)} + \tilde{C}^{(0)} \underline{F}^{(0)} \underline{C}^{(1)} = \tilde{C}^{(0)} \underline{C}^{(1)} \underline{E}^{(0)} + \tilde{C}^{(0)} \underline{C}^{(0)} \underline{E}^{(1)} \quad [122]$$

$$\underline{F}^{(1)}(k_1k_2) + \underline{E}^{(0)}(k_1k_1) \underline{A}(k_1k_2) = \underline{A}(k_1k_2) \underline{E}^{(0)}(k_2k_2) + \underline{E}^{(1)}(k_1k_2) \quad [123]$$

$$\text{Thus} \quad A_{ij}(k_1k_2) = F_{ij}^{(1)}(k_1k_2) / [E_{jj}^{(0)}(k_2k_2) - E_{ii}^{(0)}(k_1k_1)] \quad [124]$$

The normalization condition can again be used to show A is skew symmetric. Just as in the molecular case, it can be shown that only those A_{ij} where i is occupied and j vacant (or vice versa) are needed for the calculation of $P^{(1)}$; the apparent singularity in $A_{ii}(k_1k_1)$ is thus avoided. The first-order density matrix change in k space is

$$\begin{aligned} P_{\mu\nu}^{(1)}(k_1k_2) &= 2 \sum_{k_3} \sum_{\ell_3}^{oc} \{ C_{\mu\ell}^{(0)}(k_1k_3) C_{\nu\ell}^{(1)}(k_2k_3) + C_{\mu\ell}^{(1)}(k_1k_3) C_{\nu\ell}^{(0)}(k_2k_3) \} \\ &= 2 \left[\sum_{\ell_1}^{oc} C_{\mu\ell}^{(0)}(k_1k_1) C_{\nu\ell}^{(1)}(k_2k_1) + \sum_{\ell_2}^{oc} C_{\mu\ell}^{(1)}(k_1k_2) C_{\nu\ell}^{(0)}(k_2k_2) \right] \end{aligned} \quad [125]$$

since $C_{\mu\ell}^{(0)}(k_1k_2) = \partial k_1 k_2 C_{\mu\ell}^{(0)}(k_1k_1)$.

The first-order change in the electron repulsion matrix is given by the equation ($\mu \neq \nu$)

$$\begin{aligned} G_{\mu\nu}^{(1)}(k_1k_2) &= -\frac{1}{2} \left[\sum_{k_3} \sum_{\mu\nu} P_{\mu\nu}^{(0)}(k_3k_3) \langle \mu_1 \mu_3 | \nu_3 \nu_2 \rangle^{(1)} \right. \\ &\quad \left. + \sum_{k_3} \sum_{k_4} \sum_{\mu, \nu} P_{\nu\mu}^{(1)}(k_3k_4) \langle \mu_1 \mu_4 | \nu_3 \nu_2 \rangle^{(0)} \right] \end{aligned} \quad [126]$$

The summation over μ, ν implies the inclusion of contributions from both sine and cosine functions for each basis type. A list of all requisite matrix

elements is given in Table 11.

The first-order change in the total energy is given by

$$W^{(1)} = \frac{1}{2} \sum_k \sum_{\mu\nu} \{P_{\mu\nu}^{(0)}(k,k) [H_{\mu\nu}^{(1)}(k,k) + F_{\mu\nu}^{(1)}(k,k)] + P_{\mu\nu}^{(1)}(k,k) H_{\mu\nu}^{(0)}(k,k)\} + Z_{NR}^D - Z_{NR}^{(0)} \quad [127]$$

and the first-order change in the orbital energies by

$$E^{(1)} = \tilde{C}^{(0)} F^{(1)} C^{(0)} + \tilde{C}^{(1)} F^{(0)} C^{(0)} + \tilde{C}^{(0)} F^{(0)} C^{(1)} \quad [128]$$

whence

$$E_{ii}^{(1)}(k,k) = \sum_{\mu\nu} C_{\mu i}^{(0)}(k,k) F_{\mu\nu}^{(1)}(k,k) C_{\nu i}^{(0)}(k,k) \quad [129]$$

Inverting the Fourier transform to get the first-order change in the real space density matrix gives

$$\begin{aligned} \rho_{\mu\nu}^{(1)}(R,S) = & \sum_{k_1 k_2} [P_{\mu\nu}^{(1)}(k_1 k_2) \cos 2\pi k_1 R \cos 2\pi k_2 S \\ & + P_{\mu\nu}^{(1)}(k_1 k_2) \sin 2\pi k_1 R \sin 2\pi k_2 S + P_{\mu\nu}^{(1)}(k_1 k_2) \cos 2\pi k_1 R \sin 2\pi k_2 S \\ & + P_{\mu\nu}^{(1)}(k_1 k_2) \sin 2\pi k_1 R \cos 2\pi k_2 S] \sqrt{\frac{(2-\partial k_1)(2-\partial k_2)}{N}} \quad [130] \end{aligned}$$

Discussion

The equations show the pattern of the calculation. An estimate of $\underline{F}^{(1)}(k_1 k_2)$, e.g., $\underline{H}^{(1)}(k_1 k_2)$, is used to form $\underline{A}(k_1 k_2)$ and through this $\underline{P}^{(1)}(k_1 k_2)$. This, in turn, is used to recalculate $\underline{F}^{(1)}(k_1 k_2)$ and the process repeated to convergence. Clearly all submatrices $\underline{P}^{(1)}(k_1 k_2)$ (except those made redundant by the fact that the full $\underline{P}^{(1)}$ matrix is symmetric about the leading diagonal) are needed to calculate the set of $\underline{F}^{(1)}(k_1 k_2)$ submatrices.

TABLE 11

Matrix Elements of the Fock Operator for the Distorted Polymer

In the distorted polymer, the submatrices $F_{\mu\nu}^{(1)}(k_1k_2)$ are not symmetric except for $k_1 = k_2$. Explicit formulae for all requisite matrix elements can be obtained by making the appropriate substitutions in the formulae for $F_{\mu\nu}^{(1)}(k_1k_2)$ which are given here. The parameter λ has been set equal to 1. For $\mu \neq \nu$

$$H_{\mu\nu}^{(1)}(k_1k_2) = H_{\mu\nu}^D(k_1, k_2) - H_{\mu\nu}^{(0)}(k_1, k_2)$$

where the various quantities are defined in the main text.

$$\begin{aligned} G_{\mu\nu}^{(1)}(k_1k_2) = & -\frac{1}{2} \sum_{k_3} \{ P_{\nu\mu}^{(0)}(k_3) [\langle \mu_1\mu_3 | \nu_3\nu_2 \rangle^{(1)} + (1-\partial k_3) \langle \mu_1\mu_3 | \bar{\nu}_3\nu_2 \rangle^{(1)}] \\ & + P_{\nu\mu}^{(0)}(k_3) [\langle \mu_1\mu_3 | \bar{\nu}_3\nu_2 \rangle^{(1)} - \langle \mu_1\bar{\mu}_3 | \nu_3\nu_2 \rangle^{(1)}] \\ & + \sum_{k_4} [P_{\nu\mu}^{(1)}(k_3k_4) \langle \mu_1\mu_4 | \nu_3\nu_2 \rangle^{(0)} + P_{\nu\mu}^{(1)}(k_3k_4) \langle \mu_1\bar{\mu}_4 | \bar{\nu}_3\nu_2 \rangle^{(0)} \\ & + P_{\nu\mu}^{(1)}(k_3k_4) \langle \mu_1\mu_4 | \bar{\nu}_3\nu_2 \rangle^{(0)} + P_{\nu\mu}^{(1)}(k_3k_4) \langle \mu_1\bar{\mu}_4 | \nu_3\nu_2 \rangle^{(0)}] \} \end{aligned}$$

when $\mu = \nu$ the term corresponding to $H_{\mu\mu}^{(1)}(R=S)$ in the lattice sum for $H_{\mu\nu}^{(1)}(k_1k_1)$ becomes

$$\begin{aligned} H_{\mu\mu}^{(1)}(R=S) &= - \sum_B Z_B \Gamma_{AB}^{(1)} \\ \Gamma_{AB}^{(1)} &= \frac{1}{N^2} \sum_R \sum_S [\gamma_{AB}^{(0)}(R,S) - \gamma_{AB}^{(0)}(R,S)] \end{aligned}$$

In addition to the terms occurring in $G_{\mu\nu}^{(1)}(k_1k_2)$, $G_{\mu\mu}^{(1)}(k_1k_2)$ contains

$$\begin{aligned} \sum_{k_3\sigma} \{ & P_{\sigma\sigma}^{(0)}(k_3) [\langle \mu_1\mu_2 | \sigma_3\sigma_3 \rangle^{(1)} + (1-\partial k_3) \langle \mu_1\mu_2 | \bar{\sigma}_3\bar{\sigma}_3 \rangle^{(1)}] \\ & + \sum_{k_4} [P_{\sigma\sigma}^{(1)}(k_3k_4) \langle \mu_1\mu_2 | \sigma_3\sigma_4 \rangle^{(0)} + P_{\sigma\sigma}^{(1)}(k_3k_4) \langle \mu_1\mu_2 | \bar{\sigma}_3\bar{\sigma}_3 \rangle^{(0)} \\ & + P_{\sigma\sigma}^{(1)}(k_3k_4) \langle \mu_1\mu_2 | \sigma_3\bar{\sigma}_4 \rangle^{(0)} + P_{\sigma\sigma}^{(1)}(k_3k_4) \langle \mu_1\mu_2 | \bar{\sigma}_3\sigma_4 \rangle^{(0)}] \} \end{aligned}$$

Finally,

$$F_{\mu\nu}^{(1)}(k_1 k_2) = H_{\mu\nu}^{(1)}(k_1 k_2) + G_{\mu\nu}^{(1)}(k_1 k_2)$$

Apart from this, each submatrix can be treated independently. The speed of matrix multiplication, together with the independence of the submatrices, reduces the computational difficulties considerably.

A number of practical considerations cannot be stressed too strongly. First, because the distortion generally removes the equivalence of the sine and cosine functions belonging to given basis function type and k-value, all the simplifying relationships available to the zero-order theory (Table 2) must be assumed to be invalid for the perturbed equations. It then becomes essential to exercise extreme caution with the subscripting of the matrix elements and integrals. Second, the bottle-neck in the calculation as a whole is the calculation of the first-order two-electron lattice integrals. This arises, not in the calculation of the simple integrals, but in performing the lattice sums. Even where "look-up" techniques are used to find the necessary phase factors, this is a time-consuming process. However, the alternative non-transformed calculation is even less convenient; this difficulty would seem to be the price which has to be paid if the calculations are to be done.

The first-order theory which has been described here introduces all the essential techniques involved in the application of the perturbation method to the polymer problem. Second and subsequent orders involve some further algebra and a greater amount of computational effort. The second-order theory represents the barrier, in as much as all the integrals necessary for any order of calculation are available after the second order calculation has been done. In CNDO the number of coulomb and exchange integrals is determined by the number of atoms in the unit cell and the size of the Born-von Karman unit. While the number of integrals increases as the square of the number of atoms this is not as dramatic an increase as one gets in

the number of one-electron matrix elements due to the increase in the number of basis functions. Therefore the computational cost does not rise so steeply as to preclude the investigation of a wide range of systems of chemical interest which have simple unit cells.

Sample Calculations

A computer program implementing the theory to first-order (using the CNDO/2 approximation) was used to perform a number of sample calculations. The chain of hydrogen molecules was used in these examples because of its simplicity and because the small changes which might be expected to occur in this chain present a difficult test of the method.

The equilibrium configuration of the hydrogen chain obtained in the earlier calculations was used as the zero-order configuration. This is an all-linear configuration (the axis of propagation is taken to be the z-axis) in which all molecular bond-lengths are 0.748 \AA and the centres of adjacent molecules are separated by 2.500 \AA . Periodic distortions with a wavelength equal to a rational fraction of the Born-von Karman segment length were used in the calculations. Such distortions can be written in the form

$$\zeta(q) = \sum_s (u_1 + u_2) \cos 2\pi qs \quad [131]$$

where $q = 0, \dots, \frac{N-1}{2N}$,

u_i = amplitude vector of displacement for atom i .

Clearly, more general distortions involving sine functions and different wave vectors for different atoms can be constructed to satisfy the same boundary conditions but only simple waves of the above form were considered in the sample calculations. These waves cause atom 1 in cell R to be shifted

by a quantity $\underline{u}_1(R) = \underline{u}_1 \cos 2\pi qR$ and atom 2 in the same cell by $\underline{u}_2 \cos 2\pi qR$. A plot of $E^{(1)}$ against q for $\underline{u}_1 = -\underline{u}_2 = (0,0,0.05 \text{ \AA})$ is given in Figure 18. Figure 19 is a plot of $E^{(1)}$ against q for a similar distortion where $\underline{u}_1 = \underline{u}_2 = (0,0,0.05 \text{ \AA})$. Table 12 compares the estimates of $E^{(1)}$ obtained in this way with those obtained by the S.C.F. program where this was possible.

Testing a method of this kind poses a considerable problem. Comparison of results for special configurations with those of other methods is not sufficient. However, the physics of the problem provides a number of very useful checks on the method, and these will be discussed here.

Case (1), $\underline{u}_1 = -\underline{u}_2 = (0,0,0.05 \text{ \AA})$: In this example of a lattice distortion the centres of mass of the molecules remain at the positions they occupied in the regular lattice. Only the bond lengths of the individual molecules change. The distortion energy resulting from this wave has a singularity at $q = 0$ for both sine and cosine lattice waves. These singularities arise from the fact that the $q = 0$ waves are physically distinct from all other waves in the following way. Sine waves with $q = 0$ give rise to no change in the lattice while cosine waves with $q = 0$ cause each unit cell to undergo exactly the same distortion, in this case a shortening of the molecular bond. At any other value of q some of the molecules are stretched, others are contracted, the fraction of each and the extent of the distortions being determined by q and \underline{u}_1 . As formulated here the method permits the use of distortion waves having discrete q values in the range 0 to $\frac{N-1}{2N}$ in steps of $\frac{1}{N}$ only (or any distortion, repeated in each Born-von Karman unit, which can be Fourier analysed by the set of waves of this form). The condition of the lattice at $q = 0$ is of a different order or type than that obtained when $q \neq 0$. Fig. 18 demonstrates that method reproduces this predicted behaviour.

TABLE 12

Comparison of S.C.F. and P.T. Results for Lattice Distortions
in a Linear Lattice of H₂ Molecules

E(N) is energy, calculated in the CNDO/2 approximation, for N hydrogen molecules in the specified configuration.

	Method
E ⁽⁰⁾ = -1.475673 a.u./u.c.	POLYM1
= -1.475670 a.u./u.c.	[E(25) - E(21)]/4

q = 0, $\underline{u}_1 = -\underline{u}_2 = (0, 0, 0.05 \text{ \AA})$

$\Delta E_{\text{S.C.F.}}^{\text{TOTAL}} = 0.014291 \text{ a.u./u.c.}$

$\Delta E_{\text{P.T.}}^{\text{TOTAL}} = 0.014788 \text{ a.u./u.c.}$

% relative error = 3.48

$\Delta E_{\text{S.C.F.}}^{\text{ELECTRONIC}} = -0.082519 \text{ a.u./u.c.}$

$\Delta E_{\text{P.T.}}^{\text{ELECTRONIC}} = -0.082022 \text{ a.u./u.c.}$

% relative error = -0.60

q = 1/5, $\underline{u}_1 = -\underline{u}_2 = (0, 0, 0.05 \text{ \AA})$

$E(q = 1/5) - E^{(0)} = 0.005908 \quad [E(25) - E(20)]/5 - E^{(0)}$

$E^{(1)} = 0.005953 \quad \text{P.T.}$

Estimated relative error in E⁽¹⁾ = 0.76%.

TABLE 13

Comparison of Displacements Resulting from Lattice Waves
of Sine and Cosine Types

The waves have a common amplitude of 0.100 \AA along the axis of propagation and results are given for sets of waves with wave vectors of $1/5$ and $2/5$. A negative cell index refers to a cell to the left of the origin.

(i) $q = 1/5$

Cell index	-2	-1	0	1	2
Sine wave	-0.0588	-0.0951	0.0	0.0951	0.0588
Cosine wave	-0.0809	0.0309	0.100	0.0309	-0.0809

(ii) $q = 2/5$

Cell index	-2	-1	0	1	2
Sine wave	0.0951	-0.0588	0.0	0.0588	-0.0951
Cosine wave	0.0309	-0.0809	0.100	-0.0809	0.0309

Lattice waves having the same non-zero q value and amplitudes which differ only in sine/cosine character are physically indistinguishable. The choice of sine/cosine character represents a choice of phase of which the energy is independent. Other than at special values of q , the distortions arising from the sine wave bear no superficial resemblance to those due to the cosine wave of Table 13. The method correctly predicts the degeneracy of these sine and cosine waves.

Introduction of distortion waves into a lattice produces lower symmetries. The first-order real-space density-matrix is consistent in every case with these new symmetries. Here again the distinction between the sine and cosine waves is evident. Although they give rise to the same distortion energy the distorted lattices have different symmetries depending on whether the wave giving rise to the distortion is of sine or cosine type.

In a real crystal q is a quasi-continuous parameter, though for convenience the methods used here treat it as discrete. Evidence for the convergence of the method and its internal consistency is given in Fig. 18, where a single plot of $E^{(1)}$ vs q fits the results obtained by using different values N and hence different grids in q (or k) space.

The physical implications of these results are quite interesting. They show that the coupling between vibrations in individual hydrogen molecules in the chain is weak. Further, they show that the regular chain is more stable than the distorted chain. Both of these results are consistent with experimental data⁽⁹¹⁾ and elementary considerations. The first-order density matrix suggests that small but significant charge-transfer takes place when all the molecules vibrate in the rigid lattice. Clearly, a lattice

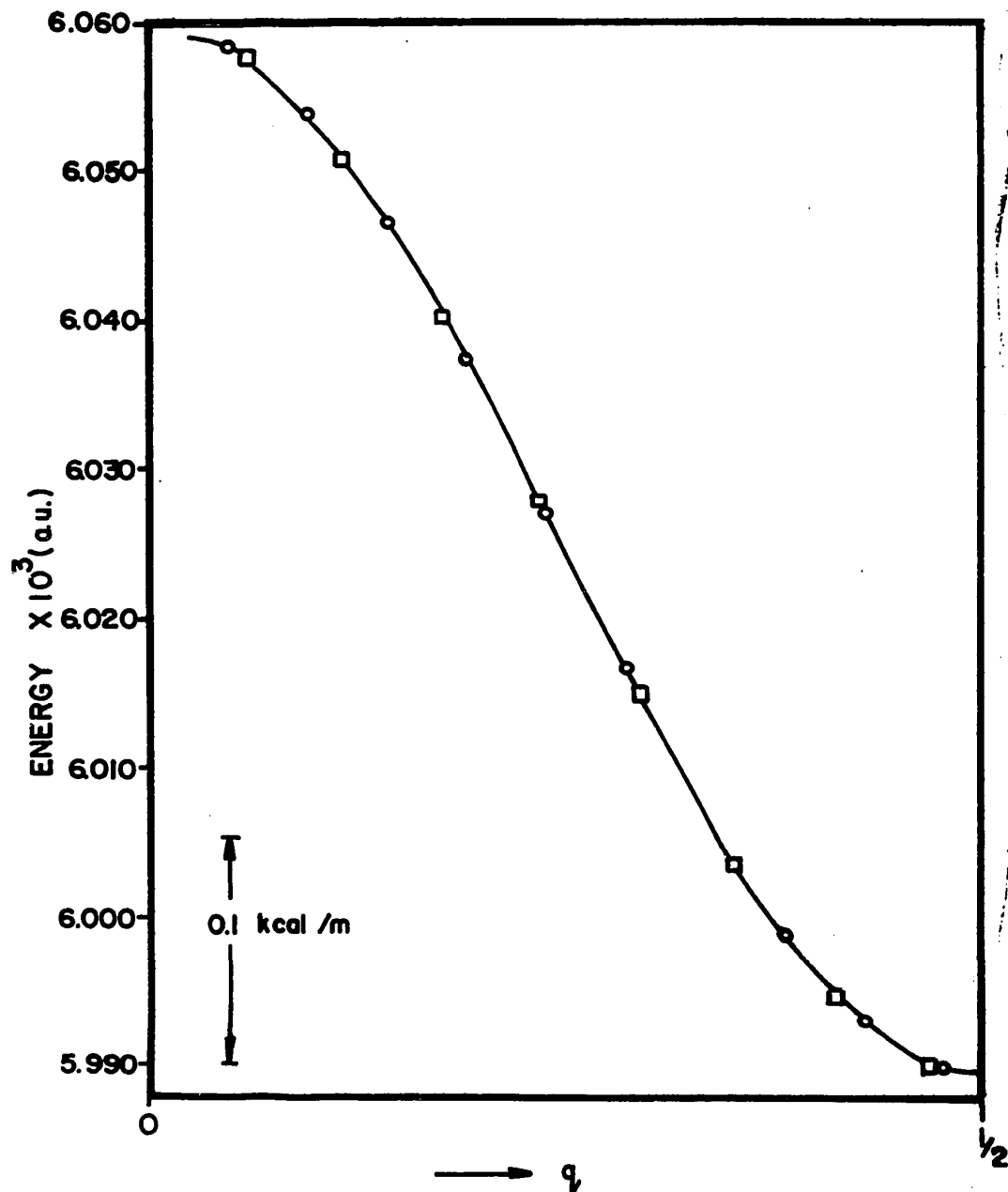


Fig. 18. A plot of the first-order energy versus the wave vector q for the lattice distortion in the hydrogen chain having $u_1 = -u_2 = (0, 0, 0.05 \text{ \AA})$.

mode where all molecules vibrate in phase with equal amplitudes gives rise to no charge transfer but a progressive wave--the distorted structure might be regarded as an instantaneous configuration of such a wave--does give rise to charge transfer even in a chain of hydrogen molecules. These results are in general agreement with qualitative considerations and deductions which can be made from experimental results on three-dimensional crystals. Because the zero-order configuration is an extremum of the density matrix (as evidenced by the degeneracy of sine and cosine waves of the same q value, and of waves differing only in the sign of the amplitude) the results are unlikely to be quantitatively correct. They do, however, establish that the method is feasible and gives reasonable results.

Case 2, $u_1 = u_2 = (0,0,0.05 \text{ \AA})$: Here both the sine and cosine waves for $q = 0$ are degenerate with the zero order result since the cosine wave represents only a net translation of the lattice. For non-zero q values the rigid molecules are displaced from their equilibrium lattice positions, some in one direction and some in the other giving rise to a longitudinal compressional wave.

Physical considerations again provide useful checks on the method. Sine and cosine waves are degenerate as they should be; the first-order density matrices have the correct symmetries; finally the result is again independent of N (Fig. 19).

The results show that the zero-order lattice is stable with respect to this deformation, although the energy required to effect the deformation is small. Charge-transfer is again evident, although the amount predicted by the first-order theory is obviously high for reasons discussed previously.

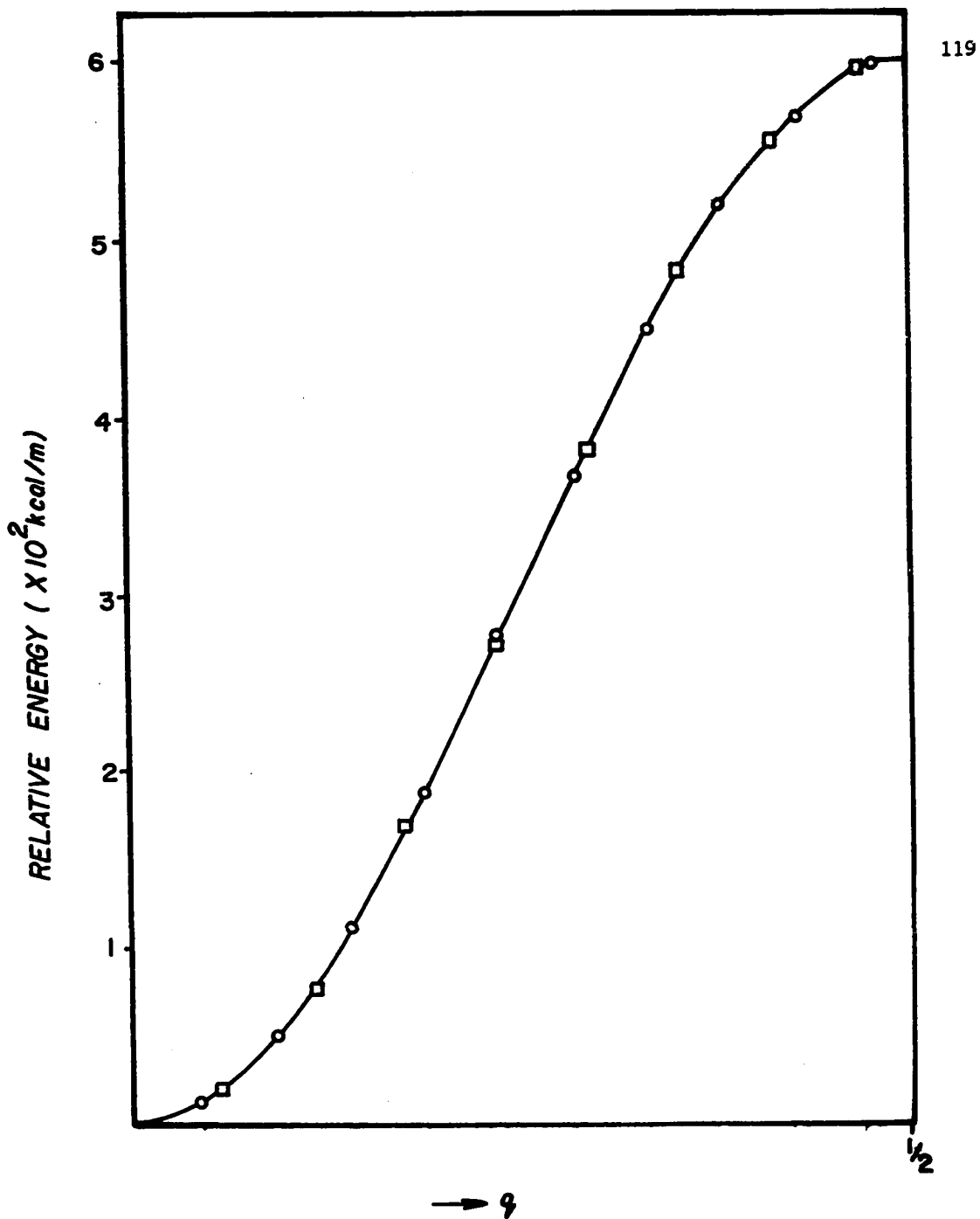


Fig. 19. A plot of the first-order energy versus the wave vector q for the lattice distortion in the hydrogen chain having $\underline{u}_1 = \underline{u}_2 = (0,0,0.05 \text{ \AA})$.

The results of these calculations give some indication of the potential uses of the method. It can be used to discuss the stability of regular lattices with respect to deformations. By the use of simple curve-fitting, or more sophisticated methods, it can be used to calculate force constants for vibrational waves with non-zero wavevectors. It provides a method of examining the effect of increasing disorder on the band-structure, charge-distribution and energy of a polymer. It is particularly powerful since it treats electron-electron interactions explicitly. For polymers, where adjacent unit cells are directly bonded to one another, this explicitness is essential; the tight-binding models⁽⁸¹⁾ used to discuss disordered chains and solids are unlikely to be successful in discussing polarization and other electronic effects in real polymers.

CHAPTER 5

FINAL DISCUSSION

The approximate molecular-orbital theory of regular polymers developed in Chapter 1 is a viable and practical method of investigating the electronic structure of these systems. The results obtained with this method, outlined in Chapter 2, are quite satisfactory. Even for model polymers which are not realized physically, the method predicts behaviour which is at least qualitatively reasonable. Each of the three monatomic chains studied is shown to be non-metallic as predicted by Peierls⁽⁷⁶⁾. The hydrogen chain is predicted to be weakly bound and linear with a molecular bond length of 0.748 Å, the free molecule value, and an intermolecular separation of 1.752 Å. Beryllium, on the other hand, has a linear structure of equally-spaced atoms. The band gap is very sensitive to the interatomic spacing and goes to zero as this spacing is decreased to 1.8975 Å, but the most stable non-metallic chain has a lattice constant of 1.963 Å. A chain of carbon atoms is predicted to have a linear structure with alternating bond lengths of 1.224 Å and 1.387 Å. A substantial band gap is predicted for this alternating chain while the chain of equally-spaced atoms has a zero band gap at this level of approximation. An alternant structure is also predicted for the infinite polyene. This structure is similar to that of the central portion of long finite polyenes having carbon-carbon bond lengths of 1.350 Å and 1.432 Å and a skeletal angle of 124.8°. Polyethylene is shown to be stable with respect to bond alternation. The dependence of the energy of helical configurations of the molecule on the helix parameter w is discussed. It is seen that the energy changes accompany-

ing conformational changes are comparable to crystal packing energies. Lithium fluoride chains are shown to be unstable with respect to structures of higher dimensionality. The optimum linear configuration of these chains consists of equally-spaced atoms, alternately lithium and fluorine, having substantial partial charges. Hydrogen fluoride chains are shown to be molecular and to have the zig-zag structure characteristic of HF in the crystalline state. A substantial increase in the bond length of the molecule is predicted on formation of the chain. The chain is shown to have a very shallow potential surface and it is suggested that the details of the chain structure are due in large part to the packing of the chains in the crystal. Finally, convergence of the method with respect to the size of the Born-von Karman segment and length of the various lattice sums is demonstrated. In the course of this discussion a modification of the Ewald transform is developed to deal with the peculiarities of one-dimensional periodicity.

Computations at this level of approximations require such modest amounts of computer time and storage that quite complex structures can be studied in this way. A machine of the size and speed of a CDC 6400 is capable of handling computations for a cellulose molecule. Clearly for such systems calculations of optimum geometries are not really feasible but wavefunctions for a representative sample of configurations would give a valuable indication of the general electronic characteristics of a given molecule. They could also provide an estimate of physical quantities which are not readily measurable or at least the trend of values of a given parameter for a series of configurations.

The use of approximate methods such as INDO⁽⁹⁾ or MINDO⁽²³⁾ would probably improve the agreement with experiment. Ab initio S.C.F. methods

are considerably more costly but with improving hardware and computational techniques the cost can be expected to decrease in the future. It is unlikely that the cost will be reduced to such an extent that large scale ab initio calculations on polymers will become commonplace. While ab initio calculations are closer to a true rigorous formulation of the problem, the results of such calculations can be further from the true result than are the results of semi-empirical methods. Since semi-empirical methods include part of the electron correlation through the use of empirical constants they sometimes give results which are much better than might be expected. Attempts to correct the correlation error for ab initio calculations involve the use of such methods as configuration interaction. These methods are very costly, and therefore are not presently feasible.

It is clear that any comparison of calculation and experimental values, an essential test of any theory, must be undertaken with caution for polymer systems. The calculated results deal largely with idealized structures in a non-interacting environment. Experimental quantities invariably relate to polymers which are in random configurations or in strongly interacting environments, or both. In this case it is unreasonable to expect detailed agreement between theory and experiment on the value of any quantity which is sensitive to these conditions. For this reason a re-examination of both theory and experiment is in order so that realistic comparisons can be made.

The theory for distorted lattices has a very useful role to play in the theoretical aspect of this analysis. It can be used to determine whether or not the regular polymer is stable with respect to arbitrary distortions. The stability of the regular hydrogen chain with respect to certain distortions was demonstrated by this method in Chapter 4. From the same results

dispersion curves such as those in Figures 18 and 19 can be obtained for the various distortions. Fourier inversion of these dispersion curves gives the real space force constants for the equivalent distortions. In this way energy level distributions for electronic and vibrational levels can be found. The resulting distributions of vibrational and electronic energy levels could probably be used to estimate the effect of temperature on the structure and spectra of the polymer. Further the use of the momentum space representation permits the interpretation of these changes in terms of scattering events. A detailed analysis of this kind even for a simple polymer represents a considerable expenditure of effort and resources. At some time in the not-too-distant future such a study may prove both feasible and useful when attention is turned to the problem of calculating the free energy of a polymer, rather than the internal energy. Because it is the free energy rather than the quantum-mechanical internal energy which determines the behaviour of the polymer, and these are significantly different for such a large system, attention must be directed to these problems before a realistic theory can be developed.

Any observed quantity for a polymer is more properly thought of as an ensemble average of the given quantity. The density matrix formalism of statistical mechanics⁽⁹¹⁾ together with Peierls' Inequality⁽⁹²⁾ provides a method of calculating such an average provided only that a suitable approximate Hamiltonian is available. In the Born-Oppenheimer⁽⁴⁰⁾ approximation this reduces to finding suitable Hamiltonians for the electronic and nuclear wavefunctions. Using the results of calculations based on the methods outlined here it may be possible to find simple forms for these effective Hamiltonians which will give reasonable ensemble averages for

observables. For example, the most difficult terms in the electronic calculation are those arising from exchange effects. A method such as that of Slater⁽²⁾ would be very useful in simplifying the theory. In fact, Slater's method is probably not appropriate for polymers from both a formal and practical viewpoint. The formal aspect is discussed by Hall⁽⁹³⁾. In practice⁽⁹⁴⁾ numerical integration of the charge density is necessary and this is too cumbersome a technique where a simple expression for the charge density is not possible. However, if a suitable simple representation of the exchange potential could be found polymer calculations could be made much simpler.

This discussion has been largely speculative, and far from exhaustive. The present time, when large scale calculations on polymer systems are beginning, is an appropriate time to decide on a strategy for these investigations. While it is likely that conventional methods are producing, and will continue to produce useful results, it is clear that for complicated systems such as those occurring in biology they are too cumbersome. They probably contain far too much detail, since it is unlikely that minute details of the electronic structure are significant in determining the behaviour of such large systems. Before too much time and effort are invested in conventional calculations some speculative studies should be undertaken to see if this is the case. This may seem like trying to run before one can walk, but sometimes it is easier to retain one's balance at speed than at a more lethargic pace.

APPENDIX 1

The convergence properties of electron repulsion and electron nuclear attraction integral lattice sums could lead to problems with respect to the application of molecular orbital theory to infinite atomic aggregates. Consider for example a phase modulated coulomb lattice sum, $\Gamma(k)$, for a one-dimensional crystal.

$$\Gamma(k) = \sum_{\ell}^{\text{lattice}} \gamma(\ell) e^{2\pi i k x(\ell)} \quad [132]$$

where $\gamma(\ell)$ is some coulomb integral between an atom centered on the origin and the ℓ th unit cells respectively, $x(\ell)$ is the lattice vector connecting these cells and k is the wave vector. The problem arises because $\gamma(\ell)$ converges as $1/x(\ell)$ so that at best, for large values of k , the series is only slowly convergent and when $k = 0$ is actually divergent. It can be seen therefore that theories based on very small summations could produce almost meaningless results and that even very long direct summations could prove unreliable.

The above problem was recognized early in the development of the theory of the lattice vibrations of ionic crystals where it was elegantly solved by Ewald⁽⁴²⁾ by means of an integral transform. Ewald's method is particularly valuable since it not only greatly increases the rate of convergence of the lattice sums but also separates out the divergent character of infinite series into a single term, thus permitting a clearer discussion and interpretation of the divergent character of the theory.

Ewald's method can be adapted to the calculation of coulomb lattice

sums for polymers. The coulomb integral γ between orbitals centered on two atoms a distance R apart can be written

$$\gamma = \frac{1}{R} - p(R)e^{-AR} \quad [133]$$

where $p(R)$ is a polynomial in R depending upon the type of orbitals under discussion and A is some positive constant. The summation over the second term of equation [133] is strongly convergent because of the exponential factor and may therefore be evaluated directly. Therefore only the $1/R$ contribution need be considered. Rewriting equation [132] more specifically,

$$\Gamma_k = \sum_{\ell} \frac{e^{2\pi i k x(\ell)}}{|x(\ell) - x|} - \sum_{\ell} p[|x(\ell) - x|] e^{-A|x(\ell) - x|} e^{2\pi i k x(\ell)} \quad [134]$$

to represent the interaction between an atom at a point x (not a lattice site) in the unit cell and all the other atoms in the polymer. If a is the unit cell length, then

$$x(\ell) = \ell a, \quad \ell \text{ being an integer.}$$

Following the above discussion only the first term is considered in detail. Using Ewald's method it can be shown that

$$\sum_{\ell} \frac{e^{2\pi i k x(\ell)}}{|x(\ell) - x|} = \frac{2}{\sqrt{\pi}} \sum_{\ell} e^{2\pi i k x(\ell)} \int_0^{\infty} e^{-[x(\ell) - x]^2 \rho^2} d\rho + \frac{2}{a} \sum_{h} e^{2\pi i [\kappa(h) + k] x} \int_0^Q e^{-\left\{(\pi[\kappa(h) + k]) / \rho^2\right\}^2 \frac{d\rho}{\rho}} \quad [135]$$

This is Ewald's theta transformation for a one-dimensional lattice. In equation [135] $\kappa(h)$ is a lattice vector from the reciprocal lattice, $\kappa(h) = h/a$, h being summed over the whole reciprocal lattice, and Q may be

regarded as a convergence parameter. Thus by means of this transformation the infinite series over the real lattice has been split into summations over both the real and the reciprocal lattices. If k and Q are not equal to zero both series are now very strongly convergent. If $k = 0$ both series still converge except now each term from the origin of the reciprocal lattice ($h = 0$) has a singularity. Thus all of the divergent properties of these series can be discussed from the analysis of this single term.

The integrals are evaluated numerically by means of Gaussian quadrature using the following equalities,

$$\int_0^Q e^{-A^2/p^2} \frac{dp}{p} = \frac{1}{2} \int_1^\infty e^{-a} \frac{da}{a} - \int_1^{A^2/Q^2} e^{-a} \frac{da}{a} \quad [136]$$

the value of the first integral being 0.219383934396.

$$\int_Q^\infty e^{-A^2 p^2} dp = \frac{\sqrt{\pi}}{2A} - \int_0^Q e^{-A^2 p^2} dp \quad [137]$$

In the case of equivalent lattice sums, between orbitals on translationally equivalent atoms, $X = 0$ so that the interaction between the origin atom with itself must be excluded. This is most conveniently accomplished by simply neglecting the first term in equation [137] when calculating the contribution from the origin unit cell in the real lattice.

As an example lattice sums of $\cos 2\pi k x(\ell) / [x(\ell) - x]$ are calculated for a one-dimensional crystal, with $a = 2.5$ a.u. and $x = 1.5$ a.u., for k values of 0.4 and 0.0125. The results for the direct summation for several thousand unit cells are given in Table 14.

The only problem encountered with Ewald's method was connected with

TABLE 14

Lattice sums for $k = 0.4$ and 0.0125 calculated by direct summation.

No. of units of cells in summation	Lattice sum for $k = 0.4$	Lattice sum for $k = 0.0125$
2,000	-0.1978982	3.2036078
4,000	-0.1980981	3.2105615
6,000	-0.1981647	3.2102750
8,000	-0.1981980	3.2104858
10,000	-0.19821803	3.2103191
12,000	-0.1982314	3.2104570
14,000	-0.1982409	3.2103394
16,000	-0.1982480	3.2104419
18,000	-0.1982536	3.2103511

TABLE 15

Recommended values of λ for various ranges of k and the value for the corresponding origin integral in k -space. $E_1 = \int_{\lambda}^{\infty} e^{-\lambda} a^{-1} da.$

k-Range	λ	E
0.5 to 0.2	1.5	0.100019582
0.2 to 0.1	0.6	0.454379503
0.1 to 0.01	0.04	2.681263689
0.01 to 0.005	0.016	3.57388711875

the numerical integration of the origin term in the reciprocal lattice. The nature of the integrand for this lattice point is such that for small values of k serious rounding errors can occur. This difficulty is easily removed by evaluating the origin integral of the reciprocal lattice very accurately for certain standard values of the limit A^2/Q^2 and inserting them into the program as constants. The value of the convergence parameter Q is then chosen, for a given value of k , so that the origin integral for the lattice sum corresponds to one of these standard values. The recommended values of Q for a given k are given by

$$Q^2 = \frac{\pi^2 k^2}{a^2 \lambda} \quad [138]$$

where values for λ are given in Table 15, together with numerical values for the $k = 0$ integral from the reciprocal lattice. With these values for the convergence parameters even the $k = 0.0125$ lattice sum converges reliably after 30 unit cells in the real lattice and 2 unit cells in the reciprocal lattice. In the case of 0.4 sum the convergence was satisfactory (10^{-12}) after about 6 unit cells in the real and 3 unit cells in the reciprocal lattice. The convergence was tested by repeating the calculations with different values of Q . The results are given in Table 16.

A comparison of the results from Tables 14 and 16 illustrates the power of the integral transform method as compared with direct summation. The sum for $k = 0.0125$ has not converged to the third decimal place after almost 20,000 terms whereas the corresponding Ewald sum has apparently converged to ten decimal places after 32 terms.

TABLE 16

Phase modulated lattice sums calculated by Ewald's method
using different values of the convergence parameter R.

Q	k = 0.0125	Q	k = 0.4
0.15708	3.21039391565	0.35	-0.198298024437
0.124182	3.21039391567	0.65	-0.198298024437
0.111072	3.21039391562	0.95	-0.198298024437

APPENDIX 2

Representative Data Relating to Convergence

Convergence with respect to the length of the lattice summation for the one-electron hamiltonian is not discussed in detail, since for all the systems studied convergence is complete within eight cells on either side of the origin. All one-electron matrix elements between basis functions separated by more than eight cells are less than $5 \cdot 10^{-11}$.

Rapid convergence with respect to N , the number of unit-cells in the Born-Von Karman segment, is found for all the systems studied. As discussed in Chapter 2 the convergence of the long-range density matrix elements (see Table 17(c)) is slower than that of the energy per unit cell.

When discussing the convergence with respect to the length of the coulomb summation it is convenient to divide the systems into two groups. The hydrogen, beryllium and polyethylene chains form one group, while the polyene, carbon, hydrogen fluoride and lithium fluoride chains form the other. In the case of the first group, a group of non-polar systems, the convergence with respect to N_c is very rapid. This can be seen in Table 18(a) and (c). The second group involves polar compounds, or systems having other long-range interactions, and the coulomb convergence is considerably slower. However, all of the systems studied do converge.

One point is worth making. The length of the coulomb sum should not exceed the size of the Born-Von Karman segment, even for systems where the direct space density matrix has converged within the Born-Von Karman segment. Because of the nature of the Fourier analysis, the density matrix elements

recur periodically with a period equal to the length of the segment. When coulomb sums become disproportionately long by comparison with segment length, errors result from this periodicity, making the convergence appear slow or erratic.

Tables 18(c) and 6 demonstrate that when the real-space density matrix has converged, in the segment, as it has in the beryllium chain, truncation has no effect. When it has not converged, as in the polyene, truncation must be done in such a way that symmetry is conserved.

TABLE 17

Data Demonstrating Convergence with Respect to N,
the Number of Cells in the Born-Von Karman Segment

(a) H₂ Chain

N	E (a.u./u.c.)	P _{HI-HII} (origin cell)
5	-1.4756730	0.99420
21	-1.4756702	0.99422
31	-1.4756702	0.99422

(b) HF Chain

N	E (a.u./u.c.)
31	-28.465593607
37	-28.465593607

(c) Polyene: Convergence of π density matrix elements with N.

Cell index	0	2	4	6
19	0.8563	0.1440	0.0483	0.0185
29	0.8570	0.1436	0.0480	0.0182
39	0.8570	0.1436	0.0480	0.0182

TABLE 18

Data Demonstrating Convergence with Respect to N_c ,
 the Number of Cells Included in the Coulomb Lattice Sum

(a) H₂ Chain

N_c	E (a.u./u.c.)
11	-1.4756702
21	-1.4756702
31	-1.4756702

(b) HF Chain

N_c	E (a.u./u.c.)	Hydrogen atom density	Fluorine p_z density
19	-27.42637	0.75652	1.64254
23	-27.42637	0.75650	1.64255

(c) Be Chain (diatomic basis)

N_c	E (a.u./u.c.)
37 balanced	-3.380518009
37 unbalanced	-3.380518009

REFERENCES

1. G. Herzberg, "Molecular Structure and Molecular Spectra", Vol. I-IV (Van Nostrand, Princeton, N.J.).
2. J. C. Slater, "Quantum Theory of Molecules and Solids", Vol. I-III (McGraw-Hill, New York).
3. L. Pauling and R. B. Corey, *Nature* 168, 550 (1951).
4. J. D. Watson and F. H. C. Crick, *Nature* 171, 964 (1953).
5. M. Perutz, *New Scientist*, 50, 676 (1971).
6. See, for example, F. L. Pilar, "Elementary Quantum Chemistry" (McGraw-Hill, New York, 1968).
7. J. M. Ziman, "Principles of the Theory of Solids" (Cambridge University Press, London, 1969).
8. J. A. Pople, D. P. Santry, and G. A. Segal, *J. Chem. Phys. Suppl.* 43, S129 (1965); J. A. Pople and G. A. Segal, *J. Chem. Phys.* *ibid* 43, S136 (1965); J. A. Pople and G. A. Segal, *J. Chem. Phys.* 44, 3289 (1966).
9. J. A. Pople and D. L. Beveridge, "Approximate Molecular Orbital Theory" (McGraw-Hill, New York, 1970).
10. R. Daudel and C. Sandorfy, "Semi-empirical Wave-mechanical Calculations on Polyatomic Molecules" (Yale University Press, New Haven, 1971).
11. J. E. Lennard-Jones, *Proc. Roy. Soc.* A158, 280 (1937).
12. C. A. Coulson, *Proc. Roy. Soc.* A164, 383 (1938).
13. K. F. Herzfeld and A. L. Sklar, *Rev. Mod. Phys.* 14, 294 (1942).
14. H. Kuhn, *J. Chem. Phys.* 17, 1198 (1949).
15. See, for example, L. Salem, "The Molecular Orbital Theory of Conjugated Systems" (W. A. Benjamin, Inc., New York, 1966).
16. Y. Ooshika, *J. Phys. Soc. Japan* 12, 1238 (1957); *ibid* 12, 1246 (1957).
17. W. L. McCubbin and R. Manne, *Chem. Phys. Letters* 2, 230 (1968).
18. G. Del Re, J. Ladik and G. Biczo, *Phys. Rev.* 155, 997 (1967). See also J. Ladik, *Acta. Phys. Acad. Sci, Hung* 11, 239 (1960); J. Ladik and G. Biczo, *J. Chem. Phys.* 42, 1658 (1965); J. Ladik, D. K. Rai and K. Appel, *J. Mol. Spectry.* 27, 72 (1968); J. Avery, J. Packer, J. Ladik and G. Biczo, *ibid* 29, 194 (1969); B. F. Rozsnyai, F. Martino, and J. Ladik, *J. Chem. Phys.* 52, 5708 (1970).

19. J. M. André, *J. Chem. Phys.* 50, 1536 (1969); J. M. André and G. Leroy, *Chem. Phys. Letters* 5, 71 (1970); J. M. André and G. Leroy, *Ann. Soc. Sci. Bruxelles, Ser. 1*, 84, 133 (1970); E. Clementi, *J. Chem. Phys.* 54, 2492 (1971).
20. K. Morokuma, *Chem. Phys. Letters* 6, 186 (1970); *J. Chem. Phys.* 54, 962 (1971); *Chem. Phys. Letters* 9, 172 (1971).
21. H. Fujita and I. Imamura, *J. Chem. Phys.* 53, 4555 (1970). A similar set of calculations in the Extended Hückel approximation is given in I. Imamura, *J. Chem. Phys.* 52, 3168 (1970).
22. Séamus O'Shea and D. P. Santry, *J. Chem. Phys.* 54, 2667 (1971).
23. D. L. Beveridge, I. Jano and J. Ladik, *J. Chem. Phys.* 56, 4744 (1972).
24. M. Tsuji, S. Huzinaga and T. Hasino, *Rev. Mod. Phys.* 32, 425 (1960).
25. H. Primas, "Problems of the Interpretation of Quantum Mechanics of Large Molecular Systems", Lecture Notes, Swiss Federal Institute of Technology, Zurich (1972).
26. F. J. Corbato, "Proc. 1957 Carbon Conf." (Pergamon Press, New York, 1957).
27. P. W. Anderson, "Concepts in Solids" (W. A. Benjamin, Inc., New York, 1963).
28. M. Born and J. R. Oppenheimer, *Ann. Physik.* 84, 457 (1927). See also Reference 40.
29. A detailed discussion of this problem is given in a series of papers beginning with W. Kolos and L. Wolniewicz, *Rev. Mod. Phys.* 35, 473 (1963).
30. H. Eyring, H. J. Walter and G. E. Kimball, "Quantum Chemistry" (John Wiley and Sons, Inc., New York, 1944).
31. G. Arfken, "Mathematical Methods for Physicists" (Academic Press, London, 1968).
32. C. C. J. Roothaan, *Rev. Mod. Phys.* 23, 69 (1951).
33. C. C. J. Roothaan, *Rev. Mod. Phys.* 32, 179 (1960).
34. V. Heine, "Group Theory in Quantum Mechanics" (Pergamon Press, London, 1960); H. Jones, "Theory of Brillouin Zones and Electronic States in Crystals" (North-Holland, Amsterdam, 1960); G. F. Koster, *Solid State Physics* 5, 174 (1957).
35. A. W. Overhauser, *Phys. Rev. Letters* 4, 415 (1960); *ibid* 4, 466 (1960).
36. J. Cizek and J. Paldus, *J. Chem. Phys.* 47, 3976 (1967).

37. R. S. Knox and A. Gold, "Symmetry in the Solid State" (W. A. Benjamin, Inc., New York, 1964).
38. "Irreducible Representations of Space Groups", J. Zak, Ed. (W. A. Benjamin, Inc., New York, 1969).
39. M. Born and Th. Von Karman, *Physik. Z.* 13, 297 (1912); *ibid* 14, 15 (1913).
40. M. Born and K. Huang, "Dynamical Theory of Crystal Lattices" (Oxford University Press, London, 1954).
41. F. E. Harris and H. J. Monkhorst, *Phys. Rev.* B2, 4400 (1970).
42. P. P. Ewald, *Ann. Physik.* 29, 1 (1916); *ibid* 49, 117 (1916); see also References 40, 41.
43. See, for example, R. J. Lee and J. C. Raich, *Phys. Rev. Letters* 27, 1137 (1971).
44. W. Hume-Rothery, "The Structures of Metals and Alloys" (Institute of Metals Monograph, London, 1936).
45. H. A. Jahn and E. Teller, *Proc. Roy. Soc.* A161, 200 (1937).
46. K. M. Middlemiss and D. P. Santry, submitted for publication to *Chem. Physics*.
47. D. P. Craig and S. H. Walmsey, "Excitons in Molecular Crystals (W. A. Benjamin, Inc., New York, 1968); see also Reference 23.
48. D. Pines, "Many-Body Problem" (W. A. Benjamin, Inc., New York, 1961).
49. H. Margenau and N. R. Kestner, "The Theory of Intermolecular Forces" (Pergamon Press, New York, 1969).
50. H. Winston and R. S. Halford, *J. Chem. Phys.* 17, 607 (1949); see also Reference 66.
51. W. Drenth and E. H. Wiebenga, *Acta Cryst.* 8, 755 (1955).
52. A. D. McLachlan, *Mol. Phys.* 2, 271 (1959).
53. L. Salem and H. C. Longuet-Higgins, *Proc. Roy. Soc.* A251, 172 (1959).
54. J. R. Platt, *J. Chem. Phys.* 25, 80 (1956).
55. M. Gouterman and G. Wagniere, *J. Chem. Phys.* 36, 1188 (1962).
56. F. A. Van Catledge and N. L. Allenger, *J. Am. Chem. Soc.* 91, 2582 (1969).
57. R. A. Harris and L. M. Falicov, *J. Chem. Phys.* 50, 4590 (1969).

58. L. Salem, *J. Chem. Phys.* 52, 1015 (1970); R. A. Harris and L. M. Falicov, *J. Chem. Phys.* 52, 1015 (1970).
59. J. M. André and G. Leroy, *Ann. Soc. Sci. Bruxelles, Ser. 1*, 133 (1970).
60. C. Tric, *J. Chem. Phys.* 51, 4778 (1969); *ibid* 55, 827 (1972).
61. R. M. Gavin, Jr. and S. A. Rice, *J. Chem. Phys.* 55, 2675 (1972).
62. J. M. André and G. Leroy, *Chem. Phys. Letters* 5, 71 (1970).
63. J. M. André, G. S. Kapsomenos and G. Leroy, *Chem. Phys. Letters* 8, 195 (1971); see also Reference 67.
64. H. A. Scheraga, *Advan. Phys. Org. Chem.* 6, 103 (1968); P. J. Flory, "Statistical Mechanics of Chain Molecules" (Wiley, New York, 1969); and references therein.
65. T. Shimanouchi and S. Mizushima, *J. Chem. Phys.* 23, 707 (1955).
66. M. C. Tobin, *J. Chem. Phys.* 23, 891 (1955); *J. Mol. Spectry.* 4, 349 (1960); W. McCubbin, *Chem. Phys. Letters* 8, 507 (1971).
67. C. W. Bunn, *Trans. Faraday Soc.* 35, 482 (1939).
68. A. Kitiagorodskii in *Advances in Structure Research by Diffraction Methods* 3, (1971).
69. R. F. W. Bader, *Mol. Phys.* 3, 137 (1960); *Can. J. Chem.* 40, 1164 (1962).
70. M. H. Wood, M. Barber, I. H. Hillier and J. M. Thomas, *J. Chem. Phys.* 56, 1788 (1972).
71. L. Salem, *J. Chem. Phys.* 37, 2100 (1962); M. J. Sparnaay, *Rec. Trav. Chim.* 9, 451 (1954).
72. H. Krauch, *J. Chem. Phys.* 28, 898 (1958).
73. I. T. Sugawara and E. Kanda, *Sci. Rep. Res. Inst. Tohoku Univ.*, P607 (1952).
74. J. H. Callomon and B. P. Stoicheff, *Can. J. Phys.* 35, 373 (1957).
75. F. London, *Trans. Faraday Soc.* 33, 8 (1937); see also Reference 49.
76. R. E. Peierls, "Quantum Theory of Solids" (Oxford University Press, London, 1955).
77. F. Perrot, *Phys. Stat. Sol. (b)* 52, 163 (1972).
78. C. A. Coulson, "Electricity" (Oliver and Boyd, Edinburgh, 1956).

79. M. R. Haynes, *J. Phys. Chem.* 5, 15 (1972).
80. M. Atoji and W. N. Lipscomb, *Acta Cryst.* 7, 173 (1954).
81. See, for example, "Structural Chemistry and Molecular Biology--A Tribute to Linus Pauling", A. Rich and N. Davidson, Eds. (W. H. Freeman and Co., San Francisco, 1966).
82. P. A. Kollman and L. C. Allen, *Chem. Rev.* 72, 283 (1972).
83. T. R. Dyke, B. J. Howard and W. Klemperer, *J. Chem. Phys.* 56, 2442 (1972).
84. J. Janzen and L. S. Bartell, *J. Chem. Phys.* 56, 3661 (1969).
85. S. P. Habuda and Tu. V. Gagarinsky, *Acta Cryst.* B27, 1677 (1971).
86. L. E. Sutton, "Interatomic Distances" (Special Publication, No. 11, The Chemical Society, London, 1958).
87. J. Bacon and D. P. Santry, *J. Chem. Phys.* 55, 3743 (1971); *ibid* 56, 2011 (1972).
88. J. Hori, "Spectral Properties of Disordered Chains and Lattices" (Pergamon Press, Oxford, 1968).
89. J. Gerratt and I. M. Mills, *J. Chem. Phys.* 49, 1719 (1968); *ibid* 49, 1730 (1968).
90. C. A. Coulson and H. C. Longuet-Higgins, *Proc. Roy. Soc.* A191, 39 (1947); R. McWeeny, *Phys. Rev.* 126, 1028 (1962); G. Diercksen and R. McWeeny, *J. Chem. Phys.* 44, 3554 (1966); A. T. Amos and G. G. Hall, *Theoret. Chim. Acta* 5, 148 (1966); R. McWeeny, *Chem. Phys. Letters* 1, 567 (1968).
91. R. C. Tolman, "Principles of Statistical Mechanics" (Oxford University Press, London, 1938).
92. D. A. Goodings, private communication.
93. G. G. Hall, *Proc. Phys. Soc.* B69, 1124 (1956).
94. J. M. Andre, J. Delhalle, J. G. Fripiat and G. Leroy, *Inter. J. of Quantum Chem.* V, 67 (1971).